uOttawa

L'Université canadienne
Canada's university

FACULTÉ DES ÉTUDES SUPÉRIEURES ET POSTOCTORALES

uOttawa

L'Université canadienne
Canada's university

FACULTY OF GRADUATE AND POSDOCTORAL STUDIES

Claudia Arauz

AUTEUR DE LA THÈSE / AUTHOR OF THESIS

M.Sc. (Cellular and Molecular Medicine)

GRADE / DEGREE

Department of Cellular and Molecular Medicine

FACULTÉ, ÉCOLE, DÉPARTEMENT / FACULTY, SCHOOL, DEPARTMENT

Genes Required for Normal Neuronal Morphology in Caenorhabditis Elegans

TITRE DE LA THÈSE / TITLE OF THESIS

Antonio Colavita

DIRECTEUR (DIRECTRICE) DE LA THÈSE / THESIS SUPERVISOR

CO-DIRECTEUR (CO-DIRECTRICE) DE LA THÈSE / THESIS CO-SUPERVISOR

John Copeland

Hsiao-Huei Chen

Hendrick de Haan

Daniel Duguay

Gary W. Slater

Le Doyen de la Faculté des études supérieures et postdoctorales / Dean of the Faculty of Graduate and Postdoctoral Studies

Genes required for normal neuronal morphology in *Caenorhabditis elegans*

Claudia Arauz

This thesis is submitted as a partial fulfillment
of the M.Sc. program in Cellular Molecular Medicine
Faculty of Medicine

University of Ottawa
Ottawa, Ontario, Canada
2010

Your file Votre référence
ISBN: 978-0-494-69043-7
Our file Notre référence
ISBN: 978-0-494-69043-7

Abstract

png-1 encodes the *Caenorhabditis elegans* homolog of Peptide: N-glycanase, a highly conserved cytosolic enzyme that cleaves N-glycans from misfolded glycoproteins. *png-1* was found to regulate several aspects of neuronal morphology including axon branching. In this study, we show that mutations in the NDR kinase pathway genes *sax-1* and *sax-2* result in *png-1* like phenotypes, including excessive branching and ectopic neurites. Furthermore, we found that *png-1; sax-1* and *png-1*; *sax-2* double mutants display enhanced defects compared to single mutants, suggesting that *png-1* and *sax-1/sax-2* act in parallel pathways to restrict axon and branch overgrowth. These interactions suggested a *sax-1* enhancer screen as a means to identify additional genes in the *png-1* pathway as enhancer mutants should phenocopy *png-1* and enhance *sax-1* branching defects.. This approach recovered at least three *sax-1 en*hancers (*sens*) that act like *png-1* to limit axon growth and branching. The identification of these genes should provide new insight into how PNG-1 regulates neuronal morphology.

Table of Contents **page**

List of Tables

List of Figures

List of Abbreviations and Gene Names

AAA	ATPases associated with various cellular activities
ACE	activator of cup1 expression
AIS	auto-inhibitory sequence
AKT	acutely transforming retrovirus AKT8 in rodent T-cell lymphoma
AMFR	autocrine motility factor receptor
APC	adenomatous polyposis coli
aPKC	atypical protein kinase C
Arp	actin related protein
AS	activation segment
Asp	aspartic acid
BAM	branching abnormal
bp	base pair
BDNF	brained-derived neurotrophic factor
BMP	bone morphogenetic protein
CAMKII	calcium/calmodulin-regulated kinase
cAMP	cyclic adenosine monophosphate
cat	abnormal catecholamine distribution
Cbk	cell wall biosynthesis kinase
Cdc42	cell division cycle 42
ced	cell death abnormality
C. elegans	*Caenorhabditis elegans*
CG	complementation group
CNS	central nervous system
Comm	commissureless
CRMP	collapsin response mediator protein
Cys	cysteine
da	dendritic arborization
Dbf	dumbbell former
DCC	deleted in colorectal cancer
D. melanogaster	*Drosophila melanogaster*
DV	dorso-ventral
Eph	ephrin
ER	endoplasmic reticulum
ERAD	ER associated protein degradation
EMS	ethylmethanesulfonate
E3	ubiquitin-protein isopeptide ligase
FGF	fibroblast growth factor
flp	FMRF-like peptide
Fry	furry
GABA	γ-aminobutyric acid
GAP	GTPase activating protein

GEF	guanine nucleotide exchange factor
GFP	green fluorescent protein
GSKβ	glycogen synthase kinase β
GTPase	guanosine-5'-triphosphate hydrolase enzyme
HEAT	Huntington, Elongation Factor 3, PR65/A, TOR
Hh	hedgehog
His	histidine
H M	hydrophobic motif
HSN	hermaphrodite-specific motor neuron
hWW	human WW domain-containing
IgCAM	Ig superfamily cell-adhesion molecules
KAL	Kallmann syndrome
KIF3A	kinesin-II
LATS	large tumour suppressor
LG	linkage group
LIM	Lin-11, Isl-1 and Mec-3
LIMK	LIM kinase
LIN	abnormal cell lineage
MAP	microtubule-associated protein
MARK	microtubule affinity regulating kinase
Mb	mega base pairs
MgSO4	magnesium sulfate
mig	mitogen-inducible gene
MOB	mps one binder
MST	mammalian sterile 20-like
MTs	microtubules
Mtl	mig-2-like
mut	mutant
NDR	nuclear Dbf2-related
N-glycans	asparagine-linked glycans
NgCAM	neuronglia cell adhesion molecule
NGF	nerve growth factor
NGM	nematode growth medium
N. crassa	*Neurospora crassa*
NTR	N-terminal regulatory
N-WASP	neural Wiskott–Aldrich syndrome protein
pag	pattern of reporter gene expression abnormal
PAK	p21-activated kinase
PAR	partitioning-defective
PCR	polymerase chain reaction
PH	pleckstrin homology
PIP2	phosphatidylinositol (4, 5)-triphosphate
PIP3	phosphatidylinositol (3, 4, 5)-triphosphate
PKB	protein kinase B
PNG	peptide: N-glycanase

PUB/PUG	peptide: N-glycanase/UBA or UBX-containing protein
P13K	phosphatidylinositol 3' kinase
Rac	Ras-related C3 botulinum toxin substrate
rad	radiation sensitive
RFLP	restriction fragment length polymorphism
RGC	retinal ganglion cell
Rho	*ras homolog*
Robo	roundabout
ROCK	Rho kinase
rol	roller
RTK	receptor tyrosine kinases
sax	sensory axon guidance
Sav	Salvador
S. cereviase	*Saccharomyces cereviase*
SCF	Skp1-cullin–F-box protein
Sec	secretory
Sema	semaphorin
sens	*sax-1* enhancers
Ser	serine
SNP	single nucleotide polymorphism
S. pombe	*Schizosaccharomyces pombe*
sul	sulfatase domain protein
TAX	abnormal chemotaxis
Tau	Tau protein
TF	transcription factor
TG	transglutaminase
Thr	threonine
Trc	tricornered
UBA	ubiquitin-associated
UBX	ubiquitin-like
UNC	uncoordinated
VC	ventral cord
VNC	ventral nerve cord
wt	wild type
Wnt	wingless-type
Yki	yorkie

Acknowledgements

I would like to thank everyone who helped and inspired me during my graduate studies.

I would like to express my deepest gratitude to my supervisor, Dr. Antonio Colavita, for his constant assistance, guidance, and support throughout this project.

I would also like to thank my advisory committee members, Dr. Marc Ekker and Dr. David Park, for their advice and direction.

To my co-workers Nasrin Habibi-Babadi, Jiravat Visanuvimol, Anna Su, Carlos Carvalho, and Andrea McEwan, I thank them for their support and making the lab an enjoyable place to work. Special thanks to Nasrin for her help, encouragement, and tea breaks.

Most of all, I would like to thank my family, especially my parents. You've always provided me with a loving, supporting, and encouraging environment throughout my life.

1. Introduction

1.1 Neuronal Morphology

The nervous system is a complex network of specialized cells including neurons and glial cells. In humans, the nervous system is made up of approximately 100 billion neurons that differ in structure, chemistry, and function (Bear et al., 2001). Neuronal cells have complex morphologies with distinctive axonal and dendritic processes which are the 'wires' that interconnect the nervous system. Proper nervous system structure and function is dependent on axons and dendrites establishing appropriate connections to other neurons and target cells. In order to establish appropriate connections, post-mitotic neurons undergo a series of distinct stages that involve the establishment of neuronal polarity, extension of axons to appropriate targets, and finally terminal arborization or branching. Since neuronal function is dependent on neuron morphology, it is essential to understand the molecular mechanisms that regulate axonal and dendritic outgrowth, guidance, and branching.

1.2 Neuronal polarization

1.2.1 Establishment of Neuronal Polarity

Axons are typically long thin processes that propagate signals, whereas dendrites are shorter and highly branched processes that receive and relay these signals. Neuronal polarization is defined as the specification of axons and dendrites. The initiation of axon outgrowth is one of the earliest events in establishing neuronal morphology (Dotti et al., 1988; Craig and Banker, 1994). Many of the key regulators of neuronal polarization have been discovered using cultured hippocampal neurons as a model system (Barnes and Polleux, 2009). Hippocampal polarization is defined by key morphological changes (Dotti et al., 1988). Early on, neurons are symmetrical

as they extend multiple short processes called neurites that are equal in length. Eventually, one of these neurites extends more rapidly than the others to form a long process that eventually becomes the axon. The remaining neurites mature into dendrites.

1.2.2 Intracellular Mechanisms

Hippocampal cells have been used to define the intrinsic programs involved in establishing neuronal polarity (Shi et al., 2003; Menager et al., 2004; Schwamborn and Puschel, 2004; Jiang et al., 2005; Nishimura et al., 2005; Yoshimura et al., 2005). Several proteins are selectively localized to the tip of the future axon including the lipid and protein kinase phosphatidylinositol 3' kinase (P13K) (Shi et al., 2003; Menager et al., 2004). Localized P13K activity at the tip of growing axons triggers a kinase signaling cascade which ultimately regulates various microtubule binding proteins and axon outgrowth. Active P13K converts phosphatidylinositol (4, 5)-triphosphate (PIP2) into phosphatidylinositol (3, 4, 5)-triphosphate (PIP3) (Menager et al., 2004). PIP3, a phospholipid second messenger, accumulates at the tip of the future axon and recruits proteins that contain the PH (Pleckstrin Homology) domain which has a high binding affinity to PIP3 (Menager et al., 2004). A protein kinase AKT (AKT/PKB) is recruited and becomes enriched in the growth cone of the future axon (Shi et al., 2003). At the tip of this axon, active AKT kinase phosphorylates and locally inactivates glycogen synthase kinase β (GSK3β), a constitutively active kinase (Jiang et al., 2005). Normally, active GSK3β inhibits axon elongation by phosphorylating proteins like the tubulin-binding protein CRMP-2 (collapsin response mediator protein-2) (Yoshimura et al., 2005), Tau protein (microtubule-associated protein) (Sperber et al., 1995; Stoothoff and Johnson, 2005) , MAP1b (microtubule associated protein-1b) (Goold et al., 1999; Gonzalez-Billault et al., 2004), and APC (adenomatous polyposis coli) (Shi et al., 2004; Zhou et al., 2004) which reduces the ability of

these proteins to bind microtubules (MTs). However, upon GSKβ inactivation, unphosphorylated CRMP-2 binds tubulin dimers to enhance MT assembly and axon elongation (Inagaki et al., 2001; Yoshimura et al., 2005).

High P13K activity is also thought to recruit the PAR (partitioning-defective) proteins PAR3 and PAR6, also key regulators of neuronal polarity, to the growing axon tip (Shi et al., 2003). The localized activity of polarity proteins, such as the PAR proteins, specifies the axon and contributes to axon elongation. These scaffolding proteins interact with one another to form a PAR3/PAR6 complex (Shi et al., 2003). Motor proteins like kinesin-II (KIF3A) are important in neuronal polarity since they transport important polarity proteins like the PAR complex from the cell body to a single neurite (Nishimura et al., 2004). The PAR3/PAR6 is able to interact and form multi-protein complexes with other proteins like atypical protein kinase C (aPKC) (Shi et al., 2003), the Rho family of GTPases (Rho GTPases) (Schwamborn and Puschel, 2004) , and Rho GTPase regulators (Nishimura et al., 2005; Zhang and Macara, 2006). The PAR3/PAR6/aPKC complex inhibits the kinase activity of microtubule affinity regulating kinase-2 (MARK2/PAR1) (Chen et al., 2006) leading to dephosphorylation of microtubule-associated proteins (MAPs), thereby promoting MT assembly and axon elongation.

The Rho family of small GTPases including Cdc42, Rac1, and RhoA , are molecular switches that regulate a variety of cellular processes (Etienne-Manneville and Hall, 2002). Guanine nucleotide exchange factors (GEFs) activate Rho GTPases; whereas, GTPase activating proteins (GAPs) deactivate Rho GTPases. Active GTP-bound Rho GTPases activate effector proteins that regulate actin/MT dynamics which leads to changes in cell morphology. In association with Cdc42 and Rac-specific GEFs, the PAR3/PAR6 complex limits Rac1 activation

and actin remodeling to the growing axon tip, thus, promoting outgrowth (Schwamborn and Puschel, 2004; Nishimura et al., 2005).

1.2.3 Extracellular Signals

P13K activity, Rho GTPases, and PAR proteins are central players in axon specification and axon outgrowth (Barnes and Polleux, 2009). However, what are the extracellular cues that trigger their activity? *In vitro* studies suggest that cell adhesion molecules like laminin and neuron-glia cell adhesion molecule (NgCAM) and neurotrophic factors like brain derived neurotrophic factor (BDNF) can specify axons. Studies have shown that the first neurite to come into contact with laminin, NgCAM, or BDNF rapidly elongates and eventually become the axon (Esch et al., 1999; Menager et al., 2004; Shelly et al., 2007) .

In vivo studies in *C. elegans* have also revealed extracellular signals that influence neuronal polarity. UNC-6/Netrin is a known axon guidance molecule which attracts or repels axons. However, UNC-6/Netrin and its receptor UNC-40/DCC have also been shown to orient and stimulate the growth of neurites specifically on the ventral side of the hermaphrodite-specific motorneuron (HSN) (Adler et al., 2006). Netrin signaling triggers the localized activity of P13K, an increase in PIP3, and the subsequent recruitment of the PH domain-containing protein MIG-10/lamellipodin which stimulates actin polymerization (Adler et al., 2006; Chang et al., 2006). Therefore, both *in vivo* and *in vitro* studies suggest that the asymmetric localization of proteins and their activity is a common mechanism that drives neuronal polarization.

1.3 Axon Guidance

1.3.1 General mechanisms of Axon Guidance

Axons and dendrites are processes that extend from the neuronal cell body and function as wires to interconnect the nervous system. Once dendrites and axons have been specified, these processes must grow in the appropriate direction and pathway towards their final target. The growth cone at the tip of the growing axons acts as a sensory and motile structure that directs axon outgrowth (Lowery and Van Vactor, 2009). The growth cone contains specific cell surface receptors that interact with guidance molecules to determine the direction and amount of axon growth (Bear et al., 2001). Extracellular molecules, membrane bound or secreted, act as guidance molecules that attract or repel growing axons (Tessier-Lavigne and Goodman, 1996). Typically, attractive cues cause growth cones to move towards the source; whereas, repulsive cues cause growth cones to move away from the source. Many of these receptor-ligand complexes initiate intracellular pathways that lead to the reorganization of the cytoskeleton in the growth cone (Huber et al., 2003; Bouquet and Nothias, 2007).

Many guidance signaling systems converge on Rho GTPases to regulate axonal growth (Jin and Strittmatter, 1997; Kaufmann et al., 1998; Wahl et al., 2000; Hu et al., 2001; Wong et al., 2001; Li et al., 2002; Shekarabi and Kennedy, 2002; Gitai et al., 2003). Guidance receptors tend to be directly or indirectly linked to GEFs and GAPs which either activate or deactivate Rho GTPase signaling (Bos et al., 2007). Rho GTPase activation of N-WASP (Neural Wiskott–Aldrich syndrome protein) causes N-WASP to bind the actin related protein (Arp) 2/3 complex to promote actin polymerization and filament assembly (Rohatgi et al., 1999). Other downstream targets of Rho GTPases include protein kinases like p21-activated kinases (PAK) (Manser et al., 1994; Hing et al., 1999) and Rho kinase (ROCK) (Leung et al., 1995; Ishizaki et

al., 1996), which are regulators of the actin cytoskeleton. ROCK phosphorylation of the serine/threonine kinase LIM kinase (LIMK) leads to inactivation of an actin depolymerizing protein, cofilin, which ultimately inhibits axon outgrowth (Arber et al., 1998; Yang et al., 1998; Maekawa et al., 1999; Ohashi et al., 2000). In general, Rho GTPase signaling pathways control the movement and morphology of axons by ultimately regulating cytoskeleton dynamics and organization.

1.3.2 Axon Guidance Molecules

Several conserved classes of guidance molecules direct axon guidance in *C. elegans* and other organisms (Araujo and Tear, 2003). Netrins, slits, semaphorins and ephrins are highly conserved families of guidance molecules (Tessier-Lavigne and Goodman, 1996; Dickson, 2002; Huber et al., 2003). Netrins (UNC-6) are a family of secreted proteins that are able to attract and repel axons both *in vitro* and *in vivo* (Hedgecock et al., 1990; Ishii et al., 1992; Harris et al., 1996; Mitchell et al., 1996; Serafini et al., 1996; Bloch-Gallego et al., 1999). These opposing actions are dependent on the specific netrin receptors present on the growth cone membrane and the intracellular pathways that are activated. The deleted in colorectal cancer (DCC/UNC-40) family of receptors mediate netrin attraction (Keino-Masu et al., 1996; Kolodziej et al., 1996), whereas the UNC-5 receptor family mediates netrin repulsion (Rothberg et al., 1990; Leung-Hagesteijn et al., 1992; Leonardo et al., 1997; Przyborski et al., 1998; Keleman and Dickson, 2001). Slits are secreted guidance proteins that repel axons. Slit repulsion is mediated through the roundabout (Robo) family of receptors (Kidd et al., 1998; Kidd et al., 1999; Hao et al., 2001). Netrins and slits are key regulators of axon guidance at the midline in vertebrates, *Drosophila*, and *C. elegans* (Brose and Tessier-Lavigne, 2000; Kaprielian et al., 2001; Bagri et al., 2002). The spinal cord floor plate in vertebrates and the ventral nerve cord (VNC) in Drosophila and *C.*

elegans serve as midline cells that separate the right and left halves of the animal and act as intermediary targets for axons (Kaprielian et al., 2001). Netrins are expressed at the midline to attract axons, whereas, slits are expressed to repel axons and ensure axons grow away from the midline (Kidd et al., 1998; Tear, 1999; Kaprielian et al., 2001; Keleman et al., 2002).

Semaphorins and their neuropilin and plexin receptors are large diverse families of guidance molecules that generally repel axons and have well established roles in neuronal development (Raper, 2000) . Ephrins, membrane bound proteins, and their receptors, Ephrin receptor tyrosine kinases (RTK), are critical for many biological processes including axon guidance (Reber et al., 2007). Ephrin/Eph binding initiates signaling pathways in both the ligand expressing cells and receptor expressing cells which mostly lead to axon repulsion. Other signaling molecules involved in axon guidance include neurotrophic factors like nerve growth factors (NGF) and BDNF (Lykissas et al., 2007) and morphogens like the bone morphogenetic protein (BMP), hedgehog (Hh), and Wnts (Charron and Tessier-Lavigne, 2007).

In conjunction with extracellular cues, the internal state of the growth cone can influence axon guidance decisions. For example, changes in levels of cAMP (Song et al., 1997) and Ca^{2+} activity (Gomez and Spitzer, 1999; Hong et al., 2000; Ming et al., 2001; Tang et al., 2003; Henley and Poo, 2004) can influence axon outgrowth and guidance. Electrical activity can cause an influx of Ca^{2+} which activates Ca^{2+}-dependent signaling kinases, Calmodulin kinases (CAMKs), inturn, CAMKs influence axonal and dendritic growth (Redmond et al., 2002; Fink et al., 2003; Gaudilliere et al., 2004; Wayman et al., 2004). Localized elevation of intracellular Ca^{2+} concentration can influence growth cone turning in the direction of high Ca^{2+} concentration (Hong et al., 2000; Wen et al., 2004). However, the link between Ca^{2+} activity and cAMP activity and cytoskeleton remodeling remain poorly understood.

1.3.3 Regulation of Axon Guidance Molecules

Axon guidance depends on the coordinated expression of guidance cues and their corresponding receptors. Transcriptional, translational, and post-translational controls are in place to regulate the spatial and temporal expression of guidance molecules in neurons and the environment (O'Donnell et al., 2009). For example, in *C. elegans*, normal dorso-ventral (DV) axon guidance requires the transcriptional repression of a guidance cue in the ventral but not dorsal muscles (Nash et al., 2000). In vertebrates, transcripts encoding the Eph2A receptor are locally translated in the growth cones which cause an upregulation of this cell surface receptor (Brittis et al., 2002). In *Drosophila* midline crossing, commissureless (Comm) downregulates the cell surface expression of Robo receptor and represses Slit/Robo mediated repulsion, thereby allowing axons to cross the midline (Keleman et al., 2002). Cell surface expressions of guidance receptors like DCC are also regulated by proteolytic cleavage of their extracellular domain by metalloproteases; in so doing Netrin/DCC signaling is attenuated (Galko and Tessier-Lavigne, 2000). It has also been shown that the netrin receptor, DCC, can be down regulated by ubiquitin-proteasome degradation in *Drosophila* (Hu et al., 1997). Apart from the guidance molecules themselves, the proteins that modulate their activity and localization are critical in regulating axonal guidance. The combined actions of many proteins involved in transcriptional regulation (Butler and Tear, 2007) , receptor trafficking (Keleman et al., 2005; Levy-Strumpf and Culotti, 2007; Watari-Goshima et al., 2007) , protein synthesis (Campbell and Holt, 2001), ubiquitination (Myat et al., 2002) , and proteolysis (Fambrough et al., 1996; Hattori et al., 2000; Hehr et al., 2005; Chen et al., 2007) all participate in the regulation of guidance signals and their receptors .

1.4 Axon and Dendritic Branching

1.4.1 General Mechanism of Axon Branching

Branching is an important step in setting up neuronal circuits and contributing to the normal structure and function of the nervous system. Axons that don't extend directly onto their targets must extend axon branches to establish appropriate connections. Axons can establish connections by extending collateral branches laterally from the primary axon shaft (interstitial branching) or through the bifurcation of the primary growth cone at the tip (O'Leary and Terashima, 1988; O'Leary et al., 1990). Interstitial branching allows neurons to project and innervate multiple targets and is the primary mode of branch formation in vertebrates (O'Leary and Terashima, 1988; O'Leary et al., 1990; Kuang and Kalil, 1994; Bastmeyer and O'Leary, 1996; Bastmeyer et al., 1998; Dent et al., 1999; Acebes and Ferrus, 2000).

Near targets, certain growth cone behaviors and morphologies are observed that are associated with axon branching (Szebenyi et al., 1998; Davenport et al., 1999; Kalil et al., 2000; Szebenyi et al., 2001; Dent et al., 2003). For example, pausing and enlargement behavior in the primary growth cone specifies the future site of an axon branch (Halloran and Kalil, 1994; Szebenyi et al., 1998; Dent et al., 2003). After a period of time, as the primary growth cone resumes forward movement, it leaves behind cytoskeletal remnants that slowly develop into a secondary growth cone that extends to form an interstitial branch (Szebenyi et al., 1998; Kalil et al., 2000; Dent and Kalil, 2001). While the primary growth cones are paused, MTs spread out and undergo localized fragmentation (Tanaka and Kirschner, 1991; Lin et al., 1994; Tanaka and Sabry, 1995; Dent et al., 1999; Kalil et al., 2000; Dent and Kalil, 2001). Fragmented MTs are able to invade, elongate, and stabilize nascent branches. Growth cone collapse, caused by actin depolymerization, is also associated with axon branching (Davenport et al., 1999). After the

initial collapse, growth cones recover and display filipodia and lamellipodia-like expansions which give rise to interstitial branches (Davenport et al., 1999).

Similar to axon guidance, intracellular responses to axon branching cues are mediated by Rho GTPases. Rho GTPases transduce extracellular signals to control various aspects of neuronal morphogenesis including axon growth, guidance, and branching through their action on cytoskeleton dynamics (Ruchhoeft et al., 1999; Luo, 2000; Nakayama et al., 2000; Ng et al., 2002). In *Drosophila*, axon growth, guidance, and branching seem to be regulated by different levels of Rac GTPase activity (Ng et al., 2002). The progressive loss of three Rac GTPases, Rac1, Rac2, and Mtl, in mushroom body neurons in *Drosophila* leads first to axon branching defects, followed by guidance defects and finally growth defects (Ng et al., 2002). The Rho GTPase signaling pathways and their downstream effectors that control branch formation are not well characterized; but likely involve a large number of effectors that are linked to regulation of the actin and MT cytoskeleton as previously described in axon guidance (Bishop and Hall, 2000; Kuhn et al., 2000; Fujita et al., 2002; Neumann et al., 2002). Similar to axon guidance, activity induced increase in Ca^{2+} activity and CAMKII can influence axon branching (Zou and Cline, 1996; Tang and Kalil, 2005; Uesaka et al., 2005).

1.4.2 Axon Branching Molecules

Although branching is important for proper neuronal structure and function, the molecular mechanisms that control branch formation remain poorly understood. However, studies suggest that axon guidance and axon branching share common mechanisms (Kalil et al., 2000; Dent et al., 2003). For example, guidance molecules that usually guide axons towards or away their targets have also been implicated in promoting or inhibiting axon branching. Slit and

semaphorin, which usually act as chemorepellants, and netrin, a chemoattractant, have been shown to promote branching (Szebenyi et al., 1998; Wang et al., 1999; Brose and Tessier-Lavigne, 2000; Dent et al., 2004; Lebrand et al., 2004) . In contrast, guidance cues like ephrins which normally repel axons have been found to suppress branching of retinal axons to control retinotectal map formation (Yates et al., 2001).

In both axon guidance and axon branching, guidance molecules elicit the reorganization of the actin and microtubule cytoskeleton in primary growth cones and branch points (Kalil et al., 2000; Dent et al., 2003). For instance, semaphorin 3A (Sema3A) reduces actin dynamics in growth cones which leads to growth cone collapse (Campbell et al., 2001). Interestingly, in *Xenopus laevis,* Sema3A induced growth cone collapse in retinal ganglion cell (RGC) axons promotes branching (Campbell et al., 2001), whereas, Sema3A induced growth cone collapse in mammalian cortical neurons reduces axon branching (Dent et al., 2004). Conversely, Netrin-1 induces the rapid formation of filopodia in cortical neurons which develop into branches (Dent et al., 2004; Tang and Kalil, 2005). Growth factors like NGF, FGF-2, BDNF, which have established roles in axon outgrowth and guidance have also been shown to promote axon branching (Cohen-Cory and Fraser, 1995; Gallo and Letourneau, 1998; Szebenyi et al., 2001). FGF-2 can regulate cortical branching by inducing growth cone pausing and enlargement (Szebenyi et al., 2001). Although guidance molecules seem to regulate branch formation and growth cone extension, evidence suggests that these two events are independently regulated. *In vivo* and *in vitro* studies have shown that interstitial branches develop only after the primary axons have stopped growing (Bagri et al., 2003; Dent et al., 2004). Overall, these extracellular guidance cues influence cytoskeleton dynamics and organization in growth cones and axon shafts to promote or inhibit branching.

1.4.3 Intrinsic Regulation of Dendritic Branching

Apart from external molecules, branching can be regulated by intrinsic mechanisms. Although many studies focus on axon branching, dendrites are extensively branched in fruit flies (*Drosophila)* and vertebrates (Bodmer and Jan, 1987; Grueber et al., 2002; Masland, 2004). Many studies have found that transcriptional programs in specific neurons regulate dendritic morphology in flies and mammals (Moore et al., 2002; Aizawa et al., 2004; Hand et al., 2005; Kim et al., 2006b; Parrish et al., 2006; Gao, 2007; Corty et al., 2009). The differential expression of two transcription factors, Knot and Cut, define the dendritic arborization (da) sensory neurons (I-IV) in *Drosophila* (Grueber et al., 2003; Hattori et al., 2007; Jinushi-Nakao et al., 2007). Furthermore, the expression of the zinc finger TFs, Abrupt and Hamlet, represses dendritic branching in *Drosophila* in some neurons (Moore et al., 2002; Li et al., 2004; Sugimura et al., 2004). Similar to external cues, internal transcription factors influence cytoskeleton dynamics and reorganization by regulating of expression of cytoskeleton interacting proteins like spastin, a microtubule severing protein (Jinushi-Nakao et al., 2007; Yu et al., 2008). For example, Knot TF promotes branching by increasing the expression of spastin that fragments MTs which are able to invade and form new branches.

1.4 Nervous System and Genetic Screens in *C. elegans*

Extensive studies have determined that neuronal structure is largely defined by external factors and interactions between neurons and their neighboring cells. As previously described, environmental factors that are secreted by target tissues and cells regulate several aspects of neuronal structure including polarization, guidance and branching. Therefore it is critical to examine neuron morphology *in vivo* in the context of other cells that influence neuronal growth

and morphology. The nematode *C. elegans* is an excellent *in vivo* model to study nervous system development as worms possess a relatively simple nervous system that contains only 302 neurons (Wood, 1988). The *C. elegans* nervous system is diverse and is composed of sensory neurons, interneurons, and motor neurons that contribute to simple behaviors like feeding, locomotion, defecation, copulation, and egg-laying (White et al., 1986). Furthermore, the position and connectivity of each of these neurons has been completely determined and many of these individual neurons can be visualized *in vivo* and followed throughout development using neuron specific GFP reporter transgenes. Neuronal morphology is relatively simple since individual neurons typically extend unbranched axons and dendrites. The simple and structurally defined nervous system of *C. elegans* makes it ideal to study neuronal development *in vivo*.

To identify the genes and genetic pathways that function in nervous system development, geneticists have traditionally performed genetic screens (Jorgensen and Mango, 2002). In typical forward genetic screens, the genome is randomly mutagenized using a mutagen. The isolation of mutants with the desired phenotype leads to the identification and characterization of genes involved in the specific process of interest. Several factors make *C. elegans* an ideal organism to perform genetic screens including, easy manipulation and growth within the lab, short generation and life cycles, easy generation of mutants through chemical mutagenesis, *in vivo* imaging of neurons using fluorescent markers, and a sequenced genome to facilitate the identification of genes of interest (Jorgensen and Mango, 2002). Previously, genetic screens in *C. elegans* have been instrumental in identifying molecules and mechanisms involved in nervous system development (Zallen et al., 1999; Araujo and Tear, 2003; Mehta et al., 2004). For example, the guidance molecule Netrin-1, its corresponding receptors and downstream signaling components were elucidated in part through the analysis of mutants with locomotion defects and misguided

axons in *C. elegans* (Hedgecock et al., 1990). Similar to Netrins, other guidance molecules and their downstream effectors have been shown to have similar functions in invertebrates and vertebrates (Kaprielian et al., 2001; Araujo and Tear, 2003). In general, the identification of molecular mechanisms in *C. elegans* has advanced our understanding of neuronal outgrowth, guidance and branching in vertebrates.

1.5 VC4 and VC5, A Model System to Study Neuronal Morphology

The egg-laying organ, the vulva, is located on the ventral surface of hermaphrodite worms (Figure 1). The motor neuron circuit that regulates egg-laying behavior consists of six VC (VC1-VC6) and two HSN motor neurons (White et al., 1986). Both the HSN and VC-class of motor neurons form synapses with egg-laying vulval muscles to stimulate egg-laying and with each other to modulate their activity (Schafer, 2006). The VC-class of motor neurons can be divided into two classes based on their morphologies. The vulval distal neurons, VC1-3 and VC6, are oriented anteroposteriorly and send processes along the ventral nerve cord, whereas the vulval proximal neurons, VC4 and VC5 (VC4/5), are oriented left-right and send processes mediolaterally along the vulval epithelium. The VC4 and VC5 motor neurons are among the most branched in *C. elegans*.

Using the neuron specific GFP reporter transgene (*cat-1::gfp*), we are able to visualize the VC4 and VC5 and follow their development using fluorescence microscopy. VC4 and VC5 are born during the first larval stage (L1), extend axons ventrally during the third larval stage (L3), and finally branch dorsally during the fourth larval stage (L4) (Lints and Hall, 2008). Based on their stereotypical morphologies and the ability to follow their development *in vivo*, VC4 and VC5 are an excellent model to study neuronal morphology. In addition, the vulva is a

known source of branch inducing signals since HSN and VC neurons lack branches in vulva-less mutants (Li and Chalfie, 1990; Garriga et al., 1993). Thus, by studying neuronal development in VC4 and VC5, we have the opportunity to identify extrinsic signals and pathways that direct proper axon branching in *C. elegans*. Previously, genes that affect VC4 andVC5 axon branching were identified through genetic screens for VC axon branch morphology defects (Colavita and Tessier-Lavigne, 2003). For example, BAM-2, a neurexin-related transmembrane protein expressed in vulval cells was found to direct proper branch termination across the midline in VC4 and VC5 (Colavita and Tessier-Lavigne, 2003).

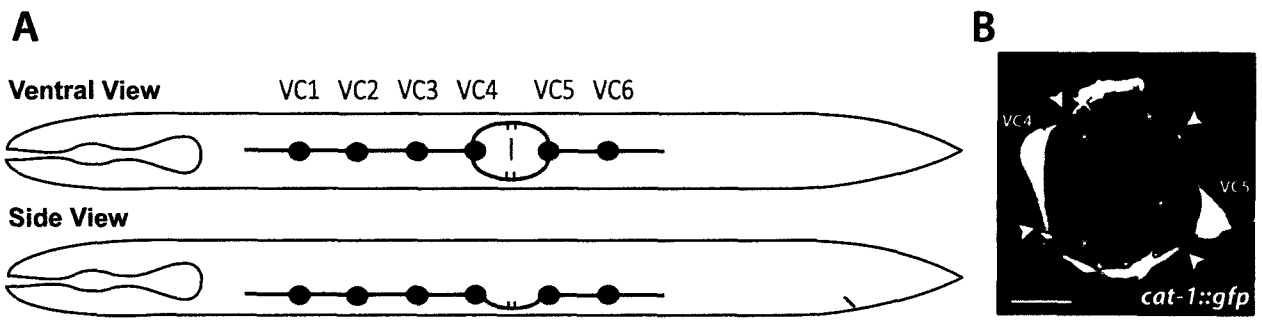

Figure 1. The VC motor neurons. (A) A schematic diagram of the C. *elegans* hermaphrodite showing the position of the six VC motor neurons and the vulva. The vulval distal neurons, VC1-3 and VC6, are oriented anteroposteriorly and send processes along the ventral nerve cord, whereas the vulval proximal neurons, VC4 and VC5 (VC4/5), are oriented left-right and send processes mediolaterally along the vulval epithelium. Anterior to the left. **(B)** Normal VC4/5 motor neuron morphology, ventral view, in a live wild type animal visualized using the neuron specific GFP reporter transgene *cyIs4[cat-1::gfp]*. VC4/5 axons and branches are indicated by arrowheads and asterisks respectively. Scale bar, 20μm

1.6 *png-1*/PNGase Pathway regulates Several Aspects of Neuronal Morphology

1.6.1 Neuron Morphological Defects in png-1 Mutants

From a genetic screen for VC axon branch morphology defects in *C. elegans*, *png-1* mutants were characterized with excessive branching phenotypes at the distal end of VC4 and VC5 axons (Habibi-Babadi et al., *in press*). These mutants also display branching defects in other neurons, such as DVB and AVL that extend axons near or adjacent to the vulva epithelium. In addition to branching defects, DVB axons in *png-1* mutants extend past their normal termination points. Behavioral assays in *png-1* mutants revealed egg-laying defects including a decrease in the number of eggs laid and a mild egg retention phenotype. The expression pattern of *png-1* is spatially broad as transcriptional activity was detected in many tissues including neurons, vulval epithelial cells, pharynx, intestine, body wall muscles, and gonads. Interestingly, *png-1* promoter activity was detected in vulval cells throughout early larval stages and into adulthood. Consistent with expression in vulval epithelial cells, cell specific rescue studies determined that *png-1* acts cell-non autonomously from vulval epithelial cells to regulate VC axon branching. These results suggest that *png-1* functions extrinsically to limit axon branching and axon growth.

1.6.2 Protein Structure of PNG-1

png-1 encodes a Peptide:N-glycanase (PNGase), a member of the transglutaminase (TGase) super family of enzymes that are highly conserved in eukaryotes (Suzuki, 2007). PNG-1 is a cytosolic enzyme that removes N-linked sugar moieties from glycoproteins or glycopeptides by cleaving the amide bond between the sugar glycan and the linker asparagine residue (Suzuki et al., 2002). The primary structure consists of a thioredoxin-like domain at the

N-terminal, a central PNGase domain which contains the catalytic triad (Cys-251, His-278, and Asp-295) required for enzymatic activity, and a conserved C-terminal domain predicted to be a mannose binding domain (Suzuki et al., 2002; Zhou et al., 2006) (Figure 2). *C. elegans* PNG-1 is unique among other PNGases since it contains a thioredoxin-like domain in the N-terminal region, whereas higher eukaryotes like flies and vertebrates contain a PUB/PUG (Peptide: N-glycanase/UBA or UBX-containing proteins) domain instead (Suzuki et al., 2001b). The PUB/PUG domain is important for protein-protein interactions, specifically with proteins in ubiquitin/proteasome protein degradation pathways (Park et al., 2001; Suzuki et al., 2001b). Despite these differences the core PNGase domain is highly conserved in all homologs from yeast to humans (Suzuki et al., 2002).

1.6.3 Biological Functions of PNGases

In vitro studies have revealed that worm PNGase has two enzymatic functions: an N-glycanase and a thioreductase (Kato et al., 2007; Suzuki et al., 2007). *In vivo*, the N-terminal thioredoxin domain and central PNGase domains are critical for regulating axon branching in *C. elegans*, although their exact function is currently unknown. The exact function of the thioredoxin domain of PNG-1 is not known although it may regulate PNGase activity as the catalytic site of PNGase contains redox sensitive residues (Suzuki et al., 1994; Suzuki et al., 1997; Suzuki et al., 1998). Alternatively, the reduction of disulphide bonds could unwind glycoproteins and prepare them for deglycosylation (Kato et al., 2007; Suzuki et al., 2007). Interestingly, PNGases are able to distinguish between native and denatured glycoproteins as they only act to remove N-glycans from denatured glycoproteins (Hirsch et al., 2004; Joshi et al., 2005; Kato et al., 2007). Structural-based studies suggest that this specificity is due to the active

site (catalytic triad) being located in a deep cleft that is spatially restrictive to folded but not denatured glycoproteins (Lee et al., 2005; Suzuki, 2007).

Prior to the *C. elegans* work showing a role in axon branching, PNGases were first implicated in the endoplasmic reticulum associated protein degradation (ERAD) quality control system that prevents the accumulation and aggregation of misfolded proteins (Park et al., 2001). ERAD is a cellular process that senses misfolded proteins, retrotranslocates them from the ER to the cytosol where they are ubiquitinated and subsequently degraded by the proteasome complex (Meusser et al., 2005). PNGase contributes to this process by removing bulky oligosaccharides from misfolded glycoproteins in order to facilitate degradation by the proteasome (Hirsch et al., 2003; Blom et al., 2004; Kim et al., 2006a). Yeast and mouse PNGases indirectly bind the proteasome via their interaction with RAD23 (Radiation sensitive)/mHR23, a DNA repair protein known to associate with the 26S proteasome and ubiquitin moieties (Park et al., 2001; Suzuki et al., 2001a; Biswas et al., 2004; Katiyar et al., 2004). Consistent with a role in ERAD, PNGase mutants in yeast display a decrease in the rate of degradation of misfolded protein (Suzuki et al., 2000); however, unlike *C. elegans*, no visible defects were detected. Interestingly, in *C. elegans*, *rad-23* mutants displayed ectopic branching and axon overextension defects similar to *png-1* mutants. Double mutant analysis showed that *png-1* and *rad-23* act in the same genetic pathway to limit axon growth and ectopic branching (Habibi-Babadi et al., 2010). Collectively, this data is consistent with PNG-1 and RAD-23 functioning in a proteolysis-dependent pathway to regulate axon outgrowth and branching; however, the molecular mechanism has not been elucidated.

Vertebrate PNGases physically interact with proteins involved in the ubiquitin-proteasome pathway via their N-terminal PUB domains (Katiyar et al., 2004; Li et al., 2005) .

These PNGase interacting proteins include a retrotranslocation protein (Derlin-1), an E3 ligase associated with the ER membrane (AMFR), an AAA ATPase (p97), and a cytosolic UBA/UBX containing protein with unknown function (Y33K) (Park et al., 2001; Katiyar et al., 2004; Li et al., 2005; Li et al., 2006). In mammalian cells, PNGase was found to be associated with the ER membrane and part of a multi-protein complex that processes misfolded proteins that are expelled from the ER to the cytosol for degradation (Katiyar et al., 2004; Katiyar et al., 2005; Li et al., 2005; Li et al., 2006). This large degradation complex links all the steps in ERAD including retrotranslocation through Derlin-1, ubiquitination by AMFR, deglycosylation by PNGase, and subsequent proteolysis by the proteasome.

1.7 *sensory axon guidance* (*sax*) Genes Regulate Morphology in Various Cells

1.7.1 Biological Functions of SAX-1 and SAX-2 Orthologs

In *C. elegans*, mutations in *sax-1* and *sax-2* genes resulted in cell shape defects and axon outgrowth defects in a subset of neurons (Zallen et al., 1999; Zallen et al., 2000; Gallegos and Bargmann, 2004). Several genetic studies have implicated orthologs of SAX-1 and SAX-2 in the development and maintenance of various cellular outgrowths like hypha, epidermal hairs, sensory bristles, and dendrites (Geng et al., 2000; Cong et al., 2001; Emoto et al., 2004; He et al., 2005a). In *Saccharomyces cereviase (S. cereviase)*, the NDR kinase Cbk-1 and scaffold protein Tao3 are required for appropriate apical growth, mating projection formation, cell separation and bud site selection in diploid cells (Bidlingmaier et al., 2001; Du and Novick, 2002). In the filamentous fungi, *Neurospora crassa (N.crassa)*, Cot-1/NDR kinase mutants display increased hyphal branching (Yarden et al., 1992; Seiler et al., 2006; Maerz et al., 2008). Mutations in *tricornered* (trc) and *furry* (fry), the fly homologs of *sax*-1 and *sax*-2 respectively, result in the branching and splitting of several cellular outgrowths like epidermal hairs, bristles, and antennas

(Geng et al., 2000; Cong et al., 2001; He et al., 2005a). In the nervous system, Trc and Fry regulate the dendritic tiling and branching of sensory neurons (Emoto et al., 2004). Combined, studies of NDR kinases in a variety of organisms have revealed roles in regulating mitosis, cell growth, cell shape, cell proliferation, apoptosis, neurite outgrowth, dendritic tiling and branching (Yarden et al., 1992; Zallen et al., 1999; Geng et al., 2000; Zallen et al., 2000; Bidlingmaier et al., 2001; Cong et al., 2001; Yang et al., 2001; Du and Novick, 2002; Nelson et al., 2003; Emoto et al., 2004; Gallegos and Bargmann, 2004; Emoto et al., 2006; Jia and Emmons, 2006). Although their physiological roles are well characterized, the targets and mechanism by which NDR kinases regulate cell morphology and other processes remain largely unknown.

1.7.2 Protein Structure of SAX-1 and SAX-2

The NDR (nuclear Dbf2-related) kinase family is a subgroup of the highly conserved serine/threonine AGC group of protein kinases that includes NDR1, NDR2, LATS1 (large tumour suppressor-1) and LATS2 in mammals, Trc (tricornered), and Lats/Warts in Drosophila, SAX-1and LATS in *C. elegans*, Dbf2, Dbf20, and Cbk1 in *S.cerevisiae*, Orb6, and Sid2 in *S. pombe and* Cot1 *in N. crassa* (Hergovich et al., 2006). NDR kinases are typically defined by an N-terminal regulatory (NTR) domain, a central kinase catalytic domain which is divided into 11 subdomains, a putative auto-inhibitory sequence (AIS) between subdomain VII and VIII, an activation segment (AS) that carries a regulatory phosphorylation site (Ser281 of human NDR1) and a hydrophobic motif (HM) located at the C-terminus which also carries a regulatory phosphorylation site (Thr444 of human NDR1) (Hanks and Hunter, 1995; Millward et al., 1995). *In vitro* studies have shown that human NDR kinase activity is controlled through multisite phosphorylation (Tamaskovic et al., 2003; Bichsel et al., 2004; Stegert et al., 2004; Stegert et al., 2005). In mammals, the phosphorylation of the threonine residue in the HM by upstream

STE20-like protein kinases is followed by the autophosphorylation of the serine residue in the AS (Mah et al., 2001; Stegert et al., 2005). The functional importance of these two regulatory sites was confirmed *in vivo* in yeast and *Drosophila* (Mah et al., 2001; Emoto et al., 2004; He et al., 2005a). For example, Trc/NDR kinase function in dendritic branching is regulated by phosphorylation of these key regulatory sites (Emoto et al., 2004). Genetic and biochemical studies indicate that another group of proteins called MOB (Mps-one binder) proteins also regulate NDR activity in yeast, flies and mammals (Luca et al., 2001; Bichsel et al., 2004; Devroe et al., 2004; He et al., 2005b; Hergovich et al., 2005; Mohl et al., 2009) . MOB binding to the conserved NTR domain is required for the activity and localization of NDR kinases in budding and fission yeast. MOB binding is postulated to release NDR kinases from auto inhibition caused by the putative AIS (Tamaskovic et al., 2003; Stegert et al., 2004).

sax-2 encodes a member of a conserved protein family that includes Tao3 and Nud1 in *S. cerevisiae*, Mor2 and Sid4 in *Schizosaccharomyces pombe (S. pombe)*, Sav (Salvador) and Fry in *Drosophila*, and hWW45, hFURRY1, and hFURRY2 in humans (Hergovich et al., 2006). SAX-2 and its orthologs are considered scaffolding proteins and contain HEAT/Armadillo repeats, which consist of α-helices with hydrophobic cores (Gallegos and Bargmann, 2004). In yeast, flies, and mammalian cells, SAX-2 orthologs have been shown to physically and genetically interact with NDR kinases (Du and Novick, 2002; Emoto et al., 2004; Chan et al., 2005; He et al., 2005a). The interaction between SAX-2 orthologs and NDR kinases is essential for NDR kinase activity and localization (Emoto et al., 2004; He et al., 2005a). Evidence suggests that SAX-2 and its orthologs function as scaffolding proteins that recruit and localize NDR kinases and facilitate their interaction with substrates (Chiba et al., 2009). In *C. elegans*, SAX-2 has

been shown to function in the same genetic pathway as SAX-1/NDR kinase to regulate neuronal morphology (Zallen et al., 2000; Gallegos and Bargmann, 2004).

1.7.3 Mechanisms of Action: NDR Kinases

In yeast and Drosophila, NDR kinases function as transcriptional regulators. In budding yeast, Cbk1 kinase activity regulates the activation and localization of Ace2, a transcription factor, by blocking its interaction with the nuclear export machinery (Colman-Lerner et al., 2001; Weiss et al., 2002; Mazanka et al., 2008) . Similar to Cbk1, Warts/Lats, a Drosophila NDR kinase, has been shown to phosphorylate and inactivate the transcription factor Yorkie (Yki) to control cell proliferation and cell death (Huang et al., 2005).

Many studies in yeast and animals have linked NDR kinases and Rho GTPases. In budding yeast, Cbk1/NDR kinase phosphorylates Sec2 (GEF); inturn Sec2 regulates the Rab GTPase exocytosis pathway which directs vesicle delivery and docking to the plasma membrane. Apart from regulating secretion, Cbk1 was found to affect Golgi dynamics through an unknown mechanism (Kurischko et al., 2008). In fission yeast, loss of Orb6/NDR kinase disrupted the restricted localization of Cdc42 GTPase resulting in its displacement from the cell tips to the cell sides thereby causing a loss of cell polarity (Das et al., 2009). In flies, Trc/NDR kinase negatively regulates Rac GTPase to control dendritic branching (Emoto et al., 2004). In general, NDR kinases have been shown to directly influence the activity and localization of Rho GTPases in a variety of organisms.

Recently, the first functions of human NDR1 kinase were reported in centrosome duplication and chromosome alignment on the metaphase plate (Hergovich et al., 2007; Chiba et al., 2009). Mammalian Fry/SAX-2 is hypothesized to act as a scaffolding protein that localizes

NDR1 and its co-activator onto mitotic MT spindles (Chiba et al., 2009). Fry is thought to directly or indirectly regulate MT dynamics by localizing and activating NDR1 kinase onto the microtubule spindle. Yeast SAX-2 homologs have also been shown to directly bind MTs (Gonzalez-Novo et al., 2009). Therefore, NDR kinases and their regulators may have a direct role in regulating the outgrowth of polarized structures by interacting with the microtubule cytoskeleton.

1.8 Summary & Rationale

png-1 mutants suggest that PNGases play a previously unknown role in neuronal development, primarily axon branching. However, the upstream and downstream components and the mechanism by which PNG-1 limits axon extension and branching are unknown. Recently, in a genetic modifier screen for enhancers or suppressors of *png-1* VC4/ VC5 axon branching defects, *sax-2* was identified as an enhancer mutation. Therefore *sax-2* and *sax-1* are candidate genes in the *png-1* genetic pathway. This study presents the phenotypic characterization of *png-1*, *sax-1*, and *sax-2* single and double mutants to determine their genetic interaction. Furthermore, a genetic screen was conducted to identify new components in the *png-1* pathway.

1.9 Objectives

Define the genetic relationship between *png-1*, *sax-1* and *sax-2* in regulating neuronal morphology and identify new genes in the *png-1* pathway.

1.10 Hypothesis

png-1 and *sax-1/sax-2* act in parallel pathways to regulate neuronal morphology in *C. elegans.*

2. Material and Methods

2.1 Strains

All *C. elegans* strains were maintained on nematode growth medium (NGM) agar plates at 20°C and manipulated using standard methods as described by Brenner (1974). The wild-type animals used in this study were of the Bristol variety, N2 strain. The following mutant strains were used in this study: LG1: *png-1(cy9)* (Habibi-Babadi et al., 2010); LGIII *sax-2(ot10)* (Altun-Gultekin et al., 2001); LGX: *sax-1(ky491)* (Zallen et al., 2000). To visualize and score neuroanatomy, we used green fluorescent protein (GFP) reporter transgenes to label specific neurons. These transgenes include: LGV: *cyIs4[cat-1::GFP + pRF4(rol-6gf)]* to label VC4 and VC5 and *otIs92[flp-10::GFP]* LGV to label DVB; Extrachromosomal array: *otEx1495[sul-1::GFP + pRF4(rol-6gf)]* to label the AVL motor neuron.

2.2 Construction of Transgenic Lines and Double Mutants

Neuron-specific GFP reporter lines were crossed into *png-1(cy9), sax-2(ot10)*, and *sax-1(ky491)* mutants using standard genetic methods (Brenner, 1974) to score for morphological defects in neurons. For example, the *sax-2(ot10); otIs92* strain was constructed by crossing *otIs92/+* heterozygous males with homozygous *sax-2(ot10)* hermaphrodites. From the F1 progeny, *sax-2(ot10)/+; otIs92/+* trans-heterozygotes were isolated (positive for GFP) and allowed to self-fertilize. Following self-fertilization, potential double homozygous *sax-2(ot10); otIs92* animals were isolated from F2 progeny and allowed to self-fertilize. Double homozygous animals were verified using polymerase chain reaction (PCR) and restriction fragment length polymorphism (RFLP) genotyping.

png-1(cy9) and *sax-2(ot10)* are both point mutations that alter restriction enzyme sites thereby generating a RFLP that can be used for genotyping purposes. The *png-1(cy9)* allele specific primers 5'CGATAATTTTACCGAATTTTCCAC and 5'TGTACCAATTTTTTGGAA TCCC were used to amplify a 250 bp fragment that was digested with MaeIII RE to detect wt (250 bp) and mutant (200 bp, 50 bp) DNA bands. *sax-2(ot10)* allele specific primers 5'TGCCTACATTCCTCCAAAGC and 5'CAAGGTGCTCCATCAACATC were used to generate a 692 bp fragment that was digested with Hyp188I RE to detect wt (405 bp, 186 bp, 70 bp, 31 bp) and mutant (475 bp, 186 bp, 31 bp) DNA bands. The *sax-1(ky491)* allele was followed by PCR that detects the presence of genomic deletion (866 bp). The PCR primers used for *ky491* are 5'TCAGGGATG AACGACTGTTC, 5'GAGCATACGCCATGTCAGAT, and 5' GTTCGCGCTGAAAGAG ACAT.

DNA template was obtained by lysing worms in lysis buffer (50 mM KCl, 10 mM Tris-HCl pH8.3, 2.5 mM MgCl2, 0.45% NP-40, 0.45% Tween-20, 0.01% gelatin, and 50 μg/mL proteinase K) at 65°C 1 hour and 95°C for 30 min. Crude lysate was used as PCR template in the PCR reaction (10X PCR buffer (10X: 100 mM Tris-HCL pH 8.3, 500 mM KCl, 20 mM $MgCl_2$), 2 mM dNTP, PCR primers (10 μM), Taq DNA polymerase (5 units/μL), and dH2O) using allele-specific primers as previously stated. The *png-1* and *sax-1* PCR products were amplified using the following cycling conditions: 95°C, 2min followed by 30 cycles of (94°C, 30s; 60°C, 30s; 72°C, 40s), and 72°C, 5min. The *sax-2* PCR product was amplified using the following cycling conditions: 95°C, 2min followed by 7 cycles of (95°C, 30s; 64°C -1°C/cycle, 30s; 72°C, 1:20 min), 28 cycles of (94°C, 30s; 57°C, 30s; 72°C, 1:20 min), and 72°C, 5 min. After amplification, PCR products were digested with appropriate enzyme as mentioned and incubated at least 3hrs at

the appropriate temperature. Digested PCR fragments were loaded and resolved on 2.5% agarose gel.

Double mutants were generated by crossing single mutants using standard genetic techniques (Brenner, 1974). For example, *sax-2* double mutants were constructed by crossing *sax-2 (ot10)/+* heterozygous males with homozygous mutant (*mut*) hermaphrodites to generate *sax-2(ot10)/+; mut/+* transheterozygote. The F1 trans-heterozygotes were then allowed to self-fertilize to generate homozygous *sax-2(ot10); mut* animals in the F2/F3 generation. Double homozygous mutants were verified using PCR-RFLP genotyping as described above.

2.3 Phenotypic Analysis of Neuron Morphology

VC4 and VC5 neurons extend two axons that circumnavigate the vulva and extend dorsally-directed branches on either side of the vulval opening. VC4 and VC5 axons typically contain approximately 3-5 branches each on the left and right sides of the vulva. VC4 and VC5 motor neurons were scored for various morphological defects including branching, axon outgrowth, and branch termination defects. Since VC4 and VC5 axons fasciculate, individual branches could not be unambiguously identified and therefore were pooled for scoring purposes. Worms were scored as having VC branching defects if they displayed an increase in branch number and/or branch length. To simplify quantification, branching defects were binned into mild, moderate, or severe categories. Animals were scored as mild, moderate, or severe if they displayed 1-3, 4-20, or greater than 20 extra branches respectively. Axon outgrowth defects were scored if either VC cell body displayed at least one ectopic process emanating at any point on the cell body. Worms were scored as having branch termination defects if at least one branch was shown to overshoot its normal termination point and cross the vulval midline.

DVB is a GABAergic motor neuron that innervates enteric muscles involved in defection. The DVB motor neuron cell body is located in the tail and extends an axon ventrally along the ventral cord and then anteriorly towards the head, terminating just posterior to the vulva. A termination defect was scored as any DVB process that extended either too far anteriorly or dorsally past the vulva. The AVL cell body is located in the head and extends an unbranched axon posteriorly towards the tail. DVB and AVL branching defects were scored if animals displayed ectopic branches, defined as a distinct axonal protrusion at least 3-5μm in length (approximately one neuronal cell body diameter). For DVB neurons, ectopic branches found on the vulva epithelium were categorized as "vulval branching" while branching outside the vulval epithelium was categorized as "non-vulval branching". .

To score morphological defects, young adult worms grown at 20°C were mounted on a 2% agarose pads in M9 buffer solution. Transgenic worms containing GFP reporter arrays were scored under 40X and 63X objectives using epifluorescence on a Zeiss Axioplan2 microscope. Confocal images were acquired using a Zeiss LSM510 Meta Confocal Microscope. Statistical analysis was performed using Student's two-tailed t-test and Z-tests as stated.

2.4 DVB Measurements

Overextension defects were scored if the DVB axon terminated either anteriorly or dorsally past the vulva. To rule out the possibility that the DVB overextension defect is due to an anterior displacement of the DVB cell body or a decrease in body length or a combination of several of these factors, we measured body length, DVB cell body position, and DVB axon length in young adult wt and mutant animals. Worm cultures were synchronized by allowing several gravid hermaphrodites to lay eggs for one hour. After the adult worm was removed, the

remaining eggs were incubated for 3 days at 20°C until they reached the young adult stage. The worms were mounted on 2% agarose pads and immobilized in M9 buffer containing 10 mM levamisole. The entire animal was photographed using 20X objective using the Zeiss LSM510 Meta Confocal Microscope. Images of animals were analyzed and measured using LSM510 Meta software. Body length was measured along the ventral length of the animal from the tip of the head to the tip of the tail. DVB cell body position was measured relative to the position of the vulva. DVB axon length was measured by tracing the entire length of the axon from the point it emerged from the cell body.

2.5 Isolation of *sax-1* Enhancer Mutations

Homozygous *sax-1(ky241); cyIs4* worms were mutagenized with 50 mM ethylmethanesulfonate (EMS) for 4 hrs at room temperature. The parental generation (Po) of mutagenized worms was then allowed to recover and produce self-progeny (F1 generation). On average, 10 F1 worms were picked and transferred to individual worm plates to produce the F2 progeny. After two to three days of growth at 20°C, approximately 100 F2 worms from each F1 plate (~200 plates) were randomly picked and mounted on slides. F2 worms were visually screened for enhanced VC4/5 branching defects using epifluorescence on a Zeiss Axioplan2 microscope. Putative *sax-1* enhancer mutants that displayed an increase in axon branches similar to the *png-1; sax-1* double mutants were recovered from the slide and transferred to a new plate and allowed to self-propagate. The self-progeny were then re-examined to confirm *sax-1* enhancement. Mutant strains were backcrossed once to the N2 wild-type strain to remove the *sax-1* mutant background and once to *cyIs4* to replace the mutagenized *cyIs4* transgene.

2.6 Complementation Tests

Complementation tests were performed using standard methods (Brenner, 1974). Complementation tests are a genetic tool used to assign mutations to genetic loci. Firstly, *sax-1* enhancers (*sens*) mutations were tested for complementation against the *cy9* allele of *png-1*, a known enhancer of the *sax-1* axon phenotype. 17 independent complementation tests were conducted by crossing heterozygous *sens* males with homozygous *png-1(cy9)* hermaphrodites. The F_1 cross progeny (trans-heterozygous) were examined for axon branching phenotype. If all the hermaphrodites in the cross progeny displayed a wild-type branching phenotype, then the mutations complemented each other (ie. the mutations are located within different genes). In contrast, if the cross progeny displayed an axon branching phenotype, then the mutations failed to complement (ie. the mutations are located within the same gene). The remaining 10 *sens* mutants were tested for complementation against each other through pair-wise combinations. *sens* mutants were placed into a complementation group based on failure to complement each other for VC branching defects.

2.7 Genetic Mapping

For mapping *sens* mutations to chromosomes, a single nucleotide polymorphism (SNP) based method was used as previously described (Wicks et al., 2001). SNPs are DNA polymorphisms distributed throughout the genome that act as genetic markers between two wild-type isolates of *C. elegans*: Bristol (England) (N2) and Hawaiian (CB4856). Briefly, the idea behind linkage mapping is to link SNPs to the particular mutation of interest since mutations and SNPs that lie in close proximity to one another will rarely be separated by a recombination event during meiosis. As a result, SNP linkage to a mutation will result in a high ratio of Bristol SNP

to Hawaiian SNP alleles if the mutation is carried on a Bristol background (Fay and Bender, 2006). Bristol and Hawaiian SNPs that alter restriction sites are referred to as snip-SNPs (RFLPs) and can be detected and distinguished based on their distinct restriction digestion patterns.

For mapping synthetic mutations like *sens* mutations, we first constructed a Hawaiian strain that harbors *sax-1* (N2 background). We mated *sax-1(ky491)* animals with the Hawaiian strain and assayed their F2/F3 progeny for the presence of *sax-1* and Hawaiian SNP markers. The line that carried Hawaiian markers along the entire length of chromosomes except chromosome VI (*sax-1* location) was selected and named *sax-1 Hw*. Initially, Hawaiian males were crossed with s*ax-1Hw* hermaphrodites, the resulting male progeny were mated with *sens; sax-1(ky491) cyIs4* hermaphrodites (N2 background) to produce F1 heterozygous animals. The F1 cross progeny was allowed to self-fertilize to regenerate *sens*; *sax-1(ky491) cyIs4* double homozygous animals. F2 *sens*; *sax-1(ky491) cyIs4* recombinants were then isolated based on their enhanced axon branching defects, cloned onto individual plates, and tested for linkage to SNPs across chromosomes I-IV (Appendix 1). Worms from each recombinant plate were lysed in 10 µL lysis buffer at 65°C 1hour and 95°C for 30 min. 1 µL of the crude lysate was used as PCR template in the PCR reaction (1µL 10X PCR buffer, 1µL 2 mM dNTP, 1µL of each PCR primer (10 µM), 0.2µL DNA polymerase (5 units/µL), and 4.8 1µL dH2O) using SNP-specific primers that flank SNP regions as listed in Table 2. All PCR products were amplified using the following cycling conditions: 95°C, 2 min followed by 30 cycles of (94°C, 30s; 60°C, 30s; 72°C, 40s), and 72°C, 5 min. After amplification, PCR products were digested with appropriate enzyme as indicated in Table 1 in a final volume of 20uL (10uL PCR product, 7.5uL H_2O, 2uL 10X buffer, 0.5uL enzyme) and incubated at least 3 hrs at the appropriate temperature. Digested PCR

fragments were loaded and resolved on 2.5% agarose gel. SNP linkage to *sens* (N2 background) mutation was deduced based on the proportion of N2 DNA bands compared to Hw DNA bands.

3. Results

3.1 Neuronal Morphology Phenotypes in *png-1*, *sax-1*, and *sax-2* Mutants

3.1.1 VC4/VC5 Axon Branching Defects

A previous genetic screen for enhancers of the *png-1* VC4/5 axon branch overgrowth phenotype identified an allele of *sax-2* as an enhancer mutant (N. Habibi-Babadi and A. Colavita, unpublished). *sax-2* encodes a scaffolding protein that has been shown to interact with NDR kinases and facilitate their activity (Emoto et al., 2004; He et al., 2005a). *sax-2* and *sax-1* (encoding a NDR kinase) have been shown to function in the same genetic pathway in a variety of species to regulate cell morphology (Bidlingmaier et al., 2001; Cong et al., 2001; Du and Novick, 2002; Emoto et al., 2004). To further characterize the role of *sax-1* and *sax-2* genes in neuronal morphology, we examined several neurons including VC4/5, DVB, and AVL in single and double mutants with *png-1* (Figure 2). All of the mutant alleles used for this study were predicted to strongly compromise protein function based on their molecular lesions (Figure 3). *sax-1 (ky491)* is a candidate null allele as the 1.3kb deletion results in an early frame shift that truncates the protein and eliminates essential kinase domains (Zallen et al., 2000). *png-1 (cy9)* is also a candidate null allele that introduces a stop within the PNGase domain; thereby abolishing PNGase activity (Habibi-Babadi et al., 2010). *sax-2(ot10)* is a loss-of-function allele that truncates the protein prematurely yet may retain some function since the HEAT repeat motif is intact (Gallegos and Bargmann, 2004).

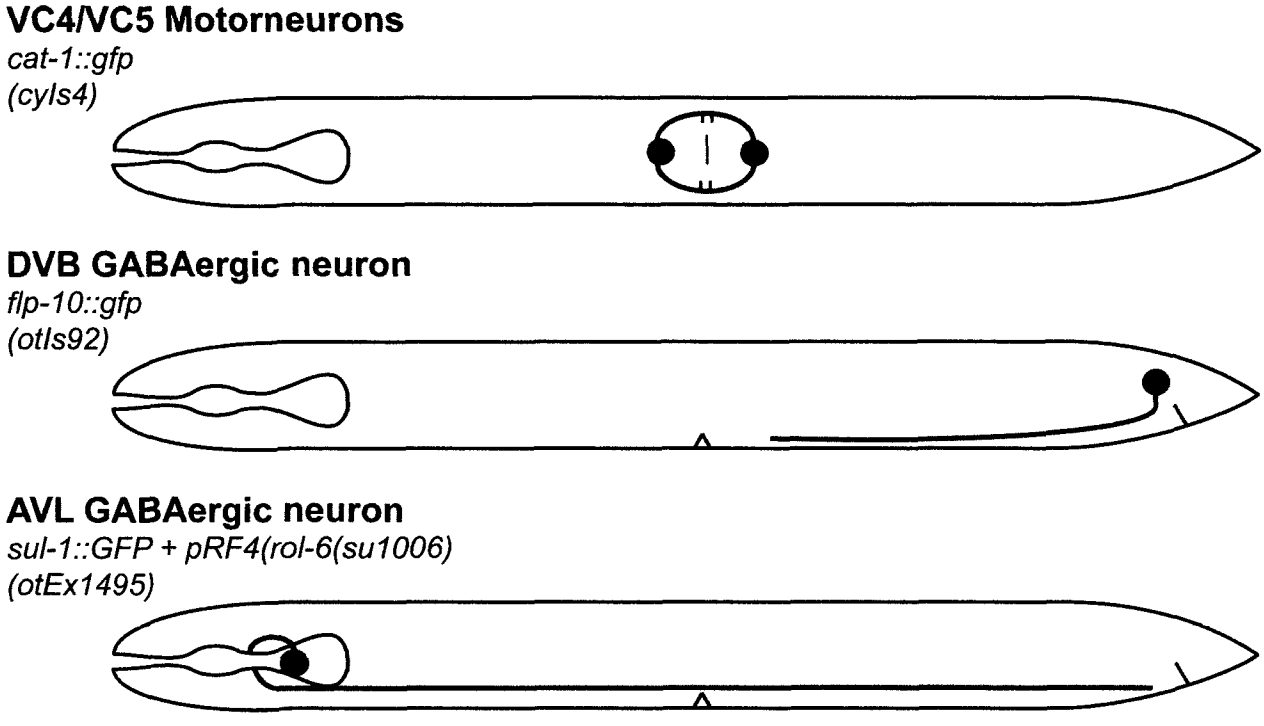

Figure 2. Schematic of neurons examined for morphological defects. VC4 and VC5 motor neurons are visualized using the *cyIs4[cat-1::gfp]* reporter gene. VC4/5 extend two axons to form a circular tract around the vulva and branch dorsally on each side of the vulval opening. The DVB motor neuron in adult hermaphrodites is visualized with a *otIs92[flp-10::gfp]* reporter gene. The DVB cell body is located in the tail and extends one axon ventrally and then anteriorly towards the head, terminating posterior to the vulva. AVL motor neuron is visualized using the *otEx1495[sul-1*::gfp*]* reporter gene. The AVL cell body that is located in the head extends a long axon posteriorly towards the tail.

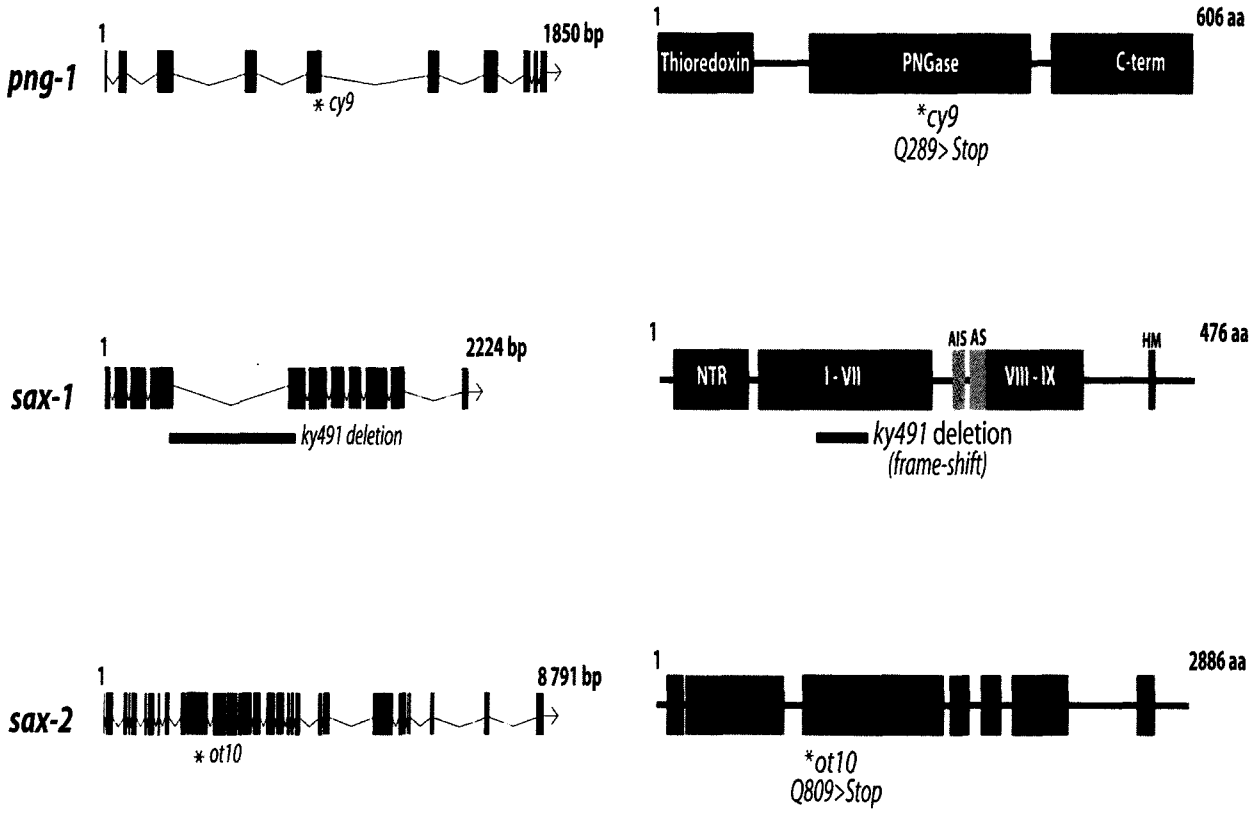

Figure 3. Genomic and protein organization of *png-1*, *sax-1*, and *sax-2*. **(A)** *png-1* encodes a PNGase with an N-terminal thioredoxin domain, a central PNGase domain, and a C-terminal mannose binding domain. **(B)** *sax-1* encodes an NDR kinase with an N-terminal regulatory (NTR) domain, a central kinase catalytic domain (subdomains I-IX), a putative auto-inhibitory sequence (AIS), an activation segment (AS), and a hydrophobic motif (HM) located at the C-terminus. AS and HM carry regulatory phosphorylation sites. **(C)** *sax-2* encodes a large scaffolding protein with mostly unknown domains except for the HEAT/Armadillo repeats at the N-terminal. Genomic structure is shown on the left. Solid black boxes represent exons. The location of point mutations and deletions are indicated by asterisks or lines respectively. Protein structure is shown on the right. Protein domains are depicted as colored boxes.

To determine if *sax-1* and *sax-2* single mutants display *png-1*-like VC4/5 branching defects, we used the VC4/5 specific *cyIs4[cat-1p::gfp]* reporter line to visualize VC4/5 in these mutants. In wild type (wt) worms, VC4/5 axons extend to form a circular tract around the vulva and project dorsally-directed branches on the left and right sides of the vulva. In wt young adults, VC4/5 axons typically contain 3-5 branches that fasciculate with each other. The natural overlap of VC4/5 axons and branches complicates phenotypic characterization as an unambiguous count of branch number or length could not be made. Branching defects in *sax-1* and *sax-2* mutants were found to be highly variable and characterized by an increase in branch number and branch length. To simplify quantification, branching defects were binned into mild, moderate, and severe categories (Figure 4). VC4/5 defects were assigned to mild, moderate, and severe categories if VC4 or VC5 displayed 1-3, ≥4-20, or >20 supernumerary or longer branches respectively. According to these criteria, 9% of wt animals displayed some branching defects (6% 'mild'; 3% 'moderate', n=176) (Figure 5A and 5H). In contrast, 91% of VC4/5 axons displayed branching defects in *png-1(cy9)* mutant animals (24% 'mild'; 66% 'moderate'; 1% 'severe', n=176) (Figure 5B and FH). The penetrance of branching defects in *sax-1* and *sax-2* were significantly lower compared to *png-1* ($P<0.01$; t-test). In *sax-1(ky491)* mutants, 60% exhibited branching defects (36% 'mild'; 24% 'moderate', n=187) while 45% of *sax-2(ot10)* mutants displayed branching defects (29% 'mild'; 16% 'moderate', n=180) (Figure 5C,5D, and 5H). Qualitatively, branching defects in *sax-1*and *sax-2* were milder than *png-1* mutants. In summary, the phenotypic penetrance and severity of axon branching defects was lower in *sax-1* and *sax-2* mutants when compared with *png-1* animals.

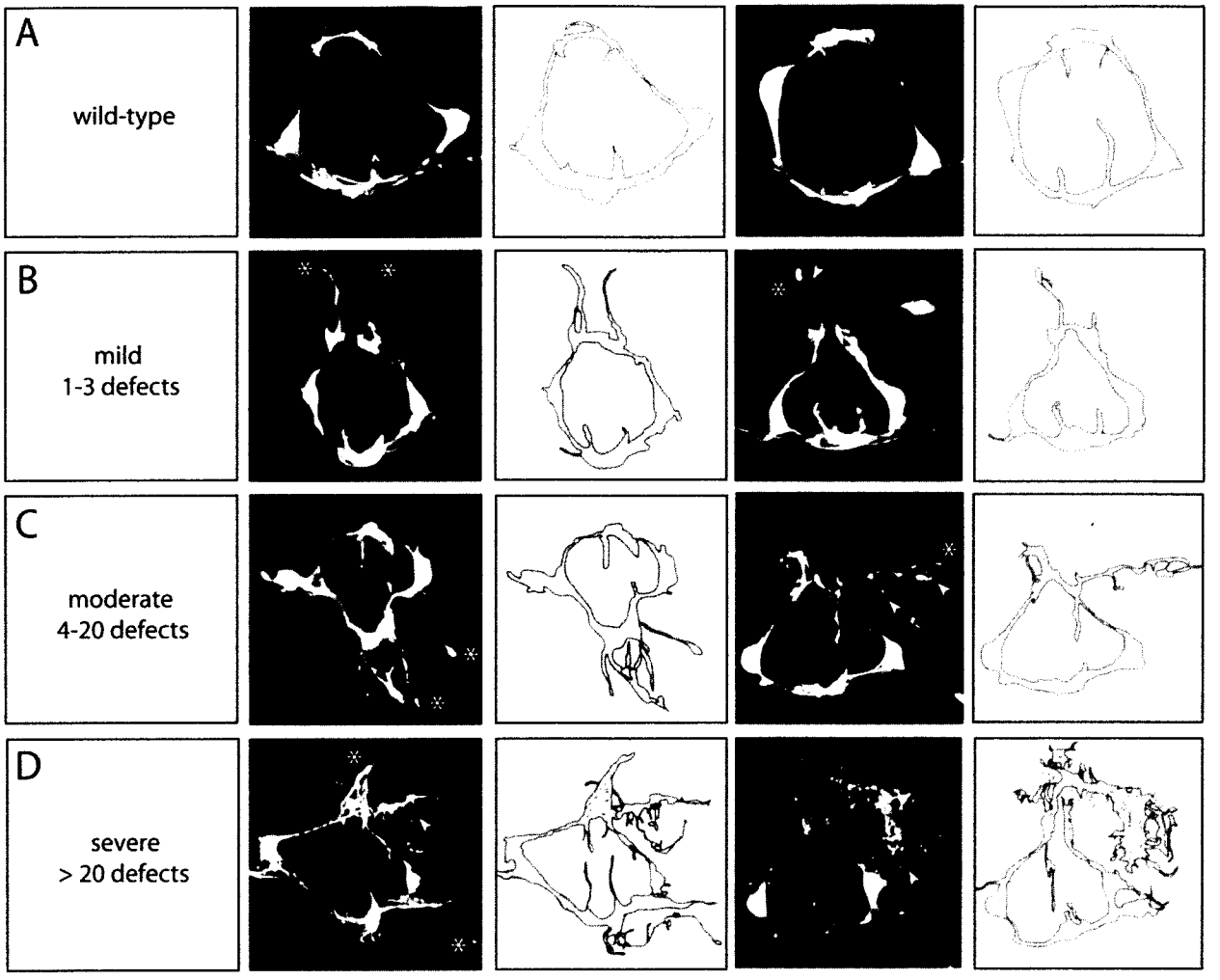

Figure 4. Phenotypic classification of VC4 and VC5 axon branching defects. Ventral view of VC motor neurons visualized using the *cyIs4[cat-1::gfp]* reporter transgene. Fluorescence micrographs and diagrams of wild-type and mutant axon morphologies are shown. (**A**) Wild type VC4/5 axons typically contain 3-5 branches on the left and right sides of the vulva. (**B**) Mild, (**C**) moderate, and (**D**) severe phenotypes are defined as animals displaying ≤3, 4-20, or >20 excess or longer branches on either the left or right sides of the vulva respectively. Examples of branch length (asterisk) and branch number (arrowhead) defects are shown.

Figure 5. VC4/VC5 axon branching defects in *png-1*, *sax-1*, and *sax-2* single and double mutants. Compared to wild type (**A**), *png-1, sax-1,* and *sax-2* single and double mutants display an increase in branch number and branch length (**B-G**). (**B-D**) Moderate branching defects are found in *png-1*, *sax-1*, and *sax-2* single mutants. (**E**) Branching defects in *sax-2; sax-1* double mutants are indistinguishable from *sax-1* and *sax-2* single mutants. (**F-G**) Branching defects in *png-1; sax-1* and *png-1; sax-2* double mutants are more severe compared to single mutants. (**A-G**) Arrowheads mark VC branching defects. Neurons were visualized with the *cyIs4[cat-1::gfp]* transgene. All images, ventral views with anterior to the left. Scale bars, 10μm. (**H**) The percentage of young adult animals with mild (≤3), moderate (≥4-20), and severe (>20) branching defects for single and double mutants. The enhancement of branching defects in *png-1; sax-1* and *png-1; sax-2* double mutants is highly significant when compared with either single mutant alone (***P<0.0001, t-tests). Error bars represent SEM of three independent counts with an n=50-60 for each set.

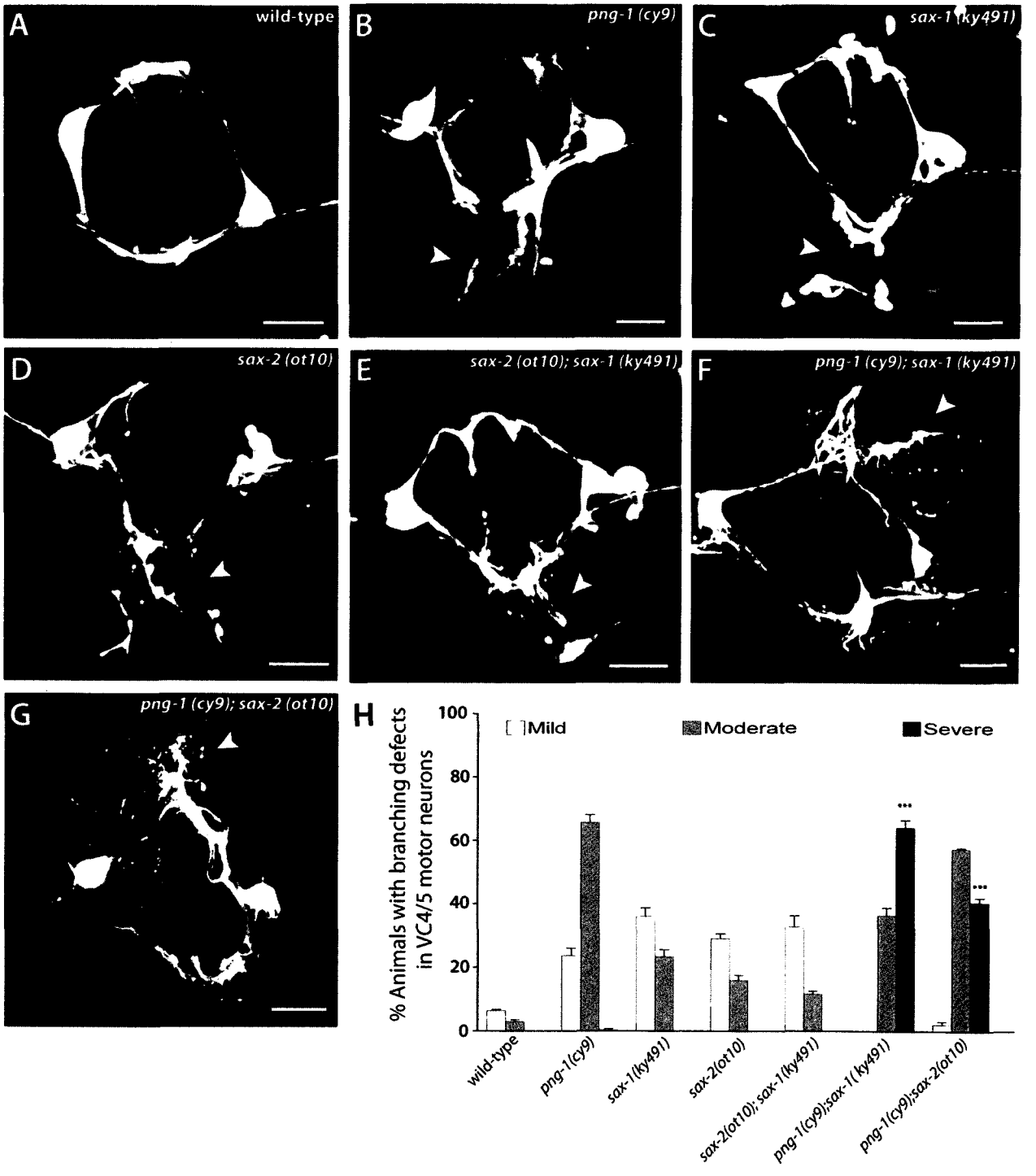
A
wild-type
B
png-1 (cy9)
C
sax-1 (ky491)
D
sax-2 (ot10)
E
sax-2 (ot10); sax-1 (ky491)
F
png-1 (cy9); sax-1 (ky491)
G
png-1 (cy9); sax-2 (ot10)
H
% Animals with branching defects in VC4/5 motor neurons
100
80
60
40
20
0
Mild
Moderate
Severe
***
***
wild-type
png-1(cy9)
sax-1(ky491)
sax-2(ot10)
sax-2(ot10); sax-1(ky491)
png-1(cy9);sax-1(ky491)
png-1(cy9);sax-2(ot10)

Double mutant analysis is a test used to determine whether two genes function in the same pathway or in parallel pathways to regulate a biological process of interest (Huang and Sternberg, 2006). If two genes function in the same pathway, a combined deficiency would result in defects similar to the single mutants because both genes are essential to the process. If two genes function in parallel pathways, a combined deficiency would result in enhanced (synthetic) defects relative to single mutants because each gene functions independently of one another to regulate a process. These genes may act redundantly with respect to one another or they may have independent functions that affect a biological process redundantly. By analyzing the double mutant phenotypes for *png-1*, *sax-1*, and *sax-2* mutants we can gain insight into the functional relationship between these genes.

To determine whether these genes are act in the same pathway or parallel pathways to limit axon branching in the VC4/5 motor neurons, we generated double mutants and examined neuronal phenotypes in VC4/5 motor neurons. In both *png-1; sax-1* and *png-1; sax-2* double mutants, 100% (n=180) of animals displayed branching defects (Figure 5H). In addition, a strong synergistic phenotype was observed in these double mutants (Figure 5F and 5G). 62% of *png-1; sax-1* animals displayed 'severe' branching defects compared to 1% (n=176) and 0% (n=180) in *png-1*and *sax-1* single mutants, respectively (Figure 5H). Similarly, 42% of *png-1; sax-2* animals displayed 'severe' branching defects compared to 1% and 0% in *png-1* and *sax-2* single mutants respectively (Figure 5H). In both cases, double mutants with *png-1* displayed significant enhancement of severe branching defects in VC4/5 compared to the single mutants ($P<0.0001$, t-test). This finding suggests that *png-1* and *sax-1/sax-2* may act in parallel pathways to inhibit VC4/5 branching as the *png-1; sax-1/2* double mutants displayed more severe phenotype than either single mutant.

In contrast, *sax-1* and *sax-2* homologs in flies are known to act in the same genetic pathway to inhibit dendritic branching (Emoto et al., 2004). To determine whether *sax-1* and *sax-2* are working in the same pathway to control branching in VC4/5, the double mutant was generated and characterized. In *sax-2; sax-1*double mutants, 45% of animals displayed branching defects (33% "mild"; 12% "moderate", n=180) compared to 60% and 45% of *sax-1* and *sax-2* single mutants respectively (Figure 5E and 5H). The penetrance of branching defects in *sax-1* and *sax-2* were not significantly different when compared with the *sax-2; sax-1* double mutant; therefore, *sax-2* and *sax-1* function in the same pathway to inhibit VC axon branching.

3.1.2 VC4/VC5 Ectopic Neurite Outgrowth and Branch Termination Defects

In addition to an axon branch overgrowth defect, VC4/5 neurons also displayed other morphological defects. VC4 and VC5 normally send out two processes that extend laterally along the vulval epithelium to form a circular tract around the vulva. In *png-1* mutants, in addition to the two normal axons, VC4/5 display ectopic neurites that extend from multiple sites on the cell body and are variable in length. The penetrance of ectopic neurites in *png-1* and *sax-2* animals, 18% (n=175) and 23% (n=180), were significantly different from wt animals (9%, n=177) ($P<0.05$; t-test) (Figure 6A, 6C and 6G). Qualitatively, we found that the majority of *png-1* and *sax-2 single* mutants display one ectopic neurite (Figure 7C). We observed no difference in ectopic neurite formation in *sax-1* mutants (9%, n=187) compared to wt (Figure 6G). Previously, in a set of sensory neuron cell bodies, *sax-1* and *sax-2* mutants were shown to function in the same pathway to prevent ectopic neurites from sprouting in older animals (Zallen et al., 2000). As expected the ectopic neurite defects in *sax-2; sax-1*double mutants were not significantly different from single mutants, suggesting that these genes act in the same genetic pathway to limit neurite outgrowth in VC neurons (Figure 6G).

Figure 6. Ectopic VC4/VC5 neurite outgrowth defects in *png-1*, *sax-1*, *sax-2* single and double mutants. (**A-F**) In addition to the two axons that normally encircle the vulva, ectopic neurites sprout from the cell bodies of VC4/5 neurons in *png-1*, *sax-1*, and *sax-2* single and double mutants. Arrows point to ectopic neurites. Neurons were visualized with the *cyIs4[cat-1::gfp]* transgene. All images, ventral views with anterior to the left. Scale bars, 10μm. (**G**) Neurite outgrowth defects are significantly more severe in *png-1; sax-1* and *png-1; sax-2* double mutants compared to single mutants (**P<0.01, t-tests). Ectopic neurites were scored if either VC cell body displayed at least one ectopic process. Error bars represent SEM of three independent counts with an n=50-60 for each set.

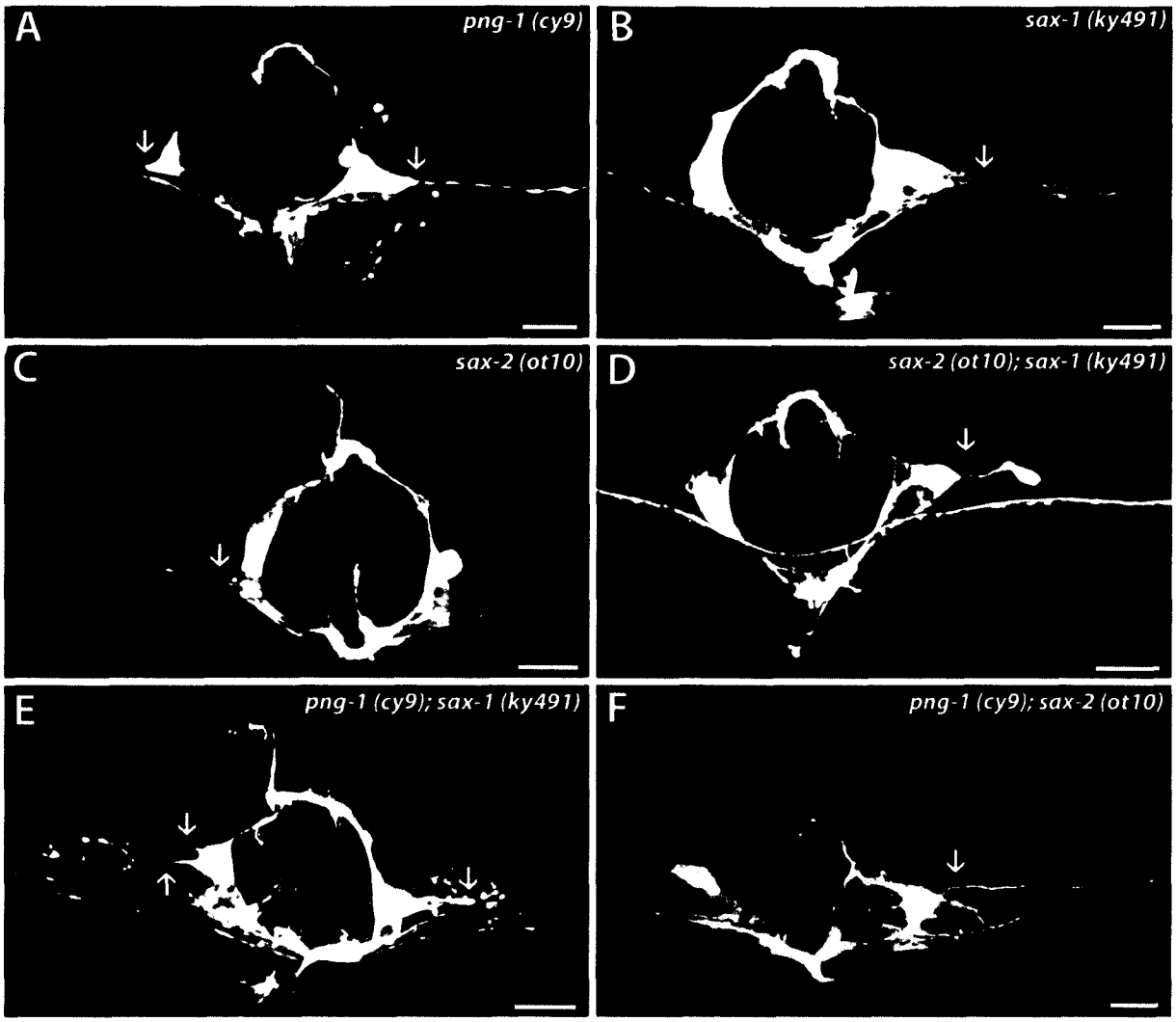
A
png-1 (cy9)
B
sax-1 (ky491)
C
sax-2 (ot10)
D
sax-2 (ot10); sax-1 (ky491)
E
png-1 (cy9); sax-1 (ky491)
F
png-1 (cy9); sax-2 (ot10)

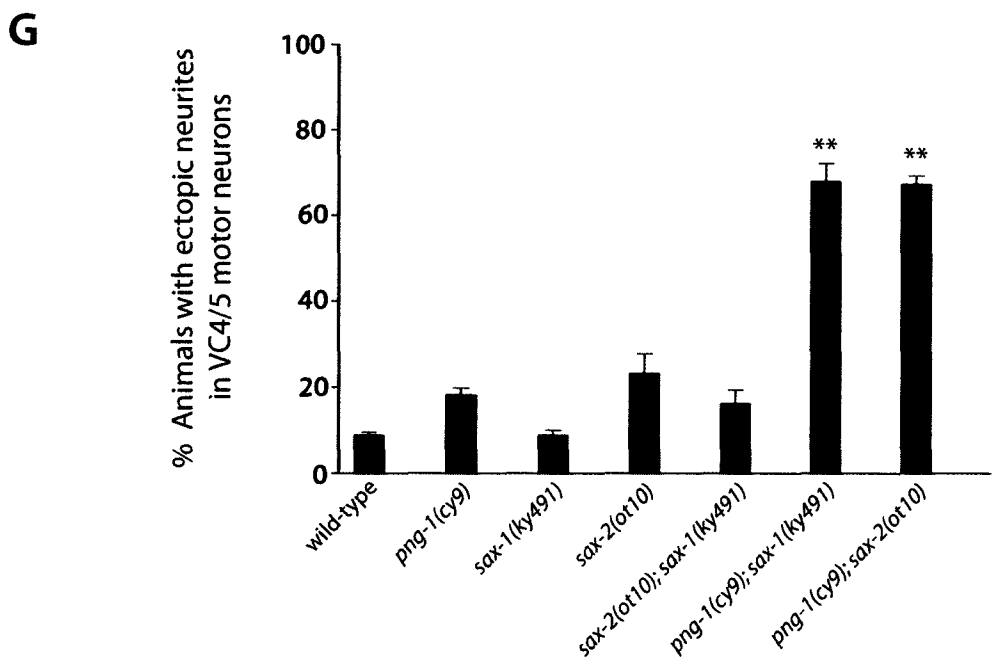
G
% Animals with ectopic neurites in VC4/5 motor neurons
100
80
60
40
20
0
**
**
wild-type
png-1(cy9)
sax-1(ky491)
sax-2(ot10)
sax-2(ot10); sax-1(ky491)
png-1(cy9); sax-1(ky491)
png-1(cy9); sax-2(ot10)

Figure 7. Quantification of ectopic VC4/VC5 neurites in *png-1, sax-1, sax-2* single and double mutants. *png-1; sax-1* (**A**) and *png-1; sax-2* (**B**) double mutants display ectopic neurites of various lengths from VC cell bodies. Normal VC4/5 axons are indicated by arrowheads and ectopic neurites are indicated by asterisks. Images on the right are high magnifications of the boxed region in the left panels. Neurons were visualized with the *cyIs4[cat-1::gfp]* transgene. All images, ventral views with anterior to the left. Scale bars, 10μm. (**C**) Quantification of VC4 and VC5 cells in single and double mutants with 1 neurite, 2 neurites, and ≥3 neurites. *png-1; sax* double mutants display significantly more ectopic neurites when compared with either single mutant (*P<0.05, t-tests). Error bars represent SEM of three independent counts with an n=50-60 for each set.

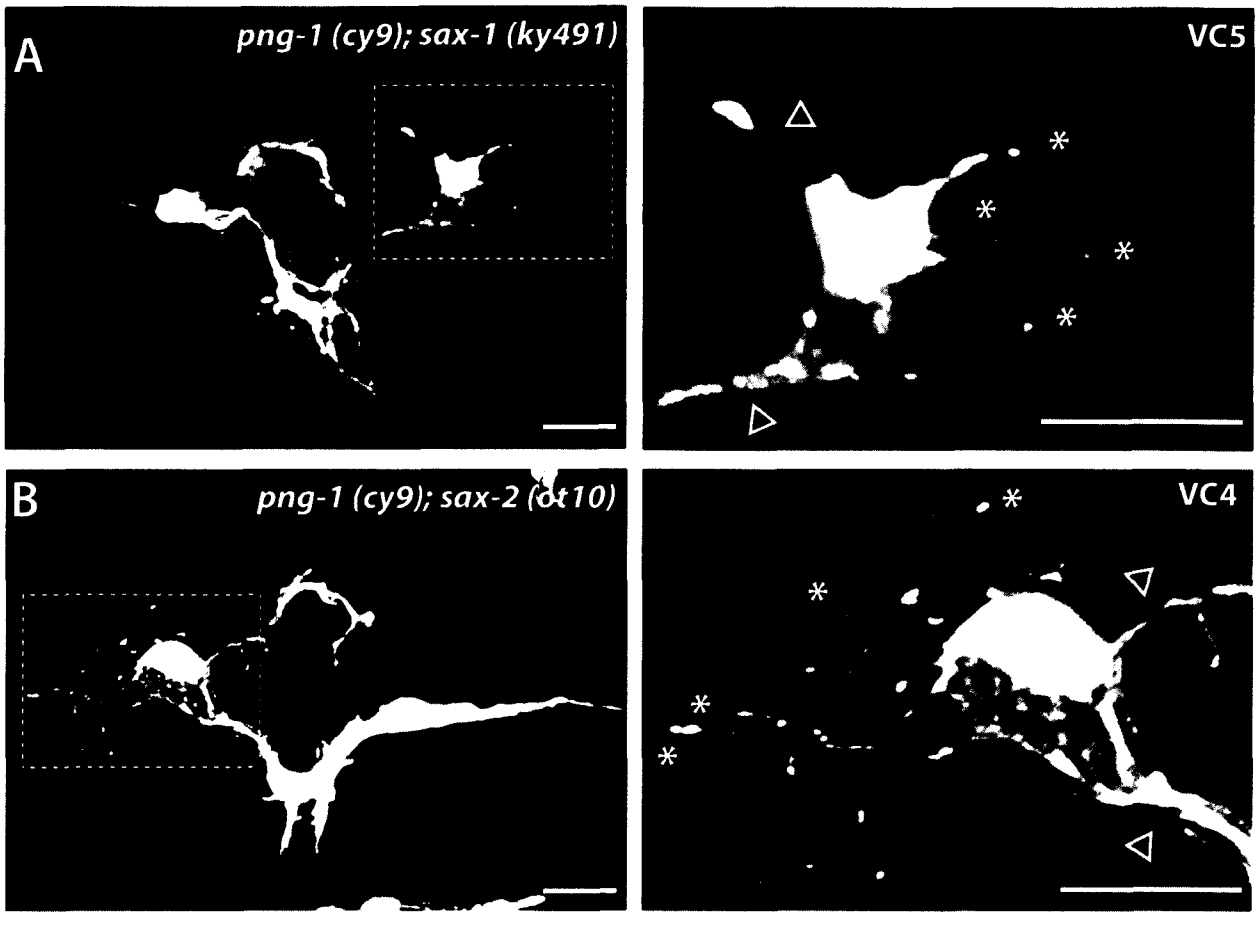
A
png-1 (cy9); sax-1 (ky491)
VC5
B
png-1 (cy9); sax-2 (ot10)
VC4

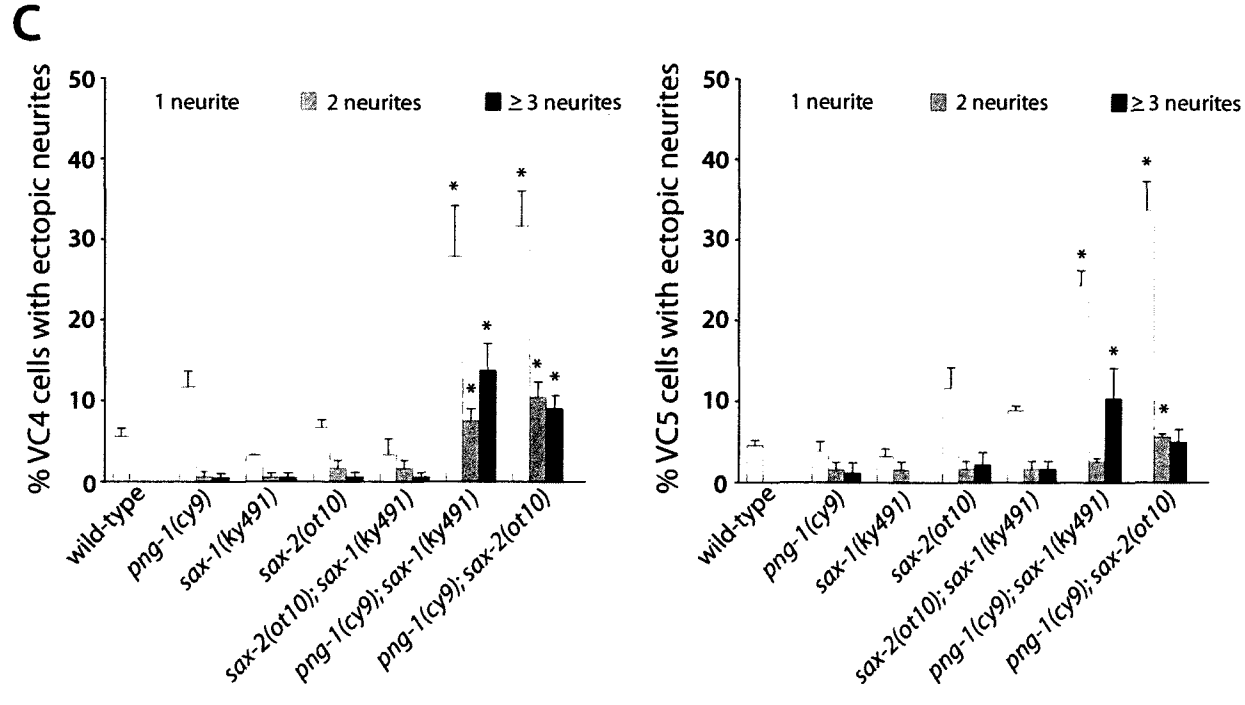
C
% VC4 cells with ectopic neurites
% VC5 cells with ectopic neurites
1 neurite
2 neurites
≥ 3 neurites
0
10
20
30
40
50
wild-type
png-1(cy9)
sax-1(ky491)
sax-2(ot10)
sax-2(ot10); sax-1(ky491)
png-1(cy9); sax-1(ky491)
png-1(cy9); sax-2(ot10)

In contrast, *sax-1* and *sax-2* double mutant analysis with *png-1* revealed severe neurite outgrowth defects. 66% (n=180) of *png-1; sax-1* and 68% (n=164) of *png-1; sax-2* animals extend ectopic neurites (Figure 6E-G). The enhancement of ectopic neurite formation in these double mutants is highly significant relative to single mutants ($P<0.01$; t-test). A significant percentage of VC4/5 neurons in *png-1*; *sax* animals were characterized as having two or more ectopic neurites compared with *png-1*, *sax-1* and *sax-2* single mutants ($P<0.05$; t-test) (Figure 7A-C). 21% of VC4 and 13% of VC5 neurons displayed two or more neurites in *png-1; sax-1;* whereas, 19% of VC4 and 10% of VC5 neurons displayed two or more neurites in *png-1; sax-2* (Figure 7C). The strong synergistic phenotypes seen in *png-1; sax-1* and *png-1; sax-2* double mutants suggest that *png-1* and *sax-1/sax-2* function in separate pathways to limit ectopic neurite outgrowth.

Further characterization of neuronal phenotypes revealed an axon branch termination defect that was previously described in *bam-2* mutants where VC axon branches were shown to overshoot their termination point and cross the midline of the vulva (Colavita and Tessier-Lavigne, 2003). *bam-2* was shown to encode a neurexin-related cell-surface protein that acts as an external branch terminating cue for VC branches. The overlap of VC4/5 branches precluded the ability to distinguish individual branches; therefore branch termination defects were scored if at least one branch or two branches crossed the midline. In *png-1*, *sax-1*, and *sax-2* mutants, 23% (n=176), 18% (n=188) and 15% (n=180) of animals displayed significant branch termination defects compared with wt animals (3%, n=176) where at least one VC axon branch passed its termination point and extended past the midline ($P<0.01$; t-test) (Figure 8A-C and 8G). In *sax-2; sax-1* double mutant the branch termination defects (25%, n=180) were no more severe than those in the single mutants (Figure 8D and 8G). In contrast, the penetrance of at least two

Figure 8. VC4/VC5 branch termination defects in *png*-1, *sax-1*, and *sax-2* single and double mutants. **(A-F)** In *png-1*, *sax-1*, and *sax-2* single and double mutants, VC branches extend past their termination point and cross the midline of the vulva. Overextended branches are indicated by asterisks. Arrowhead in (C) marks an axon branch that has terminated at a normal location. Neurons were visualized with the *cyIs4[cat-1::gfp]* transgene. All images, ventral views with anterior to the left. Scale bars, 10μm. **(G)** Quantification of branch termination defects in single and double mutants. Axon branch termination defects were scored if at least one or two branches crossed the midline. *png-1; sax-1* and *png-1; sax-2* double mutants display significantly more VC branches extending beyond their normal termination points compared to single mutants (*$P<0.05$, t-tests). Error bars represent SEM of three independent counts with an n=50-60 for each set.

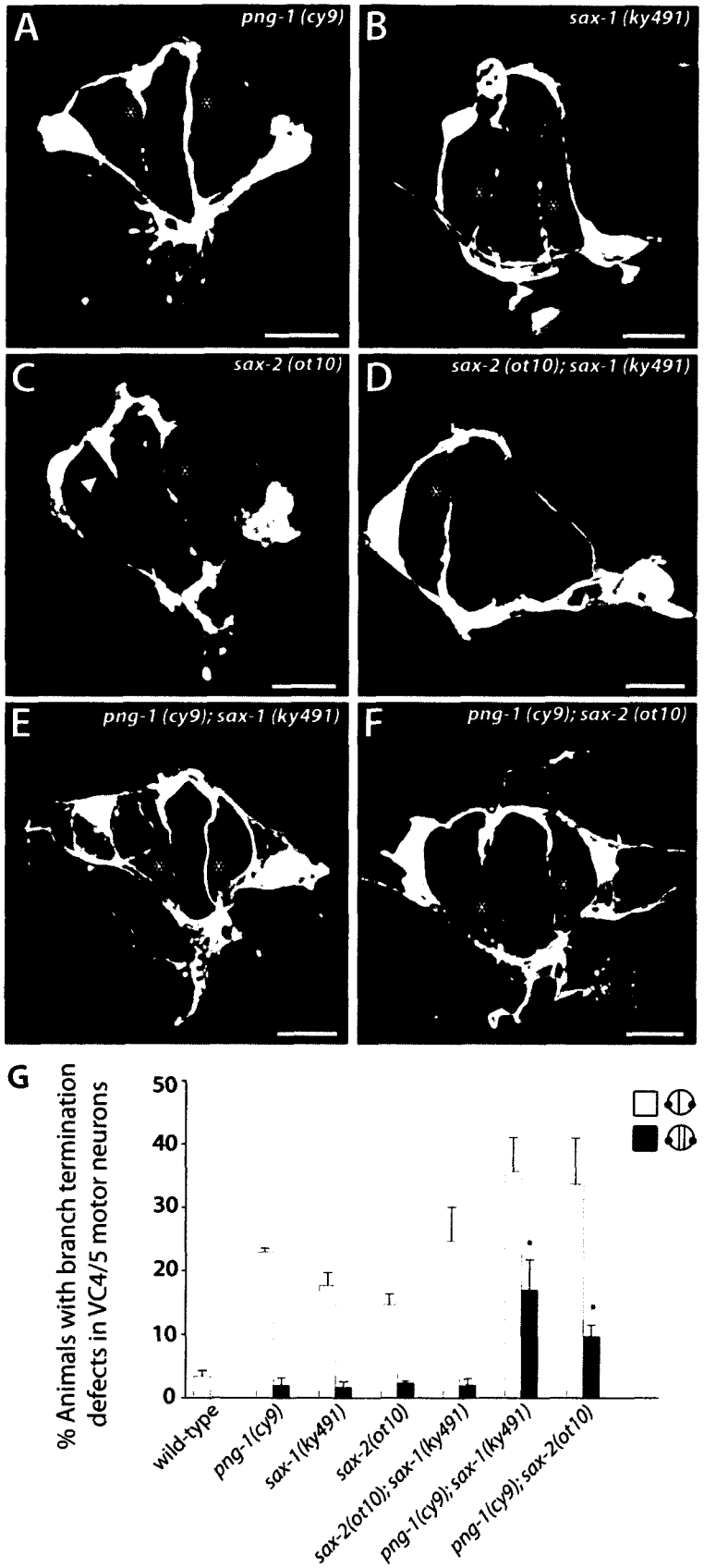
A
png-1 (cy9)
B
sax-1 (ky491)
C
sax-2 (ot10)
D
sax-2 (ot10); sax-1 (ky491)
E
png-1 (cy9); sax-1 (ky491)
F
png-1 (cy9); sax-2 (ot10)
G
% Animals with branch termination defects in VC4/5 motor neurons
50
40
30
20
10
0
wild-type
png-1(cy9)
sax-1(ky491)
sax-2(ot10)
sax-2(ot10); sax-1(ky491)
png-1(cy9); sax-1(ky491)
png-1(cy9); sax-2(ot10)

VC branches overextending past the midline was enhanced in *png-1; sax-1* and *png-1; sax-2* double mutants relative to single mutants ($P<0.05$; t-test). 17% (n=175) and 10% (n=166) of at least two VC branches overextended past the midline compared to 2% (n=176-188) in *png-1*, *sax-1*, and *sax-2* single mutants (Figure 8E-G). These results suggest that *png-1* works in a parallel pathway with a *sax-1/sax-2* pathway to control branch termination.

We have shown that VC4/5 motor neurons display significantly enhanced morphological defects in the *png-1; sax-1* and *png-1; sax-2* double mutant combinations compared with single mutants. Both the severity and penetrance of defects increased in these double mutants (Figure 9A-C). The synergy observed between *png*-1 and *sax-1/sax-2* mutants is consistent with these genes acting in parallel pathways to control or maintain neuronal morphology by restricting neurite/branch growth.

3.1.3 DVB Axon Overextension and Branching Defects

DVB is a GABAergic motor neuron that innervates enteric muscles involved in defection. The DVB cell body, located in the tail, extends an anteriorly-directed axon along the ventral nerve cord terminating just posterior to the vulva (Figure 10A). DVB in *png-1* mutants display overextension and branching defects (Habibi-Babadi et al., 2010). In *png-1* mutants, 28% (n=156) of DVB neurons displayed an overextension defect where axons either grew past the vulva or dorsally along the vulval epithelium compared to 0% in wt (n=180) (Figure 10B-C; Table 1). *png-1* mutants also display ectopic branches at the distal end of the DVB axon, located either directly adjacent to the vulva (8%, n=156) or near the vulva (3%, n=156) (Figure 11C-D; Table 1). Branching adjacent to the vulva was categorized as "vulval branching" while branching near the vulva was categorized as "non-vulval branching".

Figure 9. Neuronal morphology in *png-1; sax-1* and *png-1; sax-2* double mutants. Overall, *png-1; sax-1* (**A**) and *png-1; sax-2* (**B**) double mutants exhibit far *more* severe morphological defects compared to single mutants. VC morphology defects include excessive branching (arrowheads), ectopic neurites (arrows), and overextended branches (asterisks). Neurons were visualized with the *cyIs4[cat-1::gfp]* transgene. All images, ventral views with anterior to the left. Scale bars, 10μm. (**C**) Quantification of VC morphological defects in single and double mutants. *png-1* and *sax* double mutants displayed significantly more morphological defects than either single mutant (*$P<0.05$, t-tests). Error bars represent SEM of three independent counts with an n=50-60 for each set.

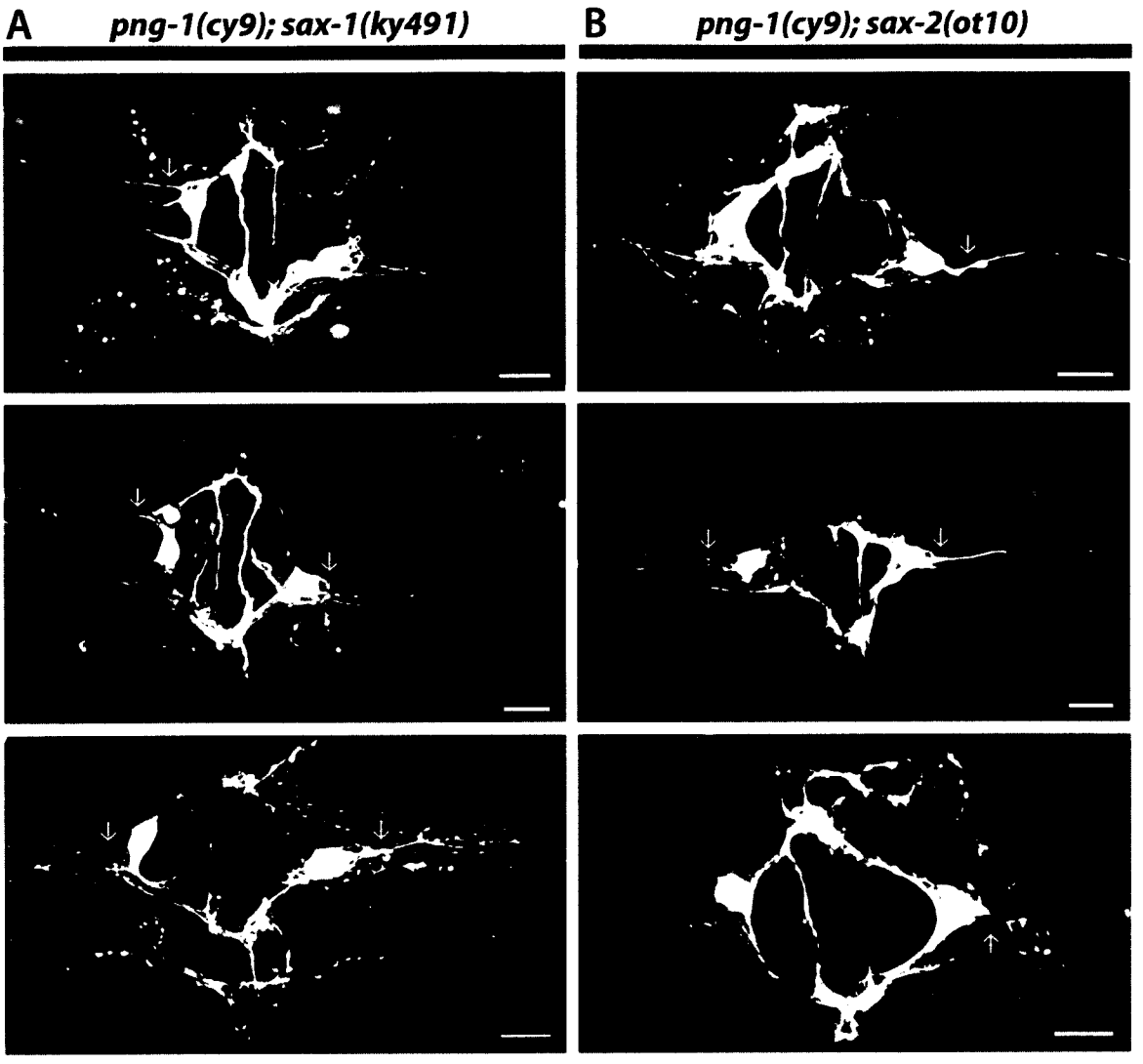
A
png-1(cy9); sax-1(ky491)
B
png-1(cy9); sax-2(ot10)

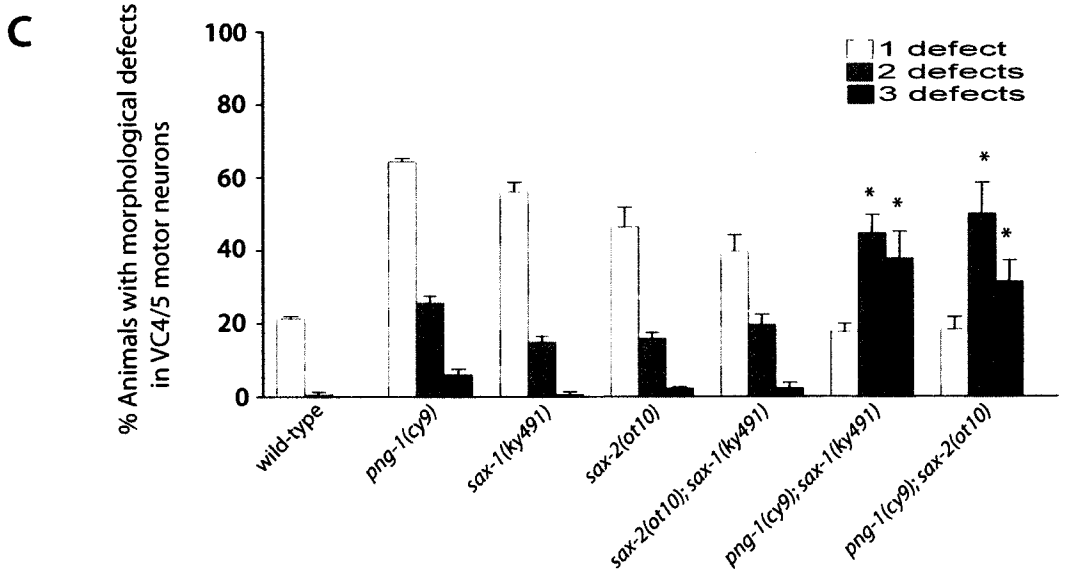
C
% Animals with morphological defects in VC4/5 motor neurons
100
80
60
40
20
0
1 defect
2 defects
3 defects
*
*
*
*
wild-type
png-1(cy9)
sax-1(ky491)
sax-2(ot10)
sax-2(ot10); sax-1(ky491)
png-1(cy9); sax-1(ky491)
png-1(cy9); sax-2(ot10)

Figure 10. DVB axon overextension defects in *png-1*, *sax-1*, and *sax-2* single and double mutants. (**A**) Schematic diagram of the DVB motor neuron in wild-type hermaphrodites. (**B-F**) (**B**) In wild-type animals, the DVB cell body in the tail extends an axon anteriorly towards the head, terminating posterior to the vulva. (**C-F**) In *png-1* single and *png-1; sax* double mutants, the DVB axon overextends past its termination point and grows past the vulva, either dorsally (**C, E-F**) or anteriorly (**D**). DVB neuron visualized with the *otIs92[flp-10::gfp]* transgene. Left images are magnifications of the boxed regions indicated in the right panels. The vulva is indicated by an asterisk. All images, anterior is to the left and dorsal at top. Scale bars, 20 μm.

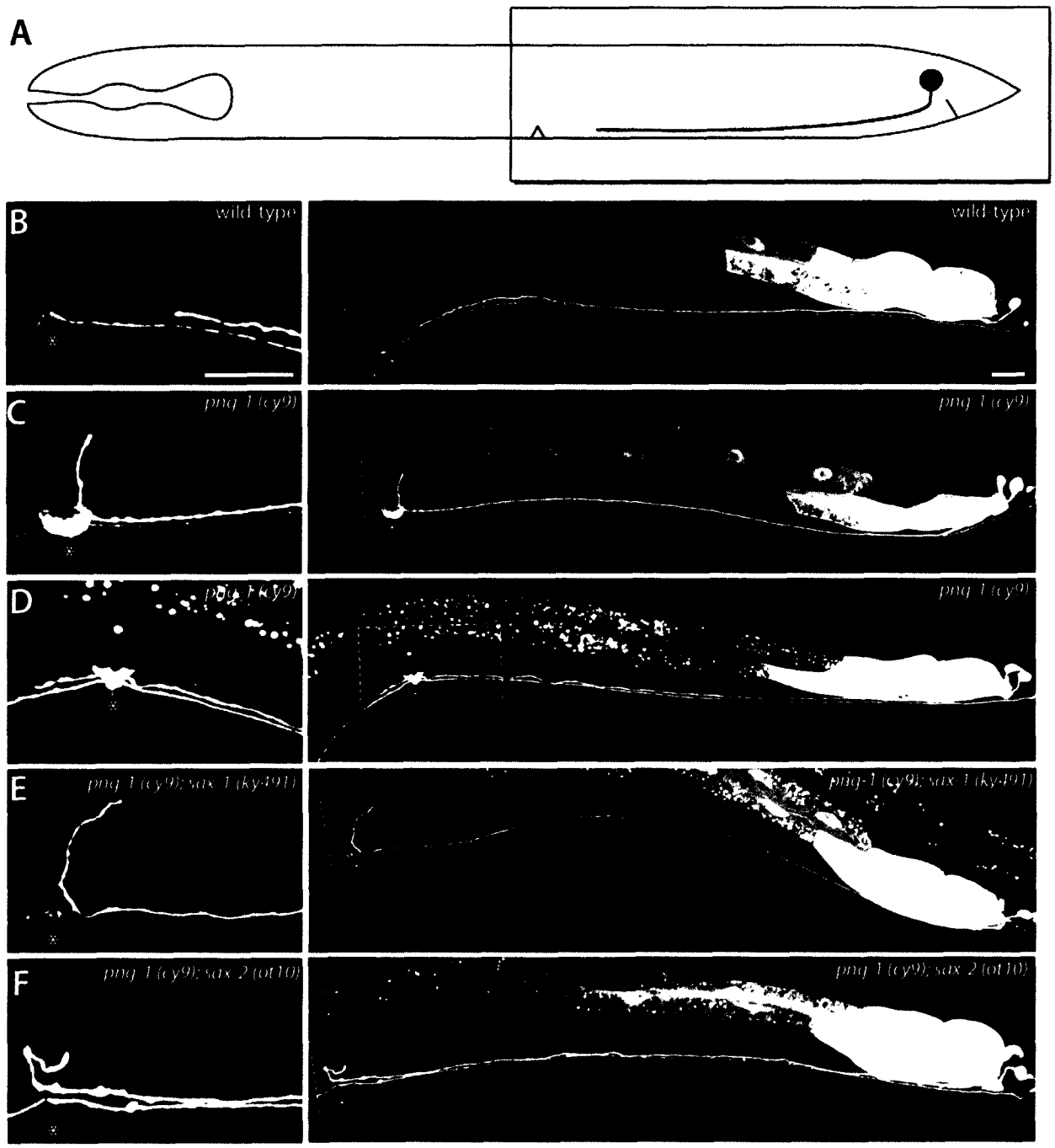
A
B
wild type
wild type
C
pnq-1(cy9)
pnq-1(cy9)
D
pnq-1(cy9)
pnq-1(cy9)
E
pnq-1(cy9); sax-1(ky491)
pnq-1(cy9); sax-1(ky491)
F
pnq-1(cy9); sax-2(ot10)
pnq-1(cy9); sax-2(ot10)

Table 1. DVB morphology defects in *png-1*, *sax-1*, and *sax-2* single and double mutants

Strain	Wild-type 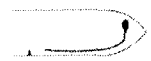	Overextension 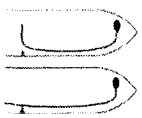	Vulval Branching 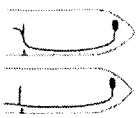	Non-Vulval Branching 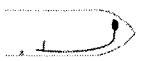	N
wild-type	100 ± 0	0 ± 0	0 ± 0	0 ± 0	180
Single mutants					
png-1(cy9)	69 ± 2	27 ± 3	8 ± 1	3 ± 1	156
sax-1 (ky491)	100 ± 0	0 ± 0	0 ± 0	0 ± 0	180
sax-2 (ot10)	97 ± 3	1 ± 1	0 ± 0	3 ± 1	174
Double mutants					
sax-2(ot10); sax-1(ky491)	93 ± 4	3 ± 1	0 ± 0	5 ± 0	180
png-1(cy9); sax-1(ky491)	11 ± 4	88 ± 6**	31 ± 5*	1 ± 1	156
png-1(cy9); sax-2(ot10)	8 ± 4	91 ± 2***	53 ± 1***	2 ± 0	168

*Young animals were scored for axon overgrowth and axon branching defects using the *otIs92[flp-10::gfp]* transgene. Axon overgrowth defects were scored if the DVB axon failed to terminate and extend past the vulva, either dorsally or anteriorly. Axon branching defects were scored if at least one ectopic branch was observed at the distal tip of the axon, either adjacent to the vulva or near the vulva. Schematic drawings show the posterior end of the animal with the vulva represented by a triangle. Animals with more than one defect were scored in multiple categories; therefore percentages do not always add up to 100%.

*Values represent the mean ± SEM of three independent counts with an n=50-60 for each set. N= total number of animals scored. Asterisks represent significant differences between single and double mutants (*P<0.05, **P<0.01, ***P<0.0001; t-test).

Figure 11. DVB axon branching defects in *png-1*, *sax-1*, and *sax-2* single and double mutants. (**A**) Schematic diagram of the DVB motor neuron in wild-type hermaphrodites. (**B**) In wild-type animals, an unbranched DVB axon terminates posterior to the vulva. (**C-D**) In *png-1* mutants, DVB axons exhibit ectopic branches at the distal tip, either directly adjacent to the vulva (**C**) or near the vulva (**D**). (**E, G**) *sax-2* and *sax-2; sax-1* mutants exhibit short branches near the vulva, while *sax-1* animals do not (**F**). (**H-K**) *png-1; sax* double mutants exhibit severely overextended DVB axons with ectopic branches in the vulval region. The vulva is indicated by an asterisk and ectopic branches are indicated by arrowheads. All images in **B-K** correspond to the boxed region in **A**. DVB neuron visualized with the *otIs92[flp-10::gfp]* transgene. All images, anterior is to the left and dorsal at top. Scale bars, 20 μm.

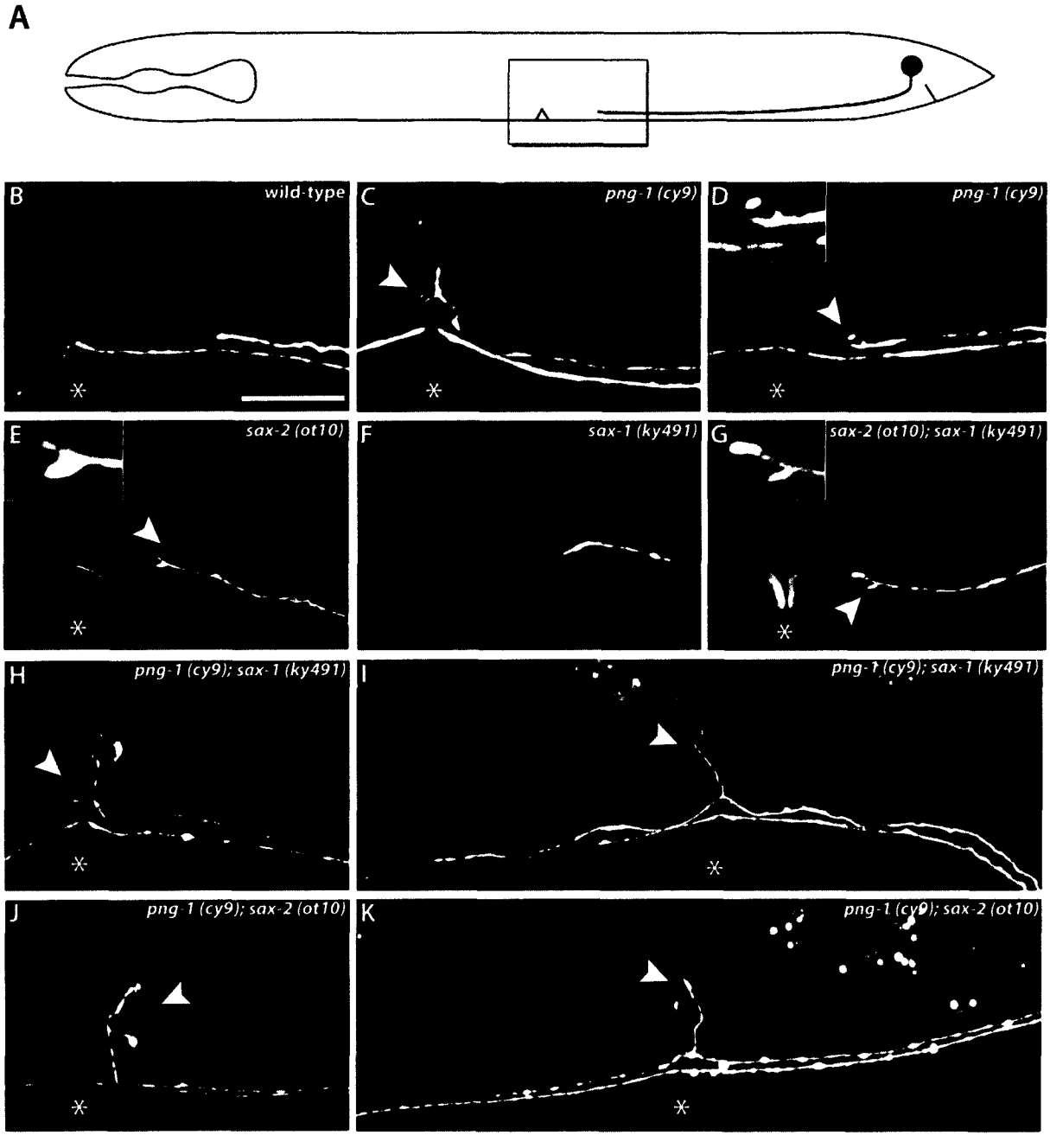
A
B wild-type
C png-1 (cy9)
D png-1 (cy9)
E sax-2 (ot10)
F sax-1 (ky491)
G sax-2 (ot10); sax-1 (ky491)
H png-1 (cy9); sax-1 (ky491)
I png-1 (cy9); sax-1 (ky491)
J png-1 (cy9); sax-2 (ot10)
K png-1 (cy9); sax-2 (ot10)

To determine whether *sax-1* and *sax-2* mutants had similar neuronal defects, DVB axon tracts were visualized in young adult worms using an *otIs92[flp-10p::gfp]* reporter line. We found that neither *sax-1* nor *sax-2* displayed significant DVB overextension and branching defects (Table 1). An examination of *sax-2; sax-1* double mutants, revealed a small non vulval branching defect (5%, n=180) that was not significantly different than single mutants (Figure 11G; Table 1).

To determine if *png-1* and *sax-1/sax-2* interact genetically in DVB neurons, I made and examined double mutants. In *png-1; sax-1* and *png-1; sax-2* doubles, 88% (n=156) and 91% (n=168) of DVB axons overextended past the vulva (Figure 10F-G; Table 1). *png-1; sax-1* and *png-1; sax-2* doubles also displayed enhanced branching defects at the distal end of the DVB axon directly adjacent to the vulva, 31% (n=156) and 53% (n =168), respectively (Figure 11H-K; Table 1). Overall, *png-1; sax-1/2* double mutants displayed significantly enhanced DVB overextension and branching phenotypes compared to single mutants suggesting that these genes act in parallel pathways to control axonal morphology in DVB neurons.

3.1.4 DVB Axon Measurements

To rule out the possibility that the DVB overextension defect is due to an anterior displacement of the DVB cell body, a decrease in body length or a combination of several of these factors, measurements of DVB axon length, DVB cell body position from the vulva, and body length were obtained in wt and mutant young adults. Body length in *png-1* (1056± 21μm, n=28), *png-1; sax-1* (1065± 18 μm, n=25) and *png-1; sax-2* (1053± 19 μm, n=25) were significantly smaller compared to wt animals (1156± 18 μm, n=21) ($P<0.05$; t-test) (Figure 12B). To control for the difference in body lengths, DVB axon length and the length from the DVB cell

Figure 12. DVB axon measurements in *png-1*, *sax-1*, and *sax-2* single and double mutants. To control for the possibility that DVB overextension defects could be caused by differences in body length and/or a displacement of the DVB cell body and not an increase in DVB axon length, we measured the body length, DVB axon length, and DVB cell body position from confocal images as shown in panel (**A**). The DVB neuron visualized with the *otIs92[flp-10::gfp]* transgene. Scale bar, 50μm. (**B**) The body lengths (μm) of *png-1* single and double mutants were significantly smaller compared to wt animals (*P<0.05, **P<0.001; t-test). (**C**) The average ratio of the DVB cell position from vulva to body length in single and double mutants were not significantly different from wt animals, thus, the overextension defect is not caused by an anterior displacement of the DVB cell body. (**D**) Instead the apparent overextension defect of DVB axons is due to an increase in axon length since the average ratio of DVB axon length to body length were significantly greater in *png-1* single and double mutants when compared to wt animals (**P<0.01, ***P<0.0001; t-test).

A

wild type otIs92

B

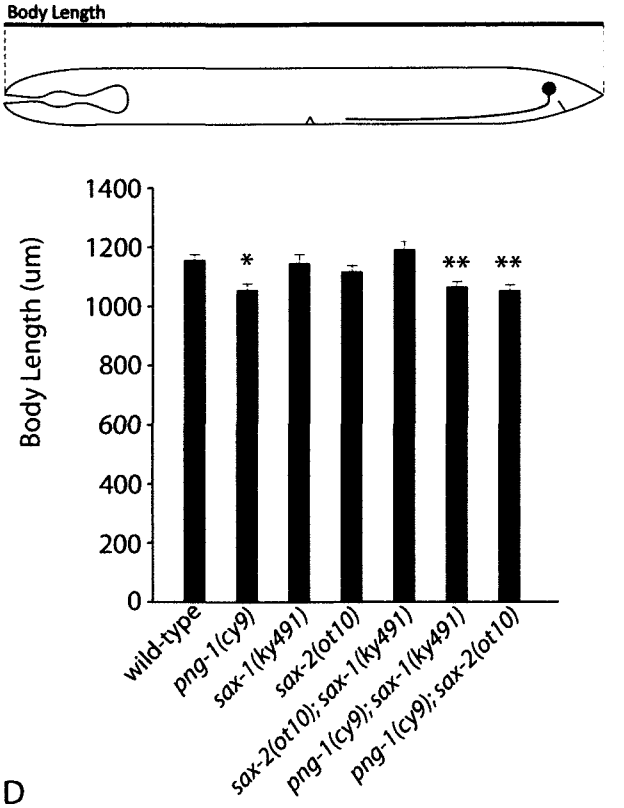

C

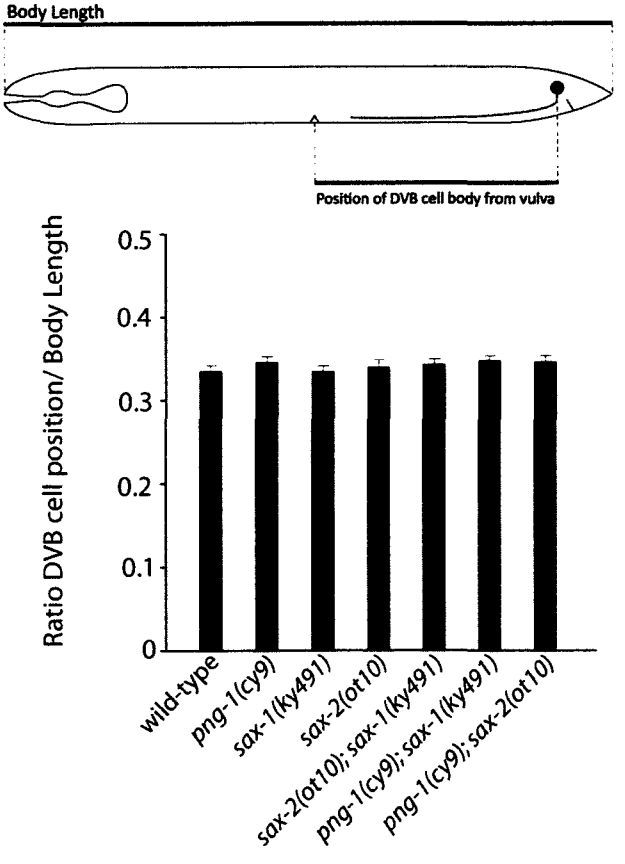

D

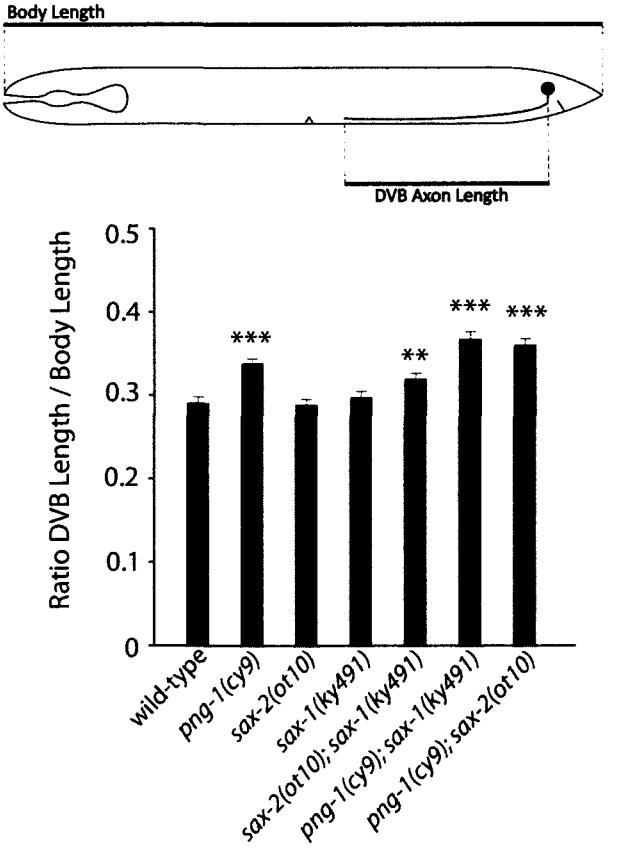

body position to the vulva were expressed as ratios with respect to body length. The DVB cell body position/body length ratio of *png-1* (0.34, n=28), *png-1; sax-1* (0.35, n=25), and *png-1; sax-2* (0.35, n=22) were not significantly different from wt animals (0.33, n=21) (Figure 12C). These findings suggest that the overextension defect in *png-1* mutants and *png-1; sax-1/2* double mutants were not due to an anterior displacement of the DVB cell body. On the contrary, the DVB axon length/body length ratio of *png-1* (0.34, n=28), *png-1; sax-1* (0.37, n=25), and *png-1; sax-2* (0.36, n=22) were significantly greater than wt animals (0.29, n=21) ($P<0.0001$; t-test) (Figure 12D). Therefore, the DVB overextension defect in these mutant backgrounds is due to an increase in axon length. On average, DVB axons in *png-1*, *sax-1*, and *sax-2* single mutants, terminated 13 ± 3 μm, 55± 6 μm, and 60± 7 μm posterior to the vulva, respectively (Figure 13). In comparison, *png-1; sax-1* and *png-1; sax-2* terminated 22 ± 7 μm (n=25) and 16± 3 μm (n=22) anteriorly or dorsally past the vulva, respectively (Figure 13).

3.1.5 AVL Axon Branching Defects

Like DVB, AVL is a GABAergic motor neuron that controls defecation. The AVL cell body, located in the head, extends a posteriorly-directed unbranched axon to the tail (Figure 14 A-B). *png-1* mutants display AVL branching defects (Habibi-Babadi et al., 2010) (Figure 14C). To determine whether *sax-1* and *sax-2* mutants display similar neuronal defects, AVL axon tracts were visualized in young adult worms using an *otEx1495[sul-1::gfp]* reporter line. *otEx1495* is on an extrachromosomal array that was not consistently expressed in AVL neurons. Nevertheless, *otEx1495* animals displayed wild-type neuronal morphology. In *sax-1* and *sax-2* mutants, the percentage of animals that display ectopic branches (25%, n=119 and 26% n=120) was significantly greater than *png-1* mutants (12%, n=122) ($P<0.01$; z-test) (Figure 14C-E and 14I). Double mutants were examined to determine whether these genes are acting in the same or

Figure 13. DVB axon termination sites in *png-1*, *sax-1*, and *sax-2* single and double mutants. Schematic diagram represents the central part of the animal. In wild-type animals, the DVB axon terminates posterior to the vulva (gray arrow). The distribution of DVB axon termination sites relative to the vulva (x-axis) is shown for wild-type, *png-1*, *sax-1*, and *sax-2* single and double mutants. The percentage (%) of DVB axons (y-axis) that terminate within each interval (10μm) is indicated. Termination sites posterior to the vulva are positive; termination sites anterior or dorsal to the vulva are negative. The % of DVB axons that terminate past the vulva in *png-1; sax* double mutants is significantly greater relative to single mutants ($P<0.0001$; t-test). n=number of DVB axons scored

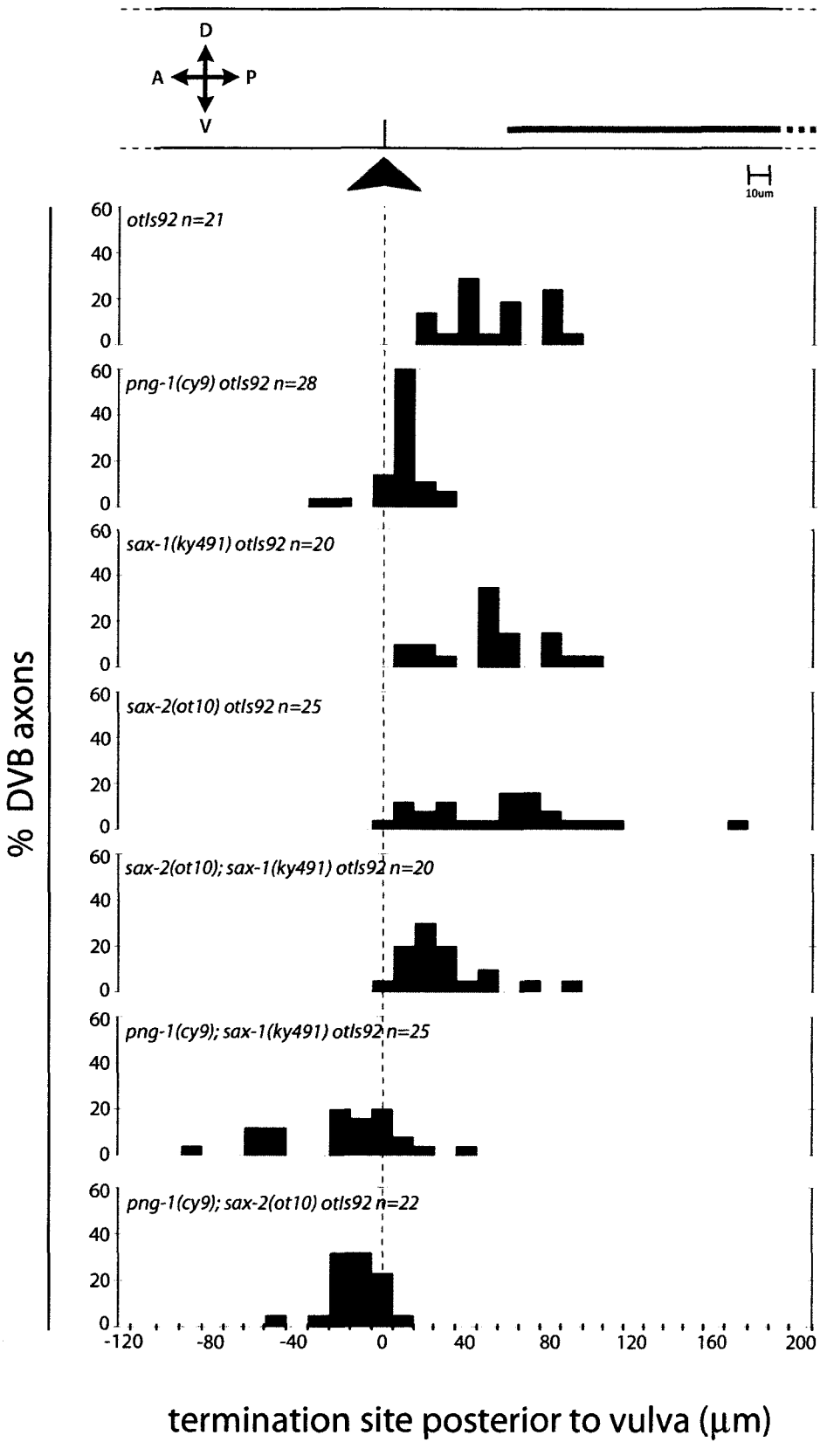
D
A
P
V
10um
otIs92 n=21
png-1(cy9) otIs92 n=28
sax-1(ky491) otIs92 n=20
sax-2(ot10) otIs92 n=25
sax-2(ot10); sax-1(ky491) otIs92 n=20
png-1(cy9); sax-1(ky491) otIs92 n=25
png-1(cy9); sax-2(ot10) otIs92 n=22
60
40
20
0
% DVB axons
-120
-80
-40
0
40
80
120
160
200
termination site posterior to vulva (µm)

Figure 14. AVL axon branching defects in *png-1*, *sax-1*, and *sax-2* single and double mutants. (**A**) Schematic diagram of the AVL motor neuron in wild-type hermaphrodites. (**B**) In wild type, AVL neurons extend an unbranched axon to the tail. (**C-H**) In *png-1*, *sax-1*, *sax-2* single and double mutants, AVL axons display ectopic branches in the vulva region. Images in **B-H** correspond to the boxed region in **A**. AVL is visualized using the *otEx1495[sul-1::gfp]* transgene. The vulva is indicated by an asterisk and ectopic branches are indicated by arrowheads. Anterior is to the left, dorsal at top. Scale bars, 20 μm. (**I**) Quantification of animals that exhibit ectopic branches in single and double mutants. The enhancement of ectopic branching in *png-1; sax* double mutants is significant when compared to single mutants (z-test; **P<0.01, ***P<0.0001). Error bars represent SE of proportion, n=113-122.

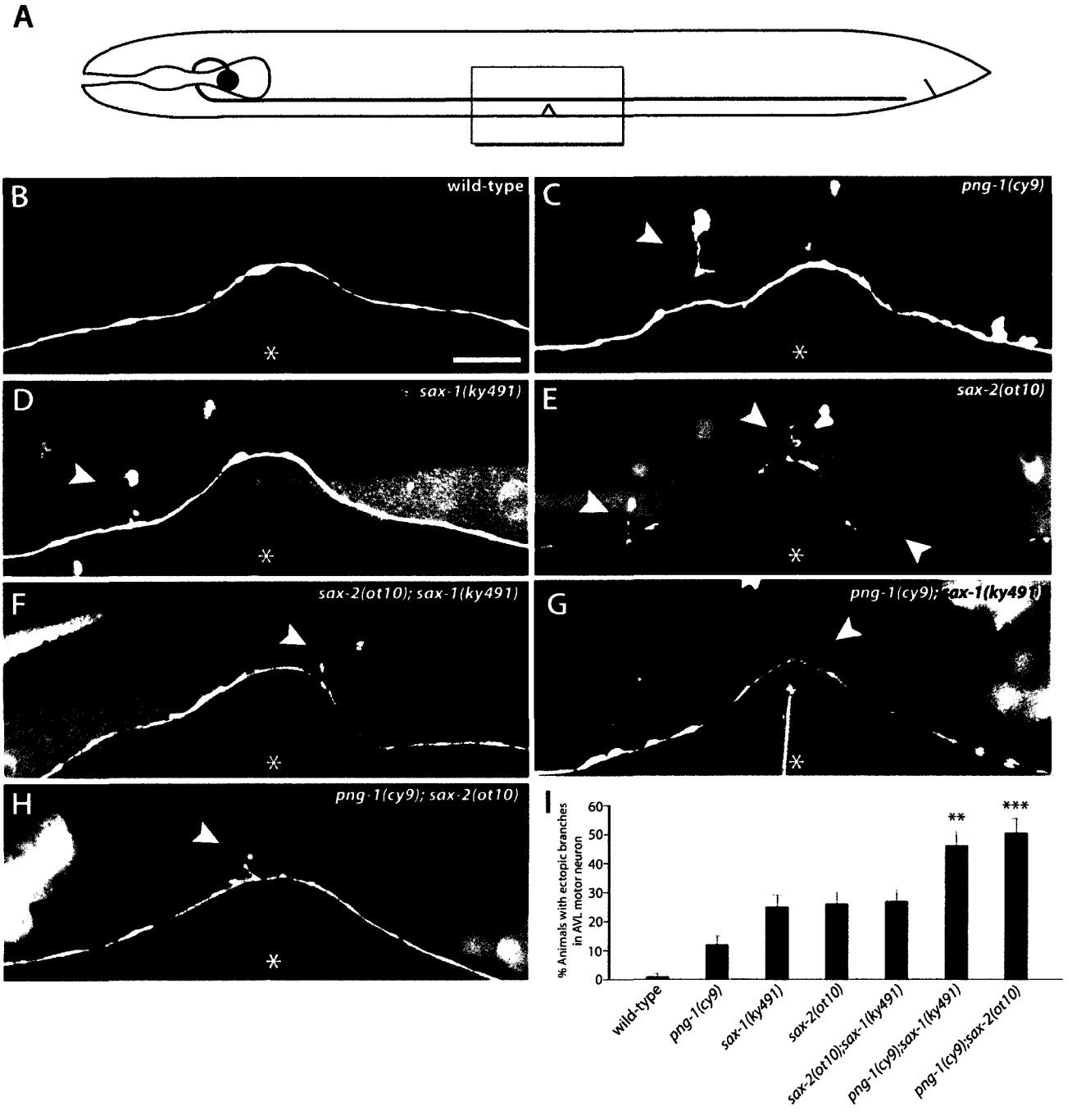
A
B
wild-type
C
png-1(cy9)
D
sax-1(ky491)
E
sax-2(ot10)
F
sax-2(ot10); sax-1(ky491)
G
png-1(cy9); sax-1(ky491)
H
png-1(cy9); sax-2(ot10)
I
% Animals with ectopic branches in AVL motor neuron
60
50
40
30
20
10
0
**
***
wild-type
png-1(cy9)
sax-1(ky491)
sax-2(ot10)
sax-2(ot10);sax-1(ky491)
png-1(cy9);sax-1(ky491)
png-1(cy9);sax-2(ot10)

parallel pathways to inhibit axon branching in AVL. The percentage of animals with ectopic branches in *sax-2; sax-1* mutants (27%, n=119) did not significantly differ compared to single mutants (Figure 14F and 14I). This implies that *sax-1* and *sax-2* act in the same genetic pathway to inhibit AVL branching. In *png-1; sax-1* and *png-1; sax-2* double mutants, 46% (n=115) and 50% (n=113) of animals displayed ectopic branching, respectively (Figure 14G-I). Thus, *png-1; sax-1*and *png-1; sax-2* double mutants resulted in significantly enhanced AVL branching phenotypes relative to single mutants ($P<0.01$; t-test) which implies that *png-1* and *sax* genes function independently in parallel pathways to limit AVL branching.

3.2 Identification and Mapping of *sax-1* Enhancer Genes

3.2.1 Genetic Screen for sax-1 Enhancer Genes

The phenotypic analysis of *png-1* and *sax-1/2* single and double mutants indicates that these genes act in parallel pathways to inhibit axon overgrowth and branching in a subset of neurons including VC4/5, DVB and AVL. These findings suggest that new components of the *png-1* pathway could be identified by screening for enhancers of *sax-1/2* axon branching defects in VC4/5 neurons. We therefore mutagenized *sax-1(ky491); cyIs4* hermaphrodites with EMS and performed a visual screen for severe branching defects (Figure 15A). In a pilot screen, 120 F1 plates with 10 worms each, in other words 1200 haploid genomes (120 x10 haploid genomes) were screened for enhancer mutants yet none were recovered. In the subsequent two screens of 4,560 haploid genomes, we isolated 17 ***s**ax-1* **en**hancer**s** (*sens*) mutants that enhanced sax-*1* branching defects (Figure 15B and 16). All the isolated mutant strains were viable and recessive.

A

sax-1 Enhancer Screen

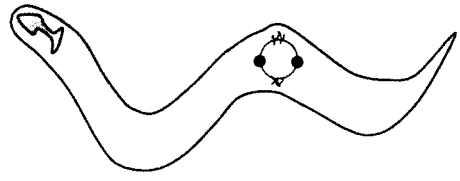

P0: *EMS mutagenesis of sax-1(ky491); cyIs4[cat-1::gfp]* worms

F1: Clone F1 worms

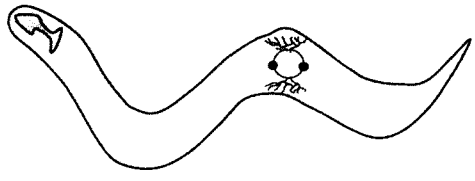

F2: Visual screen of F2 worms for ***enhanced*** axon branching defects

F3: Secondary visual screen to confirm mutant phenotypes

B

Screen	generation screened	# of genomes scored	# of enhancer mutants	enhancer mutants
1	F2	2400	0	
2	F2	3520	8	*zy26, zy27, zy28, zy29, zy30, zy31, zy32, zy33*
3	F2	5600	9	zy34,zy35,zy36,zy37,zy38, zy39, zy40, zy41, zy42

Figure 15. The *sax-1* enhancer screen. (**A**) *sax-1(ky491); cyIs4* worms, which mostly display mild VC branching defects were mutagenized with EMS and the F2 progeny were visually screened for severe VC4/5 branching defects. (**B**) Three independent screens using the *sax-1* enhancer strategy yielded 17 mutations which enhance VC branching defects.

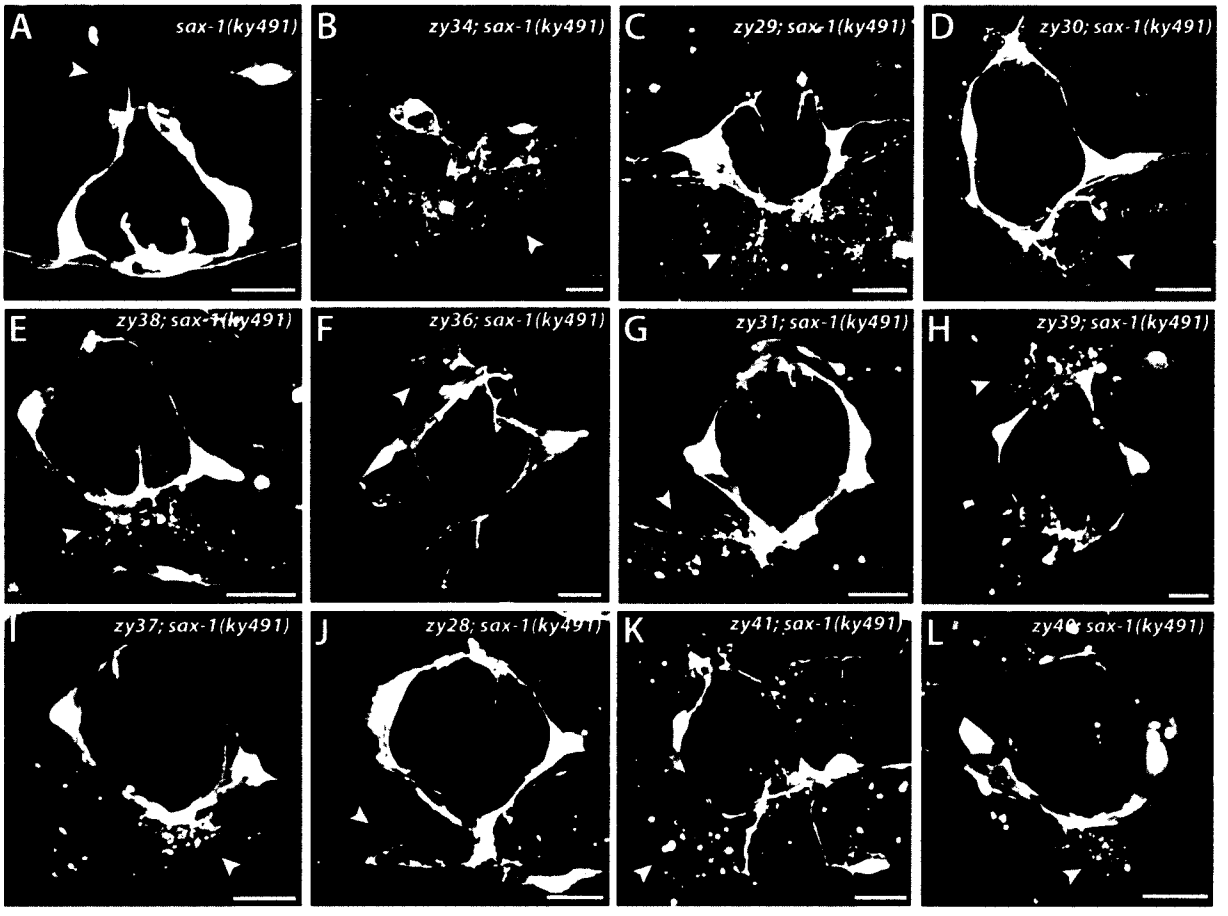

Figure 16. Axon branching phenotypes in *sax-1* enhancer mutants. (**A**) *sax-1(ky491)* mutants. (**B-L**) Representative images of mutants recovered from the *sax-1* enhancer screen. *sax-1 enhancers* (*sens*) mutants display an increase in the number of VC4/5 axon branches compared to *sax-1* single mutants. All enhancers are in the genetic background containing *sax-1(ky491); cyIs4*. Arrowheads point towards branching defects.

3.2.2 Identification of Three Complementation Groups: sens-1, sens-2, and sens-3

The *sax-1* enhancer screen yielded several mutants with similar branching defects. Complementation tests allow us to determine whether these mutant phenotypes are caused by mutations in a single gene or in different genes. Our first step was to determine whether any of the newly isolated mutants were new alleles of *png-1*. We performed pair-wise complementation tests with *png-1* and all 17 *sens* mutants. If the *png-1/sens* trans-heterozygotes examined displayed VC4/5 axon branching defects the two lines failed to complement and the *sens* allele most likely represents a new *png-1* allele. We found that four of my 17 *sax-1* enhancer mutants identified new alleles of *png-1* validating the screen as a tool to identify *png-1* pathway components (Table 2). The second step was to perform a series of pair-wise complementation tests with 10 mutants that displayed similar phenotypes in order to assign them to complementation groups (CGs). Two strains were said to complement if the trans-heterozygote displayed wt branching; whereas two strains failed to complement when branching defects were observed. These mutants mapped to at least three complementation groups and were therefore named *sax-1* enhancer-*1 (sens-1)*, *sens-2* and *sens-3* (Table 3).

Two of the original *sens* mutants, *zy32* and *zy33*, displayed multiple VC4/5 cell bodies and consequently an enhancement in axon branching was due to supernumerary axons. This phenotype resembled the supernumerary neurons found in pattern of reporter gene expression abnormal (*pag-3*) mutants (Cameron et al., 2002). Complementation tests revealed that these mutants did indeed represent new alleles of *pag-3*. Another mutant, *zy42*, displayed an uncoordinated movement phenotype. This mutant was mapped by Bobby Lanthier, a lab technician, to chromosome X, near a gene called *sensory axon guidance-3* (*sax-3*). SAX-3 is the *C. elegans* orthologue of Robo, a member of the immunoglobulin superfamily that has been

Table 2. Complementation analysis of *png-1(cy9)* and *sens* alleles

Line name	zy26[a]	zy27[a]	zy34[a]	zy35[a]	zy28[b]	zy29[b]	zy30[b]	zy31[b]	zy32[b]	zy33[b]	zy36[b]	zy37[b]	zy38[b]	zy39[b]	zy40[b]	zy41[b]	zy42[b]
png-1(cy9)	-	-	-	-	+	+	+	+	+	+	+	+	+	+	+	+	+

*The results of complementation tests between *png-1* and *sens* mutants are shown. *png-1* and *sens* trans-heterozygote animals were assayed for VC4/5 axon branching defects. Crosses that complement are indicated by "+" and crosses that fail to complement are indicated by "-"

[a] *sens* alleles that fail to complement with *png-1* and are likely to represent new alleles of *png-1*

[b] *sens* alleles that complement with *png-1* and are likely to represent new genes

Table 3. Complementation analysis of *sens* alleles

Line name	zy28	zy31	zy37	zy39	zy29	zy30	zy36	zy38	zy40
zy31	-[1]								
zy37	-[1]	-[1]							
zy39	-[1]	-[1]	-[1]						
zy29	+	ND	+	+					
zy30	+	ND	+	+	-[2]				
zy36	+	ND	+	+	-[2]	-[2]			
zy38	+	+	+	+	-[2]	-[2]	-[2]		
zy40	-	ND	+	+	+	+	ND	+	
zy41	-	ND	-	-	-	ND	+	+	-[3]

*The results of complementation tests between *sens* mutants are shown. *sens* trans-heterozygote animals were assayed for VC4/5 axon branching defects. Crosses that complement are indicated by "+" and crosses that fail to complement are indicated by "-". ND not determined.

[1]CG I named *sens-2*
[2] CG II named *sens-1*
[3] CG III named *sens-3*

shown to play a phylogenetically conserved role in axon guidance (Brose and Tessier-Lavigne, 2000). A complementation test revealed that *zy42* represents a new allele of *sax-3*. *sax-3* was previously identified as a mutant with VC4/5 morphology defects on its own (A. Colavita, unpublished) and therefore does not represent an enhancer of *sax-1* and therefore was not characterized further. Overall, the *sax-1* enhancer screen identified at least three *sens* mutants that act like *png-1* mutants to enhance the *sax-1* VC4/5 axon branching defects. Enhancer mutants were backcrossed once to the N2 wild-type strain to remove the *sax-1* mutant background and once to *cyIs4* to replace the mutagenized *cyIs4* transgene before further phenotypic characterization.

3.2.3 Genetic map positions of sens-1 and sens-2

To assign *sens* mutations to chromosomes we performed linkage mapping using single nucleotide polymorphisms as previously described (see Material and Methods). Mapping was done to first assign the 10 *sens* mutants that were not allelic to *png-1* to a chromosome. *sax-1 Hw* males were crossed with *sens; sax-1* hermaphrodites to generate a heterozygous cross progeny that were allowed to self-fertilize to generate *sens*; *sax-1 cyIs4* recombinant mutants. For several *sens* mutant, approximately 15-30 recombinants were collected and tested for SNP linkage across all chromosomes except chromosome V and VI, where the *cyIs4* GFP marker and *sax-1* mutation (both within an N2 background) were located. SNP linkage to *sens* mutation was detected as a high ratio of N2 to Hw SNP alleles. The first round of mapping allowed us to map *sens-1* alleles *(zy29, zy30, zy36)* to chromosome IV and *sens-2* alleles *(zy31, zy37)* to chromosome II. *zy40* and *zy41* (*sens-3*) mutations did not map to chromosomes I to IV and may therefore be located on chromosome V or VI.

Further mapping was done to map *sens-1* and *sens-2* alleles to smaller genetic intervals within chromosomes IV and II respectively. Subsequent analysis of SNPs spaced over the entire length of chromosome IV allowed us to map *sens-1* alleles (*zy29, zy30)* to a 7.4Mb interval on chromosome IV between the SNPs D2096 and F42A6 (Figure 17). *sens-2* alleles (*zy31,* zy37*)* were mapped to an 8Mb interval on chromosome II between the SNPs Y51B9 and F39E9 (Figure 17). The mapping of several *sens-1* alleles to the same region in chromosome IV and mapping several *sens-2* alleles to the same chromosome in II validated our complementation tests that initially defined these groups to the same genetic loci.

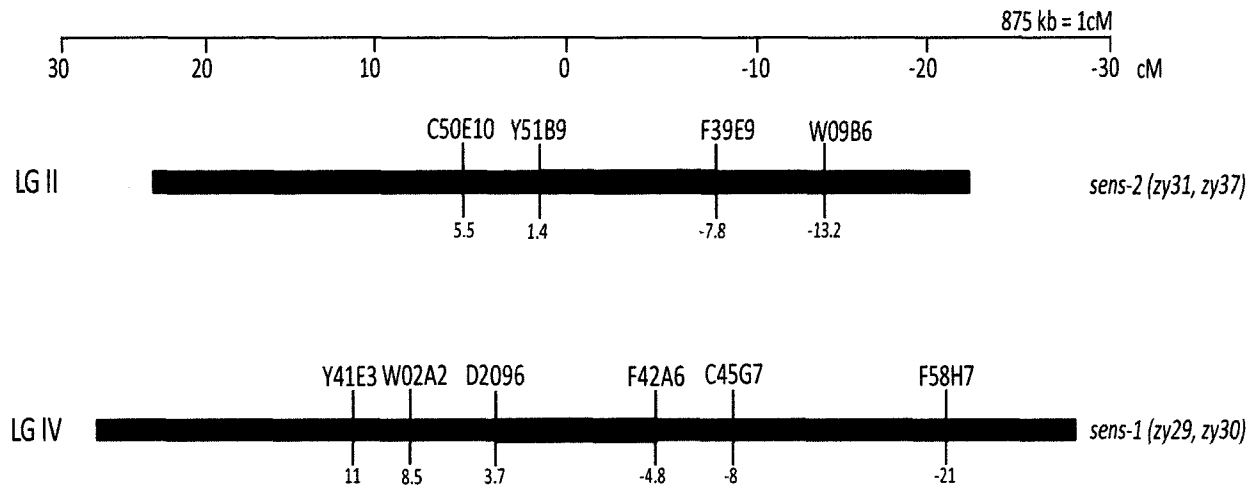

Figure 17. Chromosome mapping for *sens-1* and *sens-2* genes. A SNP-based mapping strategy was used to map *sens-1* and *sens-2* alleles to chromosomes. The position and names of SNPs used in this study are shown along the length of the chromosomes. *sens-1* alleles mapped to a large interval (red) on LGIV between SNPs D2096 and F42A6. *sens-2* alleles mapped to a large interval (red) on LGII between SNPs Y51B9 and F39E9. Note. All *sens* mutants were mapped in the *sax-1(ky491); cyIs4* genetic background.

3.3 VC4/VC5 and DVB Morphological Defects in *sens-1* and *sens-2* Mutants

To determine whether *sens-1*and *sens-2* single mutants displayed *png-1* like morphological defects, we analyzed VC4/5 and DVB for neuronal defects. When compared with wild-type animals, *sens-1* mutants, *zy29* and *zy30,* displayed significant mild branching defects, 32% (n=179) and 43% (n=166), when compared with wt animals ($P<0.05$ (wt vs. *zy29*); $P<0.01$ (wt vs. *zy30*); t-tests) (Figure 18A-D and 18G). *sens-2(zy28)* mutants displayed significant mild and moderate branching defects (49% "mild"; 23% "moderate", n=176) compared with wt animals ($P<0.01$; t-test) (Figure 18E-G). *sens* mutants also displayed other morphological defects including neurite outgrowth defects and branch termination defects. 24% (n=180) and 22% (n=165) of VC4/5 neurons in *sens-1(zy29)* and *sens-1(zy30)* displayed ectopic neurite outgrowths compared to wt ($P<0.05$; t-test) (Figure 19A-B and 19D). However, we observed no significant difference in ectopic neurite formation in *sens-2(zy28)* mutants (16%, n=173) compared to wt (Figure 19D). In wild type, 3% of animals display branch termination defects. In contrast, 13% and 17% of VC4/5 branches extend beyond the normal termination point to cross the midline in *sens-1(zy29)* and *sens-2(zy28)* mutant animals (Figure 19E-H).

To determine whether *sens-1* and *sens-2* mutants displayed *png-1*-like defects in DVB neurons, DVB axon tracts were examined in young adult worms using the *otIs92* reporter line. In evaluating the DVB axon tract in *sens-1(zy29), sens-1(zy30), and sens-2(zy28)* single mutants, no overextension defects were observed (n=120-180). However, non-vulval branching was observed. 17% (n=168) and 7% (n=180) of DVB axons in *sens-1(zy29) and sens-1(zy30)* respectively displayed non-vulval DVB branching compared to 0% in wt animals. However, we observed no significant difference in ectopic branches in *sens-2(zy28)* mutants (3%, n=173)

compared to wt. Overall, *sens-1* and *sens-2* mutants displayed a variety of defects in VC and DVB neuronal morphology that resemble defects in *png-1* mutants.

Figure 18. VC4/VC5 axon branching morphologies in *sens* mutants. (**A-F**) *sens-1* and *sens-2* mutants display mild branching defects (arrowheads). Neurons were visualized with the *cyIs4[cat-1::gfp]* transgene. All images, ventral views with anterior to the left. Scale bars, 10μm. (**G**) *sens* mutants were classified as having mild (≤3 supernumerary branches), moderate (≥4-20 supernumerary branches), or severe (>20 supernumerary branches) phenotypes. *sens* mutants display predominately mild branching phenotypes. Asterisks indicate values that are significantly different from wild type (*P<0.05, **P<0.01; t-tests). Error bars represent SEM of three independent counts with an n=50-60 for each set.

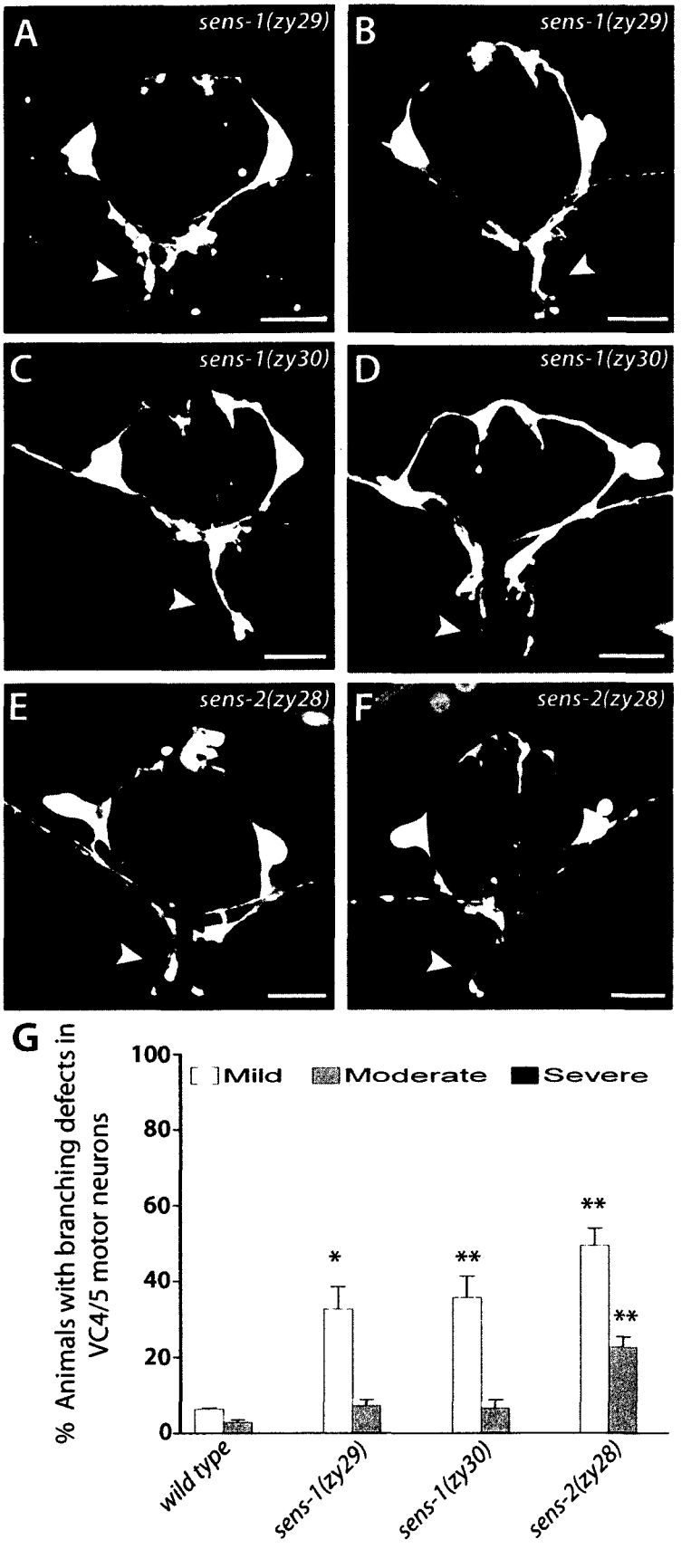
A
sens-1(zy29)
B
sens-1(zy29)
C
sens-1(zy30)
D
sens-1(zy30)
E
sens-2(zy28)
F
sens-2(zy28)
G
% Animals with branching defects in VC4/5 motor neurons
100
80
60
40
20
0
Mild
Moderate
Severe
*
**
**
**
wild type
sens-1(zy29)
sens-1(zy30)
sens-2(zy28)

Figure 19. VC4/VC5 axon branch termination and neurite outgrowth defects in *sens* mutants. (**A-G**) *sens-1* and *sens-2* mutants display branch termination defects (**A-C**) and ectopic neurites (**E-F**). Open arrowheads point to overextended VC branches and closed arrowheads point to ectopic neurites. Scale bars, 10μm. (**D, H**) Quantification of branch termination defects (**D**) and ectopic neurites (**H**) in *sens* mutants. Asterisks indicate values that are significantly different from wild type animals (*P<0.05, **P<0.01; t-tests). Error bars represent SEM of three independent counts with an n=50-60 for each set.

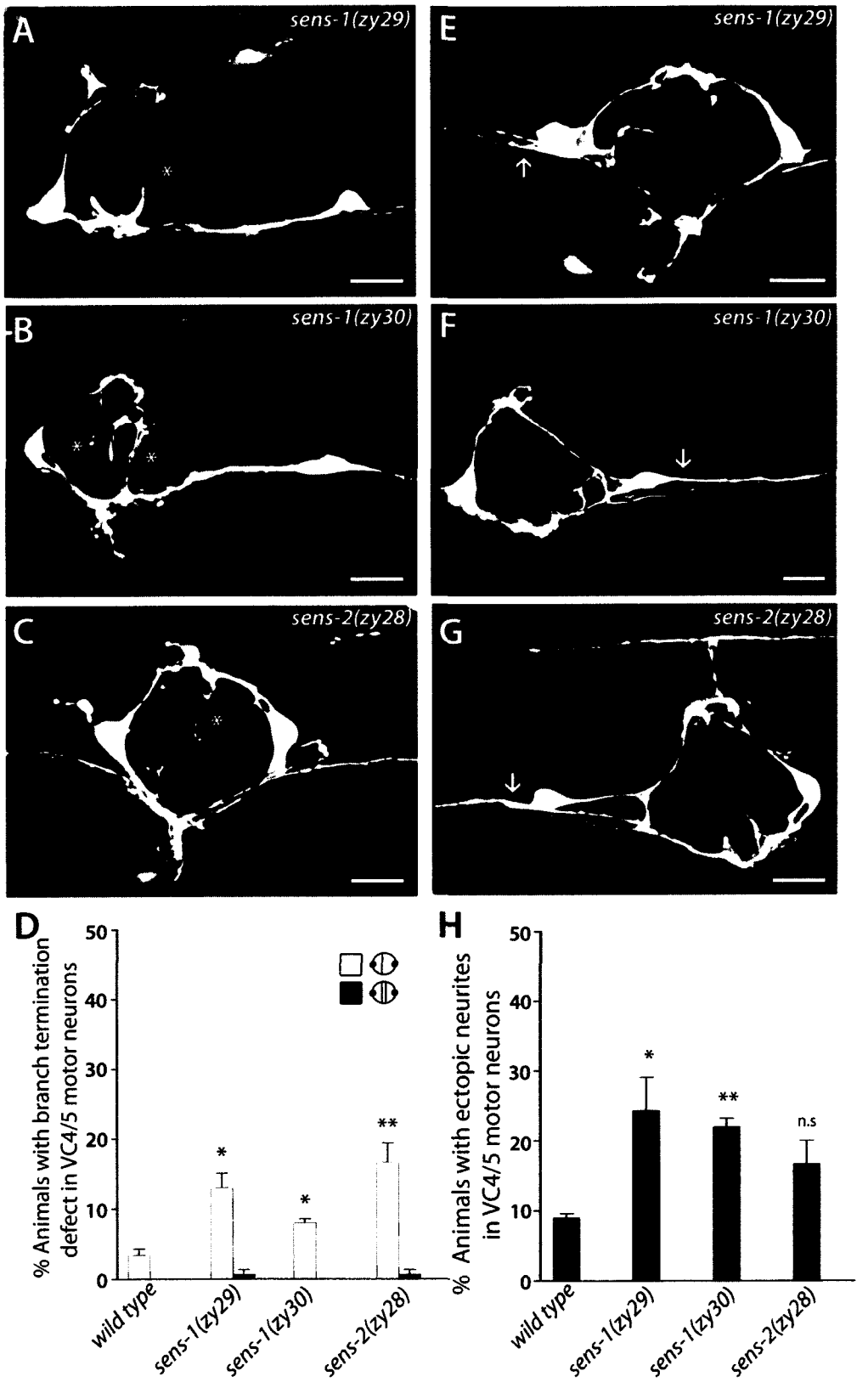
A
sens-1(zy29)
E
sens-1(zy29)
B
sens-1(zy30)
F
sens-1(zy30)
C
sens-2(zy28)
G
sens-2(zy28)
D
% Animals with branch termination defect in VC4/5 motor neurons
50
40
30
20
10
0
*
*
**
wild type
sens-1(zy29)
sens-1(zy30)
sens-2(zy28)
H
% Animals with ectopic neurites in VC4/5 motor neurons
50
40
30
20
10
0
*
**
n.s
wild type
sens-1(zy29)
sens-1(zy30)
sens-2(zy28)

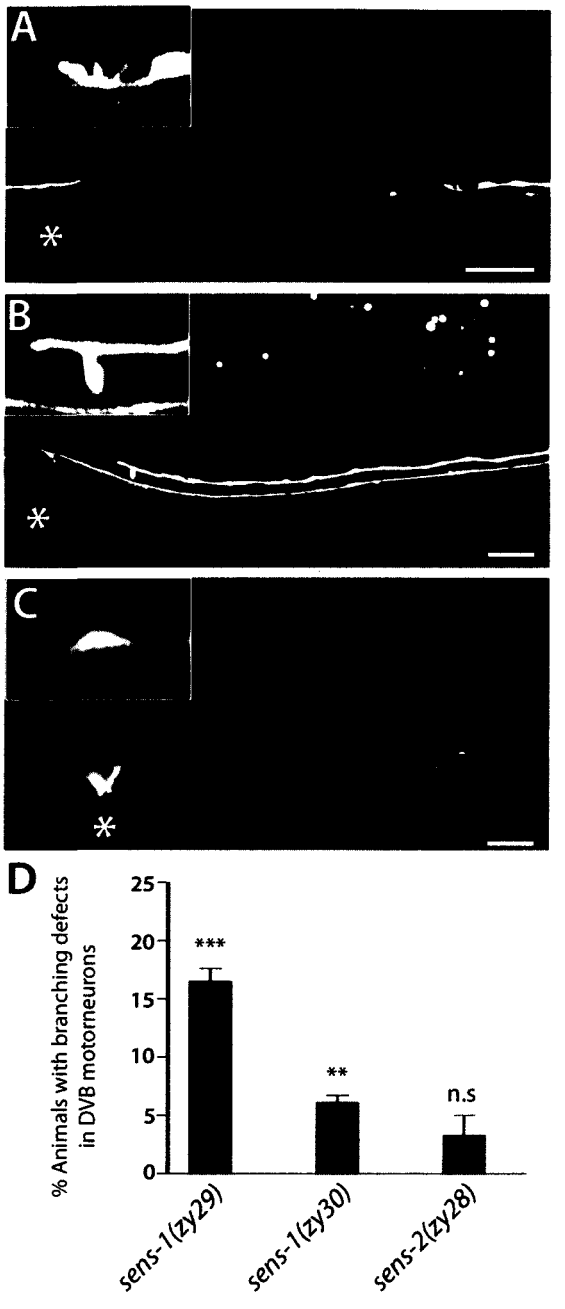

Figure 20. DVB axon branching defects in *sens* mutants. (**A-C**) In *sens* mutants, DVB axons display short ectopic branches at their distal tips. The vulva is indicated by an asterisk. Insets in the upper left corner correspond to the boxed distal tips of DVB axon. DVB neuron visualized with the *otIs92[flp-10::gfp]* transgene. Scale bars, 20 μm. (**D**) Quantification of DVB axon defects in *sens* mutants. Error bars represent SEM of three independent counts with an n=50-60 for each set.

4. Discussion

4.1 *png-1* and *sax-1/sax-2* Act in Parallel Pathways to Restrict Axon Branching and Outgrowth

In this study, we focused on the neuronal roles played by the SAX-1/NDR kinase and SAX-2 and their interactions with the PNG-1/N-glycanase. Qualitatively, *sax-1* and *sax-2* mutants displayed neuronal defects that were similar to *png-1* mutants, including excessive branching, ectopic neurite outgrowth and axon overgrowth. Axon and dendrite overbranching was the principle phenotype observed in the subset of neurons examined. In these mutants, the normally unbranched AVL and DVB neurons displayed ectopic branches; whereas, the normally branched VC4/5 neurons displayed an increase in axon branches. Notably, the axons and dendrites of these neurons were guided along their normal trajectories. In contrast, in the case of the VC4/5 neurons, mutations in the well-conserved axon guidance molecules, UNC-6/Netrin and its receptor UNC-40/DCC result in highly penetrant axon guidance defects (A. Colavita, unpublished). This suggests that *png-1*, *sax-1*, and *sax-2* play specific roles in limiting neurite outgrowth and branching, while other genes mediate the initial guidance of axons and dendrites towards their appropriate target area.

It was previously shown in *C. elegans* that *sax-1* and *sax-2* limit the primary growth of dendrites and prevents the outgrowth of ectopic neurites in adult animals (Zallen et al., 1999; Zallen et al., 2000; Gallegos and Bargmann, 2004; Jia and Emmons, 2006). In this study, we found that *sax-1* and *sax-2* also regulate axonal branching in *C. elegans*. This branching phenotype is consistent with what is known in other model organisms. Mutations in the fly homologs of *sax-1* and *sax-2*, *tricornered* (*trc*) and *furry* (*fry*) respectively, result in the formation of overly branched dendrites which are reminiscent of the VC overbranching phenotypes (Emoto et al., 2004). Thus it appears that these highly conserved proteins mediate

similar functions in fly and worm neurons. In addition, mutations in *trc* and *fry* result in the formation of branched epidermal hairs, sensory bristles, and antennas and in multi-hair phenotypes which are comparable to the overbranched and overgrown fly and worm neuronal morphologies. In filamentous fungi, mutations in the SAX-1 homolog Cot-1/NDR kinase result in hyper branched hypha (Yarden et al., 1992). Overall, these diverse but related phenotypes suggest that *sax-1* and *sax-2* homologs have conserved roles in regulating outgrowth and branching of cellular processes.

Conversely, developmental roles for PNG-1/N-glycanase homologs remain elusive. Apart from neuronal defects in *C. elegans*, an N-glycanase mutant in filamentous fungi exhibits a hyphal morphology defect, consisting of round and swollen hyphal tips (Seiler and Plamann, 2003). Thus it appears that N-glycanases may also have conserved roles in regulating cellular morphology in several organisms.

Our finding that *png-1*, *sax-1*, and *sax-2* mutants share similar phenotypes suggests two possibilities; these genes either function in the same pathway or in parallel pathways to regulate neuronal morphology. Since analysis of the *png-1; sax-1* and *png-1; sax-2* double mutants showed enhanced neuronal defects compared to either of the single mutants, *png-1* functions in a parallel pathway to *sax-1* and *sax-2*. Double mutants also displayed qualitatively much more complex morphologies including severe branching phenotypes, multiple ectopic neurites, and severely overextended axons. In contrast, analysis of s*ax-2; sax-1* double mutants displayed a phenotypic penetrance that was indistinguishable from either single mutant, suggesting that *sax-2* and *sax-1* function in the same pathway. These results are comparable to *Drosophila* studies which have shown that *trc* and *fry* act in the same genetic pathway to regulate dendritic morphology (Emoto et al., 2004). Furthermore, biochemical studies in both yeast and

Drosophila have shown that SAX-1 and SAX-2 orthologs physically interact (Du and Novick, 2002; He et al., 2005a; Seiler et al., 2006). These findings suggest that an interaction between *sax-1* and *sax-2* and their homologs is conserved over a wide range of organisms. The exact nature of this interaction is not known; although it is hypothesized that scaffolding proteins like SAX-2 facilitate SAX-1/NDR kinase activation, substrate targeting, or localization (Hergovich et al., 2006).

Our study suggest that at least two parallel pathways, the PNG-1 and SAX-1/NDR kinase pathways, regulate axon/dendrite branching and outgrowth in a subset of *C. elegans* neurons. The similar phenotypes displayed when these pathways are disrupted suggest that they may have overlapping functions. Genetic redundancy is commonly cited among members of gene families which are related in structure and perform similar, if not identical, functions. For example, one study found that the three *C. elegans* Rac GTPase-like genes, *ced-10*, *mig-2*, and *rac-2* act redundantly to regulate axon guidance (Lundquist et al., 2001). As well, several genes of the IgCAM superfamily which encode adhesion molecules display functional overlap during axon migration (Schwarz. et al, 2009). Although homologous genes are often cited in genetic redundancy; various functions can also be provided redundantly by non-homologous genes (Kadyk and Kimble, 1998; Harrington et al., 2002; Hansen et al., 2004)). For example, attractant guidance cues provided by the Netrin/DCC pathway and repellent guidance cues provided by the Slit/Robo pathway which collectively act to control ventrally-directed axon guidance in a subset of mechanosensory neurons in *C. elegans* (Hao et al., 2001). In this model, ventral axon guidance is achieved by the joint action of ventrally expressed Netrin protein attracting axons and dorsally expressed Slit protein repelling axons. In this case, parallel pathways perform different functions that collectively control a common cellular process.

Previous studies have shown that PNG-1/N-glycanase acts from vulval epithelium cells to regulate VC branching (Habibi-Babadi et al., 2010). Conversely, the SAX-1/NDR kinase pathway functions intrinsically within neurons to limit neurite outgrowth in *C. elegans* and dendritic branching in Drosophila (Zallen et al., 2000; Emoto et al., 2004; Gallegos and Bargmann, 2004). The cell-non autonomous and cell autonomous activities of PNG-1 and the SAX-1/SAX-2 pathway respectively, suggest these pathways engage different targets and work through different mechanisms. Based on differences in their biochemical functions and their site of action, we propose that the PNG-1 and SAX-1/NDR kinase pathways perform independent yet equally necessary functions that collectively control a common cellular process involved in establishing or maintaining proper neuronal morphology. Given that cytoskeleton remodeling is a common process that promotes outgrowth, extension, and branching, we propose that these parallel pathways influence cytoskeleton dynamics via independent mechanisms. Indeed, the coordinated regulation of the actin and microtubule cytoskeleton has been well established as the ultimate determinant of cellular morphology including axons/dendrite morphology (Rodriguez et al., 2003; Bouquet and Nothias, 2007; Georges et al., 2008; Li and Gundersen, 2008; Quinn and Wadsworth, 2008; Witte and Bradke, 2008). Consistent with this idea, studies in budding yeast and Drosophila have shown that disruption of the SAX-1/NDR kinase pathway results in a disorganized actin and/or microtubule structure (He and Adler, 2002; Gonzalez-Novo et al., 2009).

4.2 Possible Mechanisms to Explain PNG-1 and SAX-1/NDR Kinase Pathways in Axon Branching and Outgrowth

Worms in which the vulva has been genetically or physically ablated display axon guidance defects and the loss of axon branches; indicating that the vulval epithelium is a source of axon guidance and branching factors (Li and Chalfie, 1990; Garriga et al., 1993). When the PNG-1 and SAX-1/NDR kinase pathways are disrupted, the majority of neuronal defects were observed in the vicinity of the vulva. For example, unbranched neurons like AVL and DVB display ectopic axon branches at the vulva; whereas, the normally branched VC4/5 neurons display an increase in branches. The ectopic axon branches observed in DVB and AVL suggest that these neurons are responsive to a branching cue; yet are usually prevented from doing so.

What is preventing these axons from branching at the vulva? One possibility is that, just as the vulva emits branch promoting factors; the vulva may also provide branch inhibitory factors that prevent unnecessary or over-branching. Alternatively, the receptors that promote axon branching may be normally down regulated to prevent inappropriate branching or those that mediate branch inhibition may normally be up regulated in wild-type animals to prevent too much branching. Rho-family GTPases control various aspects of neuronal morphogenesis including axon outgrowth and branching (Ng et al., 2002). Since both PNG-1 and SAX-1/NDR pathway mutants display various neuronal morphology defects, we propose that Rho GTPases very likely lie downstream of these pathways.

Cell rescue studies suggest PNG-1 acts through a cell-non autonomous mechanism to limit VC4/5 neuronal branching suggesting PNG-1 may regulate the cell surface expression or secretion of an axon branch promoting molecule from the vulval epithelial cells (Habibi-Babadi et al., 2010). For example, an excess of a branch promoting factor or the shortage of a branch

inhibiting factor in the intercellular space may cause an overbranching phenotype. These branching cues would be relayed into the neuron via putative cell-surface receptors that trigger intracellular pathways that ultimately regulate components of the cytoskeleton machinery to influence morphological changes. The identity of this axon branching molecule is currently unknown; yet N-glycanases, based on their involvement in the degradation of misfolded glycoproteins in other systems, may regulate such a molecule through post translational modification (deglycosylation) or through a proteasomal degradation pathway (Habibi-Babadi et al., 2010).

SAX-1/NDR kinase homologs have established roles in regulating gene expression, vesicle trafficking, and exocytosis (McNemar and Fonzi, 2002; Kurischko et al., 2008; Mazanka et al., 2008)). Within neurons, the SAX-1 kinase pathway may regulate the expression or transport of signaling components that respond to or interpret axon branching factors, such as the production or localization of receptors on the axon membrane. For example, a failure to downregulate a receptor that mediates branch promoting cues may lead to an overbranching phenotype. Similar to axon guidance receptors, these putative branching receptors are likely coupled to effectors that regulate Rho-family GTPases and ultimately the actin/microtubule cytoskeleton.

Several studies have shown that the SAX-1/NDR kinase pathway regulates Rho GTPase activity and localization (Emoto et al., 2004; Kurischko et al., 2008; Das et al., 2009). In yeast and mammalian cells, SAX-2 homologs have been shown to bind MTs (Gonzalez-Novo et al., 2009; Chiba et al., 2009) and act as scaffolding proteins that bind both NDR kinases and MTs (Chiba et al., 2009). It is possible that the SAX-1/NDR kinase pathway acts intrinsically within neurons to directly organize the structure of the cytoskeleton. SAX-1/ NDR kinases have also

been shown to regulate gene expression by altering the activity and localization of transcription factors (Weiss et al., 2002; Nelson et al., 2003; Kurischko et al., 2005; Mazanka et al., 2008). Therefore, SAX-1 may regulate axonal and dendritic growth by regulating the expression of genes that encode cytoskeleton interacting proteins. Although the SAX-1 /NDR kinase pathway controls various aspects of neuronal morphology, the relevant downstream targets and mechanisms are largely unknown.

Among many possibilities, we describe one model by which these parallel pathways may collectively regulate neuronal morphology. In this model, PNGase activity within vulval epithelial cells normally downregulates levels of a putative branch promoting factor into the extracellular space. Within neurons, the SAX-1/NDR kinase pathway negatively regulates actin dynamics via regulation of RhoGTPases or actin binding proteins. A disruption in both these parallel pathways would lead to a hyper activation of branch promoting signaling pathway and actin cytoskeleton dynamics within neurons resulting in an axon/branch overgrowth phenotype.

4.3 Identification of *sens* Genes: Possible Components in *png-1* Pathway?

In the original mutagenesis screen for VC4/5 axon branching mutants, the only mutations identified were those in *png-1* (A. Colavita, unpublished). Why were other mutants with excessive branching defects not isolated? There are several possibilities. First mutations can result in pleiotropic effects, such as lethality or sterility that would preclude visualization of branching defects or recovery of mutants. Second, genetic redundancy could mask mutations that yield a visible phenotype. In this case, mutations in one gene are completely or partially compensated by the activity of other genes. Our findings suggest that the *png-1* pathway and the *sax-1*/*sax-2* pathway are partially redundant in limiting neuronal branching and outgrowth. The

milder phenotypes of *sax-1* and *sax-2* mutants compared to *png-1* likely explains why only *png-1* alleles were recovered in the original screen. Therefore, to identify other components in the *png-1* axon branching pathway, it was necessary to overcome the apparent functional redundancy regulating axon branching in VC neurons.

Enhancer screens in *C. elegans* are a good way to uncover the functional overlap among genes regulating certain biological processes (Jorgensen and Mango, 2002; Herman and Yochem, 2005). Since *png-1; sax-1* double mutants show enhanced VC4/5 branching defects, we screened for other mutants that act like *png-1* to enhance *sax-1* defects. Our *sax-1* enhancer screen identified multiple alleles in at least three *sens* (***sax-1 enhancers***) genes that limit axon branching in *C. elegans*. We propose that these genes are good candidates to regulate axon branching through a PNG-1 dependent pathway.

sens genes regulate several aspects of neuronal morphology. *sens* mutants display ectopic neurites, excessive branching, and branch termination defects, suggesting that these genes act to limit neurite and branch growth. Although these defects were mild and less penetrant, they were phenotypically similar to *png-1* mutants, consistent with disruption of a common pathway. Indeed, these mild phenotypes would have made identifying *sens* genes difficult in a conventional genetic screen as other genes like *sax-1* appear to compensate for their loss. We predict that the molecular identification of the genes obtained in the *sax-1* enhancer screen will provide insight into the pathway and mechanism involved in *png-1* mediated axon branching.

While deficits in the PNG-1 and SAX-1/NDR kinase pathways causes outgrowth and branching defects, a wide variety of genes are known to be involved in neuronal morphology in

C. elegans. Therefore, while *sens* genes may encode new PNG-1 pathway components, we cannot exclude the possibility that they instead act in a third parallel pathway, separate from the *png-1* or the *sax-1/sax-2* pathways. There are several possibilities. In both invertebrates and vertebrates, neuronal activity has been shown to influence nervous system structure (Letourneau et al., 1994; Peckol et al., 1999; Gomez and Spitzer, 2000; Ming et al., 2001; Henley and Poo, 2004). SAX-1 has already been shown to function in parallel with an activity dependent pathway consisting of TAX-4/cGMP-gated sensory transduction channel and UNC-43/Calcium/Calmodulin-regulated Kinase (CAMKII) to suppress ectopic neurite formation in sensory neurons (Zallen et.al, 2000). Intrinsic transcriptional programs have also been shown to control several aspects of neuronal morphology (Hobert et al., 1999; Clark and Chiu, 2003; Wacker et al., 2003). In *C. elegans*, transcriptional regulators like the *lim-6* homeobox gene have been shown to regulate neurite outgrowth in neurons (Hobert et al., 1999). Ubiquitin-mediated protein degradation has also been implicated in neuronal morphology since mutations in LIN-23, a component of the SCF E3 ubiquitin ligase complex, result in ectopic axons and branches (Mehta et al., 2004). Extracellular signaling molecules like KAL-1/Anosmin-1, an extracellular matrix glycoprotein, regulate axonal branching through an unknown mechanism (Bulow et al., 2002). Likewise, UNC-119, a novel conserved protein was found to maintain neuronal morphology via an unknown mechanism by suppressing axon branching in *C. elegans* (Knobel et al., 2001). Currently little is known about the upstream signals that trigger the activation of the PNG-1 and SAX-1/NDR kinase pathways, their integration into known signaling pathways or their downstream targets. The identification of *sens* genes might allow us to establish a link and integrate PNG-1 into a known molecular pathway.

4.4 Future Directions

Studies in *C. elegans* have shown *sax-1* and *sax-2* to play both developmental and maintenance roles in neuronal and dendritic development (Zallen et al., 1999; Zallen et al., 2000; Gallegos and Bargmann, 2004). However, whether they play a developmental role by inhibiting primary branch outgrowth or a maintenance role to prevent secondary branch growth remains to be studied. Since we have only characterized mutants at one time point, we cannot distinguish whether these defects are caused early in the establishment of neuronal structure or whether these genes are involved in the maintenance of neuronal morphology. Therefore time lapse studies are required to characterize neuronal morphology in single and double mutants at the larval and adult stages. Time-lapse analysis will also allow us to determine the temporal relationship between axon outgrowth and axon branching. In other words, determine whether ectopic neurites and ectopic branches appear simultaneously or separately during development in *png-1*, *sax-1*, and *sax-2* mutants.

Previous studies have shown that *png-1* is expressed in vulval cells and regulates neuronal branching of VC4/5 from the vulval epithelial cells (Habibi-Babadi et al., 2010). Studies in *C. elegans*, have found that *sax-1* and *sax-2* act cell autonomously in neurons to limit axonal/dendritic outgrowth (Zallen et al., 2000; Gallegos and Bargmann, 2004) . Similarly in yeast and Drosophila, studies have shown a cell autonomous role for *sax-1* and *sax-2* orthologs in regulating the projection of hypha and dendrites (Du and Novick, 2002; Seiler et al., 2006; Cong et al., 2001; Emoto et al., 2006). How do *sax-1* and *sax-2* regulate branching in VC4/5, AVL, and DVB? Further studies are required to determine whether they have a non cell autonomous role or cell autonomous role in limiting branching, especially in the context of the vulva. A combination of expression studies using *sax-1* and *sax-2* transcriptional and

translational fusions to GFP and cell rescue experiments should provide insight into a cellular site of action.

4.5 Summary

Our characterization of *sax-1* and *sax-2* mutants revealed qualitatively similar morphological phenotypes as previously described in *png-1* mutants such as increased axon extension and excessive branching. The synergistic phenotypes observed between *png-1* and the *sax-1* or *sax-2* mutants suggests that PNG-1 acts in parallel to the NDR kinase pathway to restrict axon outgrowth, extension, and branching in a subset of *C. elegans* neurons. Given that PNG-1 and SAX-1/NDR kinase are evolutionary conserved pathways in diverse organisms, it will be important to investigate the interplay of these two pathways in mammalian cells, especially in neuronal development. These synergistic interactions provided us with the opportunity to indentify components in the *png-1* pathway that also enhance *sax-1/sax-2* branching defects. The *sax-1* enhancer screen yielded three *sens* genes which act like *png-1* to suppress excessive axon branching in VC and DVB motor neurons. The isolation and identification of *sens* genes might provide new insight into *png-1* mediated axon branching and outgrowth. Understanding the mechanisms involved in neuronal development, especially axon outgrowth and branching, may lead to the development of treatments to promote axon regeneration following brain injury, stroke, or neurodegenerative diseases.

References

Acebes A, Ferrus A (2000) Cellular and molecular features of axon collaterals and dendrites. Trends Neurosci 23:557-565.

Adler CE, Fetter RD, Bargmann CI (2006) UNC-6/Netrin induces neuronal asymmetry and defines the site of axon formation. Nat Neurosci 9:511-518.

Aizawa H, Hu SC, Bobb K, Balakrishnan K, Ince G, Gurevich I, Cowan M, Ghosh A (2004) Dendrite development regulated by CREST, a calcium-regulated transcriptional activator. Science 303:197-202.

Altun-Gultekin Z, Andachi Y, Tsalik EL, Pilgrim D, Kohara Y, Hobert O (2001) A regulatory cascade of three homeobox genes, ceh-10, ttx-3 and ceh-23, controls cell fate specification of a defined interneuron class in C. elegans. Development 128:1951-1969.

Araujo SJ, Tear G (2003) Axon guidance mechanisms and molecules: lessons from invertebrates. Nat Rev Neurosci 4:910-922.

Arber S, Barbayannis FA, Hanser H, Schneider C, Stanyon CA, Bernard O, Caroni P (1998) Regulation of actin dynamics through phosphorylation of cofilin by LIM-kinase. Nature 393:805-809.

Bagri A, Cheng HJ, Yaron A, Pleasure SJ, Tessier-Lavigne M (2003) Stereotyped pruning of long hippocampal axon branches triggered by retraction inducers of the semaphorin family. Cell 113:285-299.

Bagri A, Marin O, Plump AS, Mak J, Pleasure SJ, Rubenstein JL, Tessier-Lavigne M (2002) Slit proteins prevent midline crossing and determine the dorsoventral position of major axonal pathways in the mammalian forebrain. Neuron 33:233-248.

Barnes AP, Polleux F (2009) Establishment of axon-dendrite polarity in developing neurons. Annu Rev Neurosci 32:347-381.

Bastmeyer M, O'Leary DD (1996) Dynamics of target recognition by interstitial axon branching along developing cortical axons. J Neurosci 16:1450-1459.

Bastmeyer M, Daston MM, Possel H, O'Leary DD (1998) Collateral branch formation related to cellular structures in the axon tract during corticopontine target recognition. J Comp Neurol 392:1-18.

Bichsel SJ, Tamaskovic R, Stegert MR, Hemmings BA (2004) Mechanism of activation of NDR (nuclear Dbf2-related) protein kinase by the hMOB1 protein. J Biol Chem 279:35228-35235.

Bidlingmaier S, Weiss EL, Seidel C, Drubin DG, Snyder M (2001) The Cbk1p pathway is important for polarized cell growth and cell separation in Saccharomyces cerevisiae. Mol Cell Biol 21:2449-2462.

Bishop AL, Hall A (2000) Rho GTPases and their effector proteins. Biochem J 348 Pt 2:241-255.

Biswas S, Katiyar S, Li G, Zhou X, Lennarz WJ, Schindelin H (2004) The N-terminus of yeast peptide: N-glycanase interacts with the DNA repair protein Rad23. Biochem Biophys Res Commun 323:149-155.

Bloch-Gallego E, Ezan F, Tessier-Lavigne M, Sotelo C (1999) Floor plate and netrin-1 are involved in the migration and survival of inferior olivary neurons. J Neurosci 19:4407-4420.

Blom D, Hirsch C, Stern P, Tortorella D, Ploegh HL (2004) A glycosylated type I membrane protein becomes cytosolic when peptide: N-glycanase is compromised. EMBO J 23:650-658.

Bodmer R, Jan YN (1987) Morphological differentiation of the embryonic peripheral neurons in Drosophila. In: Roux's Arch. Dev. Biol., pp pp. 69-77.

Bos JL, Rehmann H, Wittinghofer A (2007) GEFs and GAPs: critical elements in the control of small G proteins. Cell 129:865-877.

Bouquet C, Nothias F (2007) Molecular mechanisms of axonal growth. Adv Exp Med Biol 621:1-16.

Brenner S (1974) The genetics of Caenorhabditis elegans. Genetics 77:71-94.

Brittis PA, Lu Q, Flanagan JG (2002) Axonal protein synthesis provides a mechanism for localized regulation at an intermediate target. Cell 110:223-235.

Brose K, Tessier-Lavigne M (2000) Slit proteins: key regulators of axon guidance, axonal branching, and cell migration. Curr Opin Neurobiol 10:95-102.

Bulow HE, Berry KL, Topper LH, Peles E, Hobert O (2002) Heparan sulfate proteoglycan-dependent induction of axon branching and axon misrouting by the Kallmann syndrome gene kal-1. Proc Natl Acad Sci U S A 99:6346-6351.

Butler SJ, Tear G (2007) Getting axons onto the right path: the role of transcription factors in axon guidance. Development 134:439-448.

Cameron S, Clark SG, McDermott JB, Aamodt E, Horvitz HR (2002) PAG-3, a Zn-finger transcription factor, determines neuroblast fate in C. elegans. Development 129:1763-1774.

Campbell DS, Holt CE (2001) Chemotropic responses of retinal growth cones mediated by rapid local protein synthesis and degradation. Neuron 32:1013-1026.

Campbell DS, Regan AG, Lopez JS, Tannahill D, Harris WA, Holt CE (2001) Semaphorin 3A elicits stage-dependent collapse, turning, and branching in Xenopus retinal growth cones. J Neurosci 21:8538-8547.

Chan EH, Nousiainen M, Chalamalasetty RB, Schafer A, Nigg EA, Sillje HH (2005) The Ste20-like kinase Mst2 activates the human large tumor suppressor kinase Lats1. Oncogene 24:2076-2086.

Chang C, Adler CE, Krause M, Clark SG, Gertler FB, Tessier-Lavigne M, Bargmann CI (2006) MIG-10/lamellipodin and AGE-1/PI3K promote axon guidance and outgrowth in response to slit and netrin. Curr Biol 16:854-862.

Charron F, Tessier-Lavigne M (2007) The Hedgehog, TGF-beta/BMP and Wnt families of morphogens in axon guidance. Adv Exp Med Biol 621:116-133.

Chen YM, Wang QJ, Hu HS, Yu PC, Zhu J, Drewes G, Piwnica-Worms H, Luo ZG (2006) Microtubule affinity-regulating kinase 2 functions downstream of the PAR-3/PAR-6/atypical PKC complex in regulating hippocampal neuronal polarity. Proc Natl Acad Sci U S A 103:8534-8539.

Chen YY, Hehr CL, Atkinson-Leadbeater K, Hocking JC, McFarlane S (2007) Targeting of retinal axons requires the metalloproteinase ADAM10. J Neurosci 27:8448-8456.

Chiba S, Ikeda M, Katsunuma K, Ohashi K, Mizuno K (2009) MST2- and Furry-mediated activation of NDR1 kinase is critical for precise alignment of mitotic chromosomes. Curr Biol 19:675-681.

Clark SG, Chiu C (2003) C. elegans ZAG-1, a Zn-finger-homeodomain protein, regulates axonal development and neuronal differentiation. Development 130:3781-3794.

Cohen-Cory S, Fraser SE (1995) Effects of brain-derived neurotrophic factor on optic axon branching and remodelling in vivo. Nature 378:192-196.

Colavita A, Tessier-Lavigne M (2003) A Neurexin-related protein, BAM-2, terminates axonal branches in C. elegans. Science 302:293-296.

Colman-Lerner A, Chin TE, Brent R (2001) Yeast Cbk1 and Mob2 activate daughter-specific genetic programs to induce asymmetric cell fates. Cell 107:739-750.

Cong J, Geng W, He B, Liu J, Charlton J, Adler PN (2001) The furry gene of Drosophila is important for maintaining the integrity of cellular extensions during morphogenesis. Development 128:2793-2802.

Corty MM, Matthews BJ, Grueber WB (2009) Molecules and mechanisms of dendrite development in Drosophila. Development 136:1049-1061.

Craig AM, Banker G (1994) Neuronal polarity. Annu Rev Neurosci 17:267-310.

Das M, Wiley DJ, Chen X, Shah K, Verde F (2009) The conserved NDR kinase Orb6 controls polarized cell growth by spatial regulation of the small GTPase Cdc42. Curr Biol 19:1314-1319.

Davenport RW, Thies E, Cohen ML (1999) Neuronal growth cone collapse triggers lateral extensions along trailing axons. Nat Neurosci 2:254-259.

Dent EW, Kalil K (2001) Axon branching requires interactions between dynamic microtubules and actin filaments. J Neurosci 21:9757-9769.

Dent EW, Tang F, Kalil K (2003) Axon guidance by growth cones and branches: common cytoskeletal and signaling mechanisms. Neuroscientist 9:343-353.

Dent EW, Barnes AM, Tang F, Kalil K (2004) Netrin-1 and semaphorin 3A promote or inhibit cortical axon branching, respectively, by reorganization of the cytoskeleton. J Neurosci 24:3002-3012.

Dent EW, Callaway JL, Szebenyi G, Baas PW, Kalil K (1999) Reorganization and movement of microtubules in axonal growth cones and developing interstitial branches. J Neurosci 19:8894-8908.

Devroe E, Erdjument-Bromage H, Tempst P, Silver PA (2004) Human Mob proteins regulate the NDR1 and NDR2 serine-threonine kinases. J Biol Chem 279:24444-24451.

Dickson BJ (2002) Molecular mechanisms of axon guidance. Science 298:1959-1964.

Dotti CG, Sullivan CA, Banker GA (1988) The establishment of polarity by hippocampal neurons in culture. J Neurosci 8:1454-1468.

Du LL, Novick P (2002) Pag1p, a novel protein associated with protein kinase Cbk1p, is required for cell morphogenesis and proliferation in Saccharomyces cerevisiae. Mol Biol Cell 13:503-514.

Emoto K, Parrish JZ, Jan LY, Jan YN (2006) The tumour suppressor Hippo acts with the NDR kinases in dendritic tiling and maintenance. Nature 443:210-213.

Emoto K, He Y, Ye B, Grueber WB, Adler PN, Jan LY, Jan YN (2004) Control of dendritic branching and tiling by the Tricornered-kinase/Furry signaling pathway in Drosophila sensory neurons. Cell 119:245-256.

Esch T, Lemmon V, Banker G (1999) Local presentation of substrate molecules directs axon specification by cultured hippocampal neurons. J Neurosci 19:6417-6426.

Etienne-Manneville S, Hall A (2002) Rho GTPases in cell biology. Nature 420:629-635.

Fambrough D, Pan D, Rubin GM, Goodman CS (1996) The cell surface metalloprotease/disintegrin Kuzbanian is required for axonal extension in Drosophila. Proc Natl Acad Sci U S A 93:13233-13238.

Fay D, Bender A (2006) Genetic mapping and manipulation: chapter 4--SNPs: introduction and two-point mapping. WormBook:1-7.

Fink CC, Bayer KU, Myers JW, Ferrell JE, Jr., Schulman H, Meyer T (2003) Selective regulation of neurite extension and synapse formation by the beta but not the alpha isoform of CaMKII. Neuron 39:283-297.

Fujita H, Katoh H, Ishikawa Y, Mori K, Negishi M (2002) Rapostlin is a novel effector of Rnd2 GTPase inducing neurite branching. J Biol Chem 277:45428-45434.

Galko MJ, Tessier-Lavigne M (2000) Function of an axonal chemoattractant modulated by metalloprotease activity. Science 289:1365-1367.

Gallegos ME, Bargmann CI (2004) Mechanosensory neurite termination and tiling depend on SAX-2 and the SAX-1 kinase. Neuron 44:239-249.

Gallo G, Letourneau PC (1998) Localized sources of neurotrophins initiate axon collateral sprouting. J Neurosci 18:5403-5414.

Gao FB (2007) Molecular and cellular mechanisms of dendritic morphogenesis. Curr Opin Neurobiol 17:525-532.

Garriga G, Desai C, Horvitz HR (1993) Cell interactions control the direction of outgrowth, branching and fasciculation of the HSN axons of Caenorhabditis elegans. Development 117:1071-1087.

Gaudilliere B, Konishi Y, de la Iglesia N, Yao G, Bonni A (2004) A CaMKII-NeuroD signaling pathway specifies dendritic morphogenesis. Neuron 41:229-241.

Geng W, He B, Wang M, Adler PN (2000) The tricornered gene, which is required for the integrity of epidermal cell extensions, encodes the Drosophila nuclear DBF2-related kinase. Genetics 156:1817-1828.

Georges PC, Hadzimichalis NM, Sweet ES, Firestein BL (2008) The yin-yang of dendrite morphology: unity of actin and microtubules. Mol Neurobiol 38:270-284.

Gitai Z, Yu TW, Lundquist EA, Tessier-Lavigne M, Bargmann CI (2003) The netrin receptor UNC-40/DCC stimulates axon attraction and outgrowth through enabled and, in parallel, Rac and UNC-115/AbLIM. Neuron 37:53-65.

Gomez TM, Spitzer NC (1999) In vivo regulation of axon extension and pathfinding by growth-cone calcium transients. Nature 397:350-355.

Gonzalez-Billault C, Jimenez-Mateos EM, Caceres A, Diaz-Nido J, Wandosell F, Avila J (2004) Microtubule-associated protein 1B function during normal development, regeneration, and pathological conditions in the nervous system. J Neurobiol 58:48-59.

Gonzalez-Novo A, Labrador L, Pablo-Hernando ME, Correa-Bordes J, Sanchez M, Jimenez J, de Aldana CR (2009) Dbf2 is essential for cytokinesis and correct mitotic spindle formation in Candida albicans. Mol Microbiol.

Goold RG, Owen R, Gordon-Weeks PR (1999) Glycogen synthase kinase 3beta phosphorylation of microtubule-associated protein 1B regulates the stability of microtubules in growth cones. J Cell Sci 112 (Pt 19):3373-3384.

Grueber WB, Jan LY, Jan YN (2002) Tiling of the Drosophila epidermis by multidendritic sensory neurons. Development 129:2867-2878.

Grueber WB, Jan LY, Jan YN (2003) Different levels of the homeodomain protein cut regulate distinct dendrite branching patterns of Drosophila multidendritic neurons. Cell 112:805-818.

Habibi-Babadi N, Su A, de Carvalho CE, Colavita A (2010) The N-glycanase png-1 acts to limit axon branching during organ formation in Caenorhabditis elegans. J Neurosci 30:1766-1776.

Halloran MC, Kalil K (1994) Dynamic behaviors of growth cones extending in the corpus callosum of living cortical brain slices observed with video microscopy. J Neurosci 14:2161-2177.

Hand R, Bortone D, Mattar P, Nguyen L, Heng JI, Guerrier S, Boutt E, Peters E, Barnes AP, Parras C, Schuurmans C, Guillemot F, Polleux F (2005) Phosphorylation of Neurogenin2 specifies the migration properties and the dendritic morphology of pyramidal neurons in the neocortex. Neuron 48:45-62.

Hanks SK, Hunter T (1995) Protein kinases 6. The eukaryotic protein kinase superfamily: kinase (catalytic) domain structure and classification. FASEB J 9:576-596.

Hansen D, Wilson-Berry L, Dang T, Schedl T (2004) Control of the proliferation versus meiotic development decision in the C. elegans germline through regulation of GLD-1 protein accumulation. Development 131:93-104.

Hao JC, Yu TW, Fujisawa K, Culotti JG, Gengyo-Ando K, Mitani S, Moulder G, Barstead R, Tessier-Lavigne M, Bargmann CI (2001) C. elegans slit acts in midline, dorsal-ventral, and anterior-posterior guidance via the SAX-3/Robo receptor. Neuron 32:25-38.

Harrington RJ, Gutch MJ, Hengartner MO, Tonks NK, Chisholm AD (2002) The C. elegans LAR-like receptor tyrosine phosphatase PTP-3 and the VAB-1 Eph receptor tyrosine kinase have partly redundant functions in morphogenesis. Development 129:2141-2153.

Harris R, Sabatelli LM, Seeger MA (1996) Guidance cues at the Drosophila CNS midline: identification and characterization of two Drosophila Netrin/UNC-6 homologs. Neuron 17:217-228.

Hattori M, Osterfield M, Flanagan JG (2000) Regulated cleavage of a contact-mediated axon repellent. Science 289:1360-1365.

Hattori Y, Sugimura K, Uemura T (2007) Selective expression of Knot/Collier, a transcriptional regulator of the EBF/Olf-1 family, endows the Drosophila sensory system with neuronal class-specific elaborated dendritic patterns. Genes Cells 12:1011-1022.

He B, Adler PN (2002) The genetic control of arista lateral morphogenesis in Drosophila. Dev Genes Evol 212:218-229.

He Y, Fang X, Emoto K, Jan YN, Adler PN (2005a) The tricornered Ser/Thr protein kinase is regulated by phosphorylation and interacts with furry during Drosophila wing hair development. Mol Biol Cell 16:689-700.

He Y, Emoto K, Fang X, Ren N, Tian X, Jan YN, Adler PN (2005b) Drosophila Mob family proteins interact with the related tricornered (Trc) and warts (Wts) kinases. Mol Biol Cell 16:4139-4152.

Hedgecock EM, Culotti JG, Hall DH (1990) The unc-5, unc-6, and unc-40 genes guide circumferential migrations of pioneer axons and mesodermal cells on the epidermis in C. elegans. Neuron 4:61-85.

Hehr CL, Hocking JC, McFarlane S (2005) Matrix metalloproteinases are required for retinal ganglion cell axon guidance at select decision points. Development 132:3371-3379.

Henley J, Poo MM (2004) Guiding neuronal growth cones using Ca2+ signals. Trends Cell Biol 14:320-330.

Hergovich A, Bichsel SJ, Hemmings BA (2005) Human NDR kinases are rapidly activated by MOB proteins through recruitment to the plasma membrane and phosphorylation. Mol Cell Biol 25:8259-8272.

Hergovich A, Stegert MR, Schmitz D, Hemmings BA (2006) NDR kinases regulate essential cell processes from yeast to humans. Nat Rev Mol Cell Biol 7:253-264.

Hergovich A, Lamla S, Nigg EA, Hemmings BA (2007) Centrosome-associated NDR kinase regulates centrosome duplication. Mol Cell 25:625-634.

Herman RK, Yochem J (2005) Genetic enhancers. WormBook:1-11.

Hing H, Xiao J, Harden N, Lim L, Zipursky SL (1999) Pak functions downstream of Dock to regulate photoreceptor axon guidance in Drosophila. Cell 97:853-863.

Hirsch C, Blom D, Ploegh HL (2003) A role for N-glycanase in the cytosolic turnover of glycoproteins. EMBO J 22:1036-1046.

Hirsch C, Misaghi S, Blom D, Pacold ME, Ploegh HL (2004) Yeast N-glycanase distinguishes between native and non-native glycoproteins. EMBO Rep 5:201-206.

Hobert O, Tessmar K, Ruvkun G (1999) The Caenorhabditis elegans lim-6 LIM homeobox gene regulates neurite outgrowth and function of particular GABAergic neurons. Development 126:1547-1562.

Hong K, Nishiyama M, Henley J, Tessier-Lavigne M, Poo M (2000) Calcium signalling in the guidance of nerve growth by netrin-1. Nature 403:93-98.

Hu G, Zhang S, Vidal M, Baer JL, Xu T, Fearon ER (1997) Mammalian homologs of seven in absentia regulate DCC via the ubiquitin-proteasome pathway. Genes Dev 11:2701-2714.

Hu H, Marton TF, Goodman CS (2001) Plexin B mediates axon guidance in Drosophila by simultaneously inhibiting active Rac and enhancing RhoA signaling. Neuron 32:39-51.

Huang J, Wu S, Barrera J, Matthews K, Pan D (2005) The Hippo signaling pathway coordinately regulates cell proliferation and apoptosis by inactivating Yorkie, the Drosophila Homolog of YAP. Cell 122:421-434.

Huang LS, Sternberg PW (2006) Genetic dissection of developmental pathways. WormBook:1-19.

Huber AB, Kolodkin AL, Ginty DD, Cloutier JF (2003) Signaling at the growth cone: ligand-receptor complexes and the control of axon growth and guidance. Annu Rev Neurosci 26:509-563.

Inagaki N, Chihara K, Arimura N, Menager C, Kawano Y, Matsuo N, Nishimura T, Amano M, Kaibuchi K (2001) CRMP-2 induces axons in cultured hippocampal neurons. Nat Neurosci 4:781-782.

Ishii N, Wadsworth WG, Stern BD, Culotti JG, Hedgecock EM (1992) UNC-6, a laminin-related protein, guides cell and pioneer axon migrations in C. elegans. Neuron 9:873-881.

Ishizaki T, Maekawa M, Fujisawa K, Okawa K, Iwamatsu A, Fujita A, Watanabe N, Saito Y, Kakizuka A, Morii N, Narumiya S (1996) The small GTP-binding protein Rho binds to and activates a 160 kDa Ser/Thr protein kinase homologous to myotonic dystrophy kinase. EMBO J 15:1885-1893.

Jia L, Emmons SW (2006) Genes that control ray sensory neuron axon development in the Caenorhabditis elegans male. Genetics 173:1241-1258.

Jiang H, Guo W, Liang X, Rao Y (2005) Both the establishment and the maintenance of neuronal polarity require active mechanisms: critical roles of GSK-3beta and its upstream regulators. Cell 120:123-135.

Jin Z, Strittmatter SM (1997) Rac1 mediates collapsin-1-induced growth cone collapse. J Neurosci 17:6256-6263.

Jinushi-Nakao S, Arvind R, Amikura R, Kinameri E, Liu AW, Moore AW (2007) Knot/Collier and cut control different aspects of dendrite cytoskeleton and synergize to define final arbor shape. Neuron 56:963-978.

Jorgensen EM, Mango SE (2002) The art and design of genetic screens: caenorhabditis elegans. Nat Rev Genet 3:356-369.

Joshi S, Katiyar S, Lennarz WJ (2005) Misfolding of glycoproteins is a prerequisite for peptide: N-glycanase mediated deglycosylation. FEBS Lett 579:823-826.

Kadyk LC, Kimble J (1998) Genetic regulation of entry into meiosis in Caenorhabditis elegans. Development 125:1803-1813.

Kalil K, Szebenyi G, Dent EW (2000) Common mechanisms underlying growth cone guidance and axon branching. J Neurobiol 44:145-158.

Kaprielian Z, Runko E, Imondi R (2001) Axon guidance at the midline choice point. Dev Dyn 221:154-181.

Katiyar S, Li G, Lennarz WJ (2004) A complex between peptide:N-glycanase and two proteasome-linked proteins suggests a mechanism for the degradation of misfolded glycoproteins. Proc Natl Acad Sci U S A 101:13774-13779.

Katiyar S, Joshi S, Lennarz WJ (2005) The retrotranslocation protein Derlin-1 binds peptide:N-glycanase to the endoplasmic reticulum. Mol Biol Cell 16:4584-4594.

Kato T, Kawahara A, Ashida H, Yamamoto K (2007) Unique peptide:N-glycanase of Caenorhabditis elegans has activity of protein disulphide reductase as well as of deglycosylation. J Biochem 142:175-181.

Kaufmann N, Wills ZP, Van Vactor D (1998) Drosophila Rac1 controls motor axon guidance. Development 125:453-461.

Keino-Masu K, Masu M, Hinck L, Leonardo ED, Chan SS, Culotti JG, Tessier-Lavigne M (1996) Deleted in Colorectal Cancer (DCC) encodes a netrin receptor. Cell 87:175-185.

Keleman K, Dickson BJ (2001) Short- and long-range repulsion by the Drosophila Unc5 netrin receptor. Neuron 32:605-617.

Keleman K, Ribeiro C, Dickson BJ (2005) Comm function in commissural axon guidance: cell-autonomous sorting of Robo in vivo. Nat Neurosci 8:156-163.

Keleman K, Rajagopalan S, Cleppien D, Teis D, Paiha K, Huber LA, Technau GM, Dickson BJ (2002) Comm sorts robo to control axon guidance at the Drosophila midline. Cell 110:415-427.

Kidd T, Bland KS, Goodman CS (1999) Slit is the midline repellent for the robo receptor in Drosophila. Cell 96:785-794.

Kidd T, Brose K, Mitchell KJ, Fetter RD, Tessier-Lavigne M, Goodman CS, Tear G (1998) Roundabout controls axon crossing of the CNS midline and defines a novel subfamily of evolutionarily conserved guidance receptors. Cell 92:205-215.

Kim I, Ahn J, Liu C, Tanabe K, Apodaca J, Suzuki T, Rao H (2006a) The Png1-Rad23 complex regulates glycoprotein turnover. J Cell Biol 172:211-219.

Kim MD, Jan LY, Jan YN (2006b) The bHLH-PAS protein Spineless is necessary for the diversification of dendrite morphology of Drosophila dendritic arborization neurons. Genes Dev 20:2806-2819.

Knobel KM, Davis WS, Jorgensen EM, Bastiani MJ (2001) UNC-119 suppresses axon branching in C. elegans. Development 128:4079-4092.

Kolodziej PA, Timpe LC, Mitchell KJ, Fried SR, Goodman CS, Jan LY, Jan YN (1996) frazzled encodes a Drosophila member of the DCC immunoglobulin subfamily and is required for CNS and motor axon guidance. Cell 87:197-204.

Kuang RZ, Kalil K (1994) Development of specificity in corticospinal connections by axon collaterals branching selectively into appropriate spinal targets. J Comp Neurol 344:270-282.

Kuhn TB, Meberg PJ, Brown MD, Bernstein BW, Minamide LS, Jensen JR, Okada K, Soda EA, Bamburg JR (2000) Regulating actin dynamics in neuronal growth cones by ADF/cofilin and rho family GTPases. J Neurobiol 44:126-144.

Kurischko C, Weiss G, Ottey M, Luca FC (2005) A role for the Saccharomyces cerevisiae regulation of Ace2 and polarized morphogenesis signaling network in cell integrity. Genetics 171:443-455.

Kurischko C, Kuravi VK, Wannissorn N, Nazarov PA, Husain M, Zhang C, Shokat KM, McCaffery JM, Luca FC (2008) The yeast LATS/Ndr kinase Cbk1 regulates growth via Golgi-dependent glycosylation and secretion. Mol Biol Cell 19:5559-5578.

Lebrand C, Dent EW, Strasser GA, Lanier LM, Krause M, Svitkina TM, Borisy GG, Gertler FB (2004) Critical role of Ena/VASP proteins for filopodia formation in neurons and in function downstream of netrin-1. Neuron 42:37-49.

Lee JH, Choi JM, Lee C, Yi KJ, Cho Y (2005) Structure of a peptide:N-glycanase-Rad23 complex: insight into the deglycosylation for denatured glycoproteins. Proc Natl Acad Sci U S A 102:9144-9149.

Leonardo ED, Hinck L, Masu M, Keino-Masu K, Ackerman SL, Tessier-Lavigne M (1997) Vertebrate homologues of C. elegans UNC-5 are candidate netrin receptors. Nature 386:833-838.

Leung-Hagesteijn C, Spence AM, Stern BD, Zhou Y, Su MW, Hedgecock EM, Culotti JG (1992) UNC-5, a transmembrane protein with immunoglobulin and thrombospondin type 1 domains, guides cell and pioneer axon migrations in C. elegans. Cell 71:289-299.

Leung T, Manser E, Tan L, Lim L (1995) A novel serine/threonine kinase binding the Ras-related RhoA GTPase which translocates the kinase to peripheral membranes. J Biol Chem 270:29051-29054.

Levy-Strumpf N, Culotti JG (2007) VAB-8, UNC-73 and MIG-2 regulate axon polarity and cell migration functions of UNC-40 in C. elegans. Nat Neurosci 10:161-168.

Li C, Chalfie M (1990) Organogenesis in C. elegans: positioning of neurons and muscles in the egg-laying system. Neuron 4:681-695.

Li G, Zhou X, Zhao G, Schindelin H, Lennarz WJ (2005) Multiple modes of interaction of the deglycosylation enzyme, mouse peptide N-glycanase, with the proteasome. Proc Natl Acad Sci U S A 102:15809-15814.

Li G, Zhao G, Zhou X, Schindelin H, Lennarz WJ (2006) The AAA ATPase p97 links peptide N-glycanase to the endoplasmic reticulum-associated E3 ligase autocrine motility factor receptor. Proc Natl Acad Sci U S A 103:8348-8353.

Li R, Gundersen GG (2008) Beyond polymer polarity: how the cytoskeleton builds a polarized cell. Nat Rev Mol Cell Biol 9:860-873.

Li W, Wang F, Menut L, Gao FB (2004) BTB/POZ-zinc finger protein abrupt suppresses dendritic branching in a neuronal subtype-specific and dosage-dependent manner. Neuron 43:823-834.

Li X, Saint-Cyr-Proulx E, Aktories K, Lamarche-Vane N (2002) Rac1 and Cdc42 but not RhoA or Rho kinase activities are required for neurite outgrowth induced by the Netrin-1 receptor DCC (deleted in colorectal cancer) in N1E-115 neuroblastoma cells. J Biol Chem 277:15207-15214.

Lin CH, Thompson CA, Forscher P (1994) Cytoskeletal reorganization underlying growth cone motility. Curr Opin Neurobiol 4:640-647.

Lowery LA, Van Vactor D (2009) The trip of the tip: understanding the growth cone machinery. Nat Rev Mol Cell Biol 10:332-343.

Luca FC, Mody M, Kurischko C, Roof DM, Giddings TH, Winey M (2001) Saccharomyces cerevisiae Mob1p is required for cytokinesis and mitotic exit. Mol Cell Biol 21:6972-6983.

Luo L (2000) Rho GTPases in neuronal morphogenesis. Nat Rev Neurosci 1:173-180.

Lykissas MG, Batistatou AK, Charalabopoulos KA, Beris AE (2007) The role of neurotrophins in axonal growth, guidance, and regeneration. Curr Neurovasc Res 4:143-151.

Maekawa M, Ishizaki T, Boku S, Watanabe N, Fujita A, Iwamatsu A, Obinata T, Ohashi K, Mizuno K, Narumiya S (1999) Signaling from Rho to the actin cytoskeleton through protein kinases ROCK and LIM-kinase. Science 285:895-898.

Maerz S, Ziv C, Vogt N, Helmstaedt K, Cohen N, Gorovits R, Yarden O, Seiler S (2008) The nuclear Dbf2-related kinase COT1 and the mitogen-activated protein kinases MAK1 and MAK2 genetically interact to regulate filamentous growth, hyphal fusion and sexual development in Neurospora crassa. Genetics 179:1313-1325.

Mah AS, Jang J, Deshaies RJ (2001) Protein kinase Cdc15 activates the Dbf2-Mob1 kinase complex. Proc Natl Acad Sci U S A 98:7325-7330.

Manser E, Leung T, Salihuddin H, Zhao ZS, Lim L (1994) A brain serine/threonine protein kinase activated by Cdc42 and Rac1. Nature 367:40-46.

Masland RH (2004) Neuronal cell types. Curr Biol 14:R497-500.

Mazanka E, Alexander J, Yeh BJ, Charoenpong P, Lowery DM, Yaffe M, Weiss EL (2008) The NDR/LATS family kinase Cbk1 directly controls transcriptional asymmetry. PLoS Biol 6:e203.

McNemar MD, Fonzi WA (2002) Conserved serine/threonine kinase encoded by CBK1 regulates expression of several hypha-associated transcripts and genes encoding cell wall proteins in Candida albicans. J Bacteriol 184:2058-2061.

Mehta N, Loria PM, Hobert O (2004) A genetic screen for neurite outgrowth mutants in Caenorhabditis elegans reveals a new function for the F-box ubiquitin ligase component LIN-23. Genetics 166:1253-1267.

Menager C, Arimura N, Fukata Y, Kaibuchi K (2004) PIP3 is involved in neuronal polarization and axon formation. J Neurochem 89:109-118.

Meusser B, Hirsch C, Jarosch E, Sommer T (2005) ERAD: the long road to destruction. Nat Cell Biol 7:766-772.

Millward T, Cron P, Hemmings BA (1995) Molecular cloning and characterization of a conserved nuclear serine(threonine) protein kinase. Proc Natl Acad Sci U S A 92:5022-5026.

Ming G, Henley J, Tessier-Lavigne M, Song H, Poo M (2001) Electrical activity modulates growth cone guidance by diffusible factors. Neuron 29:441-452.

Mitchell KJ, Doyle JL, Serafini T, Kennedy TE, Tessier-Lavigne M, Goodman CS, Dickson BJ (1996) Genetic analysis of Netrin genes in Drosophila: Netrins guide CNS commissural axons and peripheral motor axons. Neuron 17:203-215.

Mohl DA, Huddleston MJ, Collingwood TS, Annan RS, Deshaies RJ (2009) Dbf2-Mob1 drives relocalization of protein phosphatase Cdc14 to the cytoplasm during exit from mitosis. J Cell Biol 184:527-539.

Moore AW, Jan LY, Jan YN (2002) hamlet, a binary genetic switch between single- and multiple- dendrite neuron morphology. Science 297:1355-1358.

Myat A, Henry P, McCabe V, Flintoft L, Rotin D, Tear G (2002) Drosophila Nedd4, a ubiquitin ligase, is recruited by Commissureless to control cell surface levels of the roundabout receptor. Neuron 35:447-459.

Nakayama AY, Harms MB, Luo L (2000) Small GTPases Rac and Rho in the maintenance of dendritic spines and branches in hippocampal pyramidal neurons. J Neurosci 20:5329-5338.

Nash B, Colavita A, Zheng H, Roy PJ, Culotti JG (2000) The forkhead transcription factor UNC-130 is required for the graded spatial expression of the UNC-129 TGF-beta guidance factor in C. elegans. Genes Dev 14:2486-2500.

Nelson B, Kurischko C, Horecka J, Mody M, Nair P, Pratt L, Zougman A, McBroom LD, Hughes TR, Boone C, Luca FC (2003) RAM: a conserved signaling network that regulates Ace2p transcriptional activity and polarized morphogenesis. Mol Biol Cell 14:3782-3803.

Neumann H, Schweigreiter R, Yamashita T, Rosenkranz K, Wekerle H, Barde YA (2002) Tumor necrosis factor inhibits neurite outgrowth and branching of hippocampal neurons by a rho-dependent mechanism. J Neurosci 22:854-862.

Ng J, Nardine T, Harms M, Tzu J, Goldstein A, Sun Y, Dietzl G, Dickson BJ, Luo L (2002) Rac GTPases control axon growth, guidance and branching. Nature 416:442-447.

Nishimura T, Kato K, Yamaguchi T, Fukata Y, Ohno S, Kaibuchi K (2004) Role of the PAR-3-KIF3 complex in the establishment of neuronal polarity. Nat Cell Biol 6:328-334.

Nishimura T, Yamaguchi T, Kato K, Yoshizawa M, Nabeshima Y, Ohno S, Hoshino M, Kaibuchi K (2005) PAR-6-PAR-3 mediates Cdc42-induced Rac activation through the Rac GEFs STEF/Tiam1. Nat Cell Biol 7:270-277.

O'Donnell M, Chance RK, Bashaw GJ (2009) Axon growth and guidance: receptor regulation and signal transduction. Annu Rev Neurosci 32:383-412.

O'Leary DD, Terashima T (1988) Cortical axons branch to multiple subcortical targets by interstitial axon budding: implications for target recognition and "waiting periods". Neuron 1:901-910.

O'Leary DD, Bicknese AR, De Carlos JA, Heffner CD, Koester SE, Kutka LJ, Terashima T (1990) Target selection by cortical axons: alternative mechanisms to establish axonal connections in the developing brain. Cold Spring Harb Symp Quant Biol 55:453-468.

Ohashi K, Nagata K, Maekawa M, Ishizaki T, Narumiya S, Mizuno K (2000) Rho-associated kinase ROCK activates LIM-kinase 1 by phosphorylation at threonine 508 within the activation loop. J Biol Chem 275:3577-3582.

Park H, Suzuki T, Lennarz WJ (2001) Identification of proteins that interact with mammalian peptide:N-glycanase and implicate this hydrolase in the proteasome-dependent pathway for protein degradation. Proc Natl Acad Sci U S A 98:11163-11168.

Parrish JZ, Kim MD, Jan LY, Jan YN (2006) Genome-wide analyses identify transcription factors required for proper morphogenesis of Drosophila sensory neuron dendrites. Genes Dev 20:820-835.

Przyborski SA, Knowles BB, Ackerman SL (1998) Embryonic phenotype of Unc5h3 mutant mice suggests chemorepulsion during the formation of the rostral cerebellar boundary. Development 125:41-50.

Quinn CC, Wadsworth WG (2008) Axon guidance: asymmetric signaling orients polarized outgrowth. Trends Cell Biol 18:597-603.

Raper JA (2000) Semaphorins and their receptors in vertebrates and invertebrates. Curr Opin Neurobiol 10:88-94.

Reber M, Hindges R, Lemke G (2007) Eph receptors and ephrin ligands in axon guidance. Adv Exp Med Biol 621:32-49.

Redmond L, Kashani AH, Ghosh A (2002) Calcium regulation of dendritic growth via CaM kinase IV and CREB-mediated transcription. Neuron 34:999-1010.

Rodriguez OC, Schaefer AW, Mandato CA, Forscher P, Bement WM, Waterman-Storer CM (2003) Conserved microtubule-actin interactions in cell movement and morphogenesis. Nat Cell Biol 5:599-609.

Rohatgi R, Ma L, Miki H, Lopez M, Kirchhausen T, Takenawa T, Kirschner MW (1999) The interaction between N-WASP and the Arp2/3 complex links Cdc42-dependent signals to actin assembly. Cell 97:221-231.

Rothberg JM, Jacobs JR, Goodman CS, Artavanis-Tsakonas S (1990) slit: an extracellular protein necessary for development of midline glia and commissural axon pathways contains both EGF and LRR domains. Genes Dev 4:2169-2187.

Ruchhoeft ML, Ohnuma S, McNeill L, Holt CE, Harris WA (1999) The neuronal architecture of Xenopus retinal ganglion cells is sculpted by rho-family GTPases in vivo. J Neurosci 19:8454-8463.

Schafer WF (2006) Genetics of egg-laying in worms. Annu Rev Genet 40:487-509.

Schwamborn JC, Puschel AW (2004) The sequential activity of the GTPases Rap1B and Cdc42 determines neuronal polarity. Nat Neurosci 7:923-929.

Seiler S, Plamann M (2003) The genetic basis of cellular morphogenesis in the filamentous fungus Neurospora crassa. Mol Biol Cell 14:4352-4364.

Seiler S, Vogt N, Ziv C, Gorovits R, Yarden O (2006) The STE20/germinal center kinase POD6 interacts with the NDR kinase COT1 and is involved in polar tip extension in Neurospora crassa. Mol Biol Cell 17:4080-4092.

Serafini T, Colamarino SA, Leonardo ED, Wang H, Beddington R, Skarnes WC, Tessier-Lavigne M (1996) Netrin-1 is required for commissural axon guidance in the developing vertebrate nervous system. Cell 87:1001-1014.

Shekarabi M, Kennedy TE (2002) The netrin-1 receptor DCC promotes filopodia formation and cell spreading by activating Cdc42 and Rac1. Mol Cell Neurosci 19:1-17.

Shelly M, Cancedda L, Heilshorn S, Sumbre G, Poo MM (2007) LKB1/STRAD promotes axon initiation during neuronal polarization. Cell 129:565-577.

Shi SH, Jan LY, Jan YN (2003) Hippocampal neuronal polarity specified by spatially localized mPar3/mPar6 and PI 3-kinase activity. Cell 112:63-75.

Shi SH, Cheng T, Jan LY, Jan YN (2004) APC and GSK-3beta are involved in mPar3 targeting to the nascent axon and establishment of neuronal polarity. Curr Biol 14:2025-2032.

Song HJ, Ming GL, Poo MM (1997) cAMP-induced switching in turning direction of nerve growth cones. Nature 388:275-279.

Sperber BR, Leight S, Goedert M, Lee VM (1995) Glycogen synthase kinase-3 beta phosphorylates tau protein at multiple sites in intact cells. Neurosci Lett 197:149-153.

Stegert MR, Tamaskovic R, Bichsel SJ, Hergovich A, Hemmings BA (2004) Regulation of NDR2 protein kinase by multi-site phosphorylation and the S100B calcium-binding protein. J Biol Chem 279:23806-23812.

Stegert MR, Hergovich A, Tamaskovic R, Bichsel SJ, Hemmings BA (2005) Regulation of NDR protein kinase by hydrophobic motif phosphorylation mediated by the mammalian Ste20-like kinase MST3. Mol Cell Biol 25:11019-11029.

Stoothoff WH, Johnson GV (2005) Tau phosphorylation: physiological and pathological consequences. Biochim Biophys Acta 1739:280-297.

Sugimura K, Satoh D, Estes P, Crews S, Uemura T (2004) Development of morphological diversity of dendrites in Drosophila by the BTB-zinc finger protein abrupt. Neuron 43:809-822.

Suzuki T (2007) Cytoplasmic peptide:N-glycanase and catabolic pathway for free N-glycans in the cytosol. Semin Cell Dev Biol 18:762-769.

Suzuki T, Park H, Lennarz WJ (2002) Cytoplasmic peptide:N-glycanase (PNGase) in eukaryotic cells: occurrence, primary structure, and potential functions. FASEB J 16:635-641.

Suzuki T, Park H, Kitajima K, Lennarz WJ (1998) Peptides glycosylated in the endoplasmic reticulum of yeast are subsequently deglycosylated by a soluble peptide: N-glycanase activity. J Biol Chem 273:21526-21530.

Suzuki T, Park H, Kwofie MA, Lennarz WJ (2001a) Rad23 provides a link between the Png1 deglycosylating enzyme and the 26 S proteasome in yeast. J Biol Chem 276:21601-21607.

Suzuki T, Park H, Till EA, Lennarz WJ (2001b) The PUB domain: a putative protein-protein interaction domain implicated in the ubiquitin-proteasome pathway. Biochem Biophys Res Commun 287:1083-1087.

Suzuki T, Seko A, Kitajima K, Inoue Y, Inoue S (1994) Purification and enzymatic properties of peptide:N-glycanase from C3H mouse-derived L-929 fibroblast cells. Possible widespread occurrence of post-translational remodification of proteins by N-deglycosylation. J Biol Chem 269:17611-17618.

Suzuki T, Kitajima K, Emori Y, Inoue Y, Inoue S (1997) Site-specific de-N-glycosylation of diglycosylated ovalbumin in hen oviduct by endogenous peptide: N-glycanase as a quality control system for newly synthesized proteins. Proc Natl Acad Sci U S A 94:6244-6249.

Suzuki T, Park H, Hollingsworth NM, Sternglanz R, Lennarz WJ (2000) PNG1, a yeast gene encoding a highly conserved peptide:N-glycanase. J Cell Biol 149:1039-1052.

Suzuki T, Tanabe K, Hara I, Taniguchi N, Colavita A (2007) Dual enzymatic properties of the cytoplasmic peptide: N-glycanase in C. elegans. Biochem Biophys Res Commun 358:837-841.

Szebenyi G, Callaway JL, Dent EW, Kalil K (1998) Interstitial branches develop from active regions of the axon demarcated by the primary growth cone during pausing behaviors. J Neurosci 18:7930-7940.

Szebenyi G, Dent EW, Callaway JL, Seys C, Lueth H, Kalil K (2001) Fibroblast growth factor-2 promotes axon branching of cortical neurons by influencing morphology and behavior of the primary growth cone. J Neurosci 21:3932-3941.

Tamaskovic R, Bichsel SJ, Rogniaux H, Stegert MR, Hemmings BA (2003) Mechanism of Ca2+-mediated regulation of NDR protein kinase through autophosphorylation and phosphorylation by an upstream kinase. J Biol Chem 278:6710-6718.

Tanaka E, Sabry J (1995) Making the connection: cytoskeletal rearrangements during growth cone guidance. Cell 83:171-176.

Tanaka EM, Kirschner MW (1991) Microtubule behavior in the growth cones of living neurons during axon elongation. J Cell Biol 115:345-363.

Tang F, Kalil K (2005) Netrin-1 induces axon branching in developing cortical neurons by frequency-dependent calcium signaling pathways. J Neurosci 25:6702-6715.

Tang F, Dent EW, Kalil K (2003) Spontaneous calcium transients in developing cortical neurons regulate axon outgrowth. J Neurosci 23:927-936.

Tear G (1999) Axon guidance at the central nervous system midline. Cell Mol Life Sci 55:1365-1376.

Tessier-Lavigne M, Goodman CS (1996) The molecular biology of axon guidance. Science 274:1123-1133.

Uesaka N, Hirai S, Maruyama T, Ruthazer ES, Yamamoto N (2005) Activity dependence of cortical axon branch formation: a morphological and electrophysiological study using organotypic slice cultures. J Neurosci 25:1-9.

Wacker I, Schwarz V, Hedgecock EM, Hutter H (2003) zag-1, a Zn-finger homeodomain transcription factor controlling neuronal differentiation and axon outgrowth in C. elegans. Development 130:3795-3805.

Wahl S, Barth H, Ciossek T, Aktories K, Mueller BK (2000) Ephrin-A5 induces collapse of growth cones by activating Rho and Rho kinase. J Cell Biol 149:263-270.

Wang KH, Brose K, Arnott D, Kidd T, Goodman CS, Henzel W, Tessier-Lavigne M (1999) Biochemical purification of a mammalian slit protein as a positive regulator of sensory axon elongation and branching. Cell 96:771-784.

Watari-Goshima N, Ogura K, Wolf FW, Goshima Y, Garriga G (2007) C. elegans VAB-8 and UNC-73 regulate the SAX-3 receptor to direct cell and growth-cone migrations. Nat Neurosci 10:169-176.

Wayman GA, Kaech S, Grant WF, Davare M, Impey S, Tokumitsu H, Nozaki N, Banker G, Soderling TR (2004) Regulation of axonal extension and growth cone motility by calmodulin-dependent protein kinase I. J Neurosci 24:3786-3794.

Weiss EL, Kurischko C, Zhang C, Shokat K, Drubin DG, Luca FC (2002) The Saccharomyces cerevisiae Mob2p-Cbk1p kinase complex promotes polarized growth and acts with the mitotic exit network to facilitate daughter cell-specific localization of Ace2p transcription factor. J Cell Biol 158:885-900.

Wen Z, Guirland C, Ming GL, Zheng JQ (2004) A CaMKII/calcineurin switch controls the direction of Ca(2+)-dependent growth cone guidance. Neuron 43:835-846.

Wicks SR, Yeh RT, Gish WR, Waterston RH, Plasterk RH (2001) Rapid gene mapping in Caenorhabditis elegans using a high density polymorphism map. Nat Genet 28:160-164.

Witte H, Bradke F (2008) The role of the cytoskeleton during neuronal polarization. Curr Opin Neurobiol 18:479-487.

Wong K, Ren XR, Huang YZ, Xie Y, Liu G, Saito H, Tang H, Wen L, Brady-Kalnay SM, Mei L, Wu JY, Xiong WC, Rao Y (2001) Signal transduction in neuronal migration: roles of GTPase activating proteins and the small GTPase Cdc42 in the Slit-Robo pathway. Cell 107:209-221.

Yang N, Higuchi O, Ohashi K, Nagata K, Wada A, Kangawa K, Nishida E, Mizuno K (1998) Cofilin phosphorylation by LIM-kinase 1 and its role in Rac-mediated actin reorganization. Nature 393:809-812.

Yang X, Li DM, Chen W, Xu T (2001) Human homologue of Drosophila lats, LATS1, negatively regulate growth by inducing G(2)/M arrest or apoptosis. Oncogene 20:6516-6523.

Yarden O, Plamann M, Ebbole DJ, Yanofsky C (1992) cot-1, a gene required for hyphal elongation in Neurospora crassa, encodes a protein kinase. EMBO J 11:2159-2166.

Yates PA, Roskies AL, McLaughlin T, O'Leary DD (2001) Topographic-specific axon branching controlled by ephrin-As is the critical event in retinotectal map development. J Neurosci 21:8548-8563.

Yoshimura T, Kawano Y, Arimura N, Kawabata S, Kikuchi A, Kaibuchi K (2005) GSK-3beta regulates phosphorylation of CRMP-2 and neuronal polarity. Cell 120:137-149.

Yu W, Qiang L, Solowska JM, Karabay A, Korulu S, Baas PW (2008) The microtubule-severing proteins spastin and katanin participate differently in the formation of axonal branches. Mol Biol Cell 19:1485-1498.

Zallen JA, Kirch SA, Bargmann CI (1999) Genes required for axon pathfinding and extension in the C. elegans nerve ring. Development 126:3679-3692.

Zallen JA, Peckol EL, Tobin DM, Bargmann CI (2000) Neuronal cell shape and neurite initiation are regulated by the Ndr kinase SAX-1, a member of the Orb6/COT-1/warts serine/threonine kinase family. Mol Biol Cell 11:3177-3190.

Zhang H, Macara IG (2006) The polarity protein PAR-3 and TIAM1 cooperate in dendritic spine morphogenesis. Nat Cell Biol 8:227-237.

Zhou FQ, Zhou J, Dedhar S, Wu YH, Snider WD (2004) NGF-induced axon growth is mediated by localized inactivation of GSK-3beta and functions of the microtubule plus end binding protein APC. Neuron 42:897-912.

Zhou X, Zhao G, Truglio JJ, Wang L, Li G, Lennarz WJ, Schindelin H (2006) Structural and biochemical studies of the C-terminal domain of mouse peptide-N-glycanase identify it as a mannose-binding module. Proc Natl Acad Sci U S A 103:17214-17219.

Zou DJ, Cline HT (1996) Expression of constitutively active CaMKII in target tissue modifies presynaptic axon arbor growth. Neuron 16:529-539.

Appendix1. snip-SNP used for chromosome and interval mapping of *sens* mutants. SNP primers, their locations, PCR and restriction fragment band sizes are indicated.

LG	Marker	Map position	Primers (5'-3')	PCR product (bp)	Enzyme	Fragment sizes (bp)	
						Bristol digest	Hw digest
I	VF39H2L	3	TTCAGGCTCCACTTTATGCC CATCTGGGACGTTCTTTCAC	641	DraI	641	421, 219
II	T01D1	-18	AAGAGGTGTTCTTCTGCAGC ACCATCCACGCAGTTCATTC	619	DraI	402, 172, 44	574, 44
II	W09B6	-13	TAATTTCTAGCACCAGTGAGGC CCCAAATTTCCACCTGTAATCC	728	DdeI	480, 250	730
II	F39E9	-8	ATGCCTTCGCAAACTCTG GAGTCATGCAACAACGCATATG	276	XbaI	276	146, 130
II	F54D10	-5	TTGAGTCTCAAATGGCGCTG GGGTGTCTTTGCCATGTTTG	450	DraI	450	253, 196
II	Y51B9	1	CTAGGAGATGCTCCAACTTCTG TCGCATCAAGTCCATCTCTG	656	EcoRI	656	328, 327
II	ZK666	3	TCAACCTTCATACGTGTCGC GGAATGACTGATAAAGGTGTCG	760	XbaI	460, 300	760
II	C50E10	5	CTCCTTCAGTACCATATGGCTC TCGGGTCTCTCCAAAAACTC	666	EcoRI	666	391, 274
III	W03A5	-2	CAGACATTTAGGAGTAGGCAGG GAGTACGCGGGTCATTTTTG	365	MseI	365	210, 163
III	B0280	-1	GCGGTGTATCGTCCATTTC AATTCCACGAGTTCCATGTCTG	240	BamHI	150, 90	240
III	T28D6	9	TTTCGTGTACGAACGTCTCC CATTTCTCCCACTCTTGCTG	500	DraI	500	283, 217
IV	F58H7	-21	CAGATATTGGCTGAGCAGTG CTGCAAAGAAGCGAGAACAG	659	SspI	361, 244, 54	361, 298
IV	C45G7	-8	TCCGCTCTGGTTGACATTAC AAATCTACATGGACGCGC	491	DraI	491	253, 238
IV	F42A6	-5	ACTTTCAGCTGCTCGTACTCTC TCTGCCTTTTCACTTGCC	397	DraI	234, 163	397
IV	F38a5	3	GCACCATCTTCTGCTCCAAC TTAACCTTTGGAGTGACTGCG	405	XbaI	405	143, 262
IV	D2096	4	ACGAAAAATCACAGAGCGGG AATCAACAACGGACGACGAG	852	EcoRI	651, 206	852
IV	W02A2	9	AATTCTCGGCTTCATACCCG GTGCGTTTGTATCCTCCATG	485	SspI	218,136, 131	349, 136
IV	Y41E3	11	GCGTTACCCTACTTATGTCCAC AAGTAGCTTCGTAACTGCGC	609	DraI	391, 217	609